THE EFFECT OF SHEAR ON SWEEP FLOCCULATION IN STABLE WATER-IN-OIL EMULSIONS

by

Aakanksha Bhargava

A thesis submitted in partial fulfilment of the requirements for the degree of

Master of Science

in

Chemical Engineering

Department of Chemical and Materials Engineering
University of Alberta

Abstract

Naphthenic Froth Treatment (NFT) is employed to remove water droplets and solids from the bitumen froth recovered from the extracted oilsands ore. In the process, bitumen froth is diluted with naphtha to reduce the viscosity and induce density difference to promote settling of water droplets and solids. The diluted bitumen froth is then mixed with a demulsifier and passed through Inclined Plate Settlers (IPSs) and centrifuges. The IPS units separate most water and solids from the diluted bitumen froth, leaving the final concentration of around 1.5 -2.5 wt % water and 0.5 wt% solids in the final product. The remaining water is present in the form of very stable droplets that are difficult to separate without the assistance of induced flocculation or coalescence. These water droplets in diluted bitumen are detrimental to upgrading facilities as they may cause corrosion problems. The selection of operating conditions for separating equipment (IPS) such as demulsifier selection/optimal concentration depends on the data obtained from laboratory scale bottle or jar tests. These tests are done under static conditions that are not representative of the shear/flow experienced at the industrial scale. The main objective of the project is to understand the effect of shear on the flocculation of water droplets. This project uses water-in-light mineral oil emulsions as analogs for water-in-diluted bitumen emulsions.

Several experiments were conducted to determine the effect of shear rate on the flocculation of water droplets in water-in-light mineral oil emulsions. The effect of shear was studied using a custom-built Couette cell, which has a shear rate range similar to IPS. The shear rate selected is 12.2 – 29.3 s^{-1}, similar to that experienced by the water droplets between the parallel plates in an IPS. The emulsion was sheared in the Couette cell using a precisely defined protocol and then allowed to settle for one hour.

The laminar shear rate ($12.2 - 29.3$ s^{-1}) induced in the water-in-light mineral oil emulsion forces water droplets/ flocs to come in contact with each other, increasing the number of collisions and promoting floc formation. Furthermore, the formed flocs have higher settling velocities than individual droplets. The faster settling flocs sweep away single water droplets or small flocs present in their settling path, leading to further growth of the flocs, which increases their settling velocity; this mechanism is called sweep flocculation. Sweep flocculation promotes the removal of small water droplets from the oil that would otherwise take many days or hours to settle. It can be inferred from the experiments that shearing the emulsion promotes the formation of flocs, which further induces sweep flocculation in the emulsion and results in a cleaner oil as compared to the emulsions, that have not been sheared in the Couette cell.

Preface

This thesis is original work by Aakanksha Bhargava. No part of this thesis has been published previously.

Dedicated to my parents, who always believed in me.

Acknowledgments

Table of Content

List of Figures

List of Tables

List of Symbols

Symbol	Description	Unit
α	Collision efficiency	-
β	Collision frequency function	-
n_j	Concentration of particle of size i	-
n_j	Concentration of particle of size j	-
du/dy or G	Velocity gradient/ Average shear rate	s^{-1}
d_i	Diameter of the ith particle	L
d_j	Diameter of the jth particle	L
g	Acceleration of gravity	m/s^2
ρ_p	Density of particle	kg/m^3
ρ_l	Density of fluid	kg/m^3
μ_l	Dynamic viscosity of the fluid	Pa. s
v_i	Settling velocity of the ith particle	m/s
v_j	Settling velocity of the jth particle	m/s
$v_{p,\infty}$	Settling velocity of the particle in Stokes 'regime	m/s
Ta	Taylor number	-
ω	Angular velocity	rad/s
R_i	Couette cell inner cylinder radius	mm
R_o	Couette cell outer cylinder radius	mm
d_{10}	Number mean diameter	µm
d_{32}	Sauter mean diameter	µm
d_{43}	Volume mean diameter	µm

Chapter 1 : Introduction

1.1 Background

In 2020, Alberta produced 83 % of Canada's total oil, and 66 % of it was bitumen [1]. The crude bitumen production was close to 3.2 million barrels per day in 2020 and is expected to increase by 56 % by 2030 [1]. Consequently, Alberta oilsands will significantly impact the Canadian and global energy markets in the coming years.

Alberta oilsands, also known as bituminous sands, are a mixture of sand, water, clay, minerals, and bitumen [2]. Crude bitumen is a heavy crude oil with high sulfur and heavy metal percentages and relatively low hydrogen content [2]. It must be treated and separated from the water and solids before being fractioned in refineries to produce gasoline, heating oils, diesel, and jet fuels.

In bitumen extraction from oil sands, the excavated ore is crushed, treated with water, and passed through a Primary Separation Vessel (PSV), where bitumen is recovered through as bitumen froth [2,3]. The recovered bitumen froth, on average, has 60 wt. % bitumen, 30 wt.% water, and 10 wt.% solids [2–5]. The water in bitumen froth contains salts that can contribute to serious corrosion-related hazards, while coarse solids can cause equipment wear in upgrading operations [2,4,6]. It is, therefore, crucial to remove the water and solids before feeding the bitumen to upgrading units [2,4,6].

Froth treatment units are employed to remove water droplets and solids, and the first step in froth treatment is the addition of a solvent (light hydrocarbon). The solvent is added to induce density difference as bitumen density is extremely close to that of water, making separation by gravity settling too slow for commercial interest [2,4]. The addition of solvent also reduces the viscosity of bitumen, further enhancing the separation process [2,4].

There are two technologies in froth treatment categorized based on the type of solvent used: Paraffinic Froth Treatment (PFT) and Naphthenic Froth Treatment (NFT) [2,4]. Paraffinic froth treatment (PFT) uses aliphatic/paraffinic solvents to separate water and solids from bitumen [2,4]. The final diluted bitumen has a negligible amount of water and solids; less than 0.2 wt.% water and less than 0.01 wt.% solids [2,4]. Naphthenic froth treatment (NFT) uses naphtha as a solvent. The naphtha is a mixture of aliphatic, naphthenic, and aromatic hydrocarbons [7]. The final water content in the diluted bitumen is greater than 0.5 wt. % [2,4]. Therefore, the focus of the project is NFT, as it produces a product with a higher water content. A schematic of a typical NFT process employed in the industry is shown in Figure 1.1.
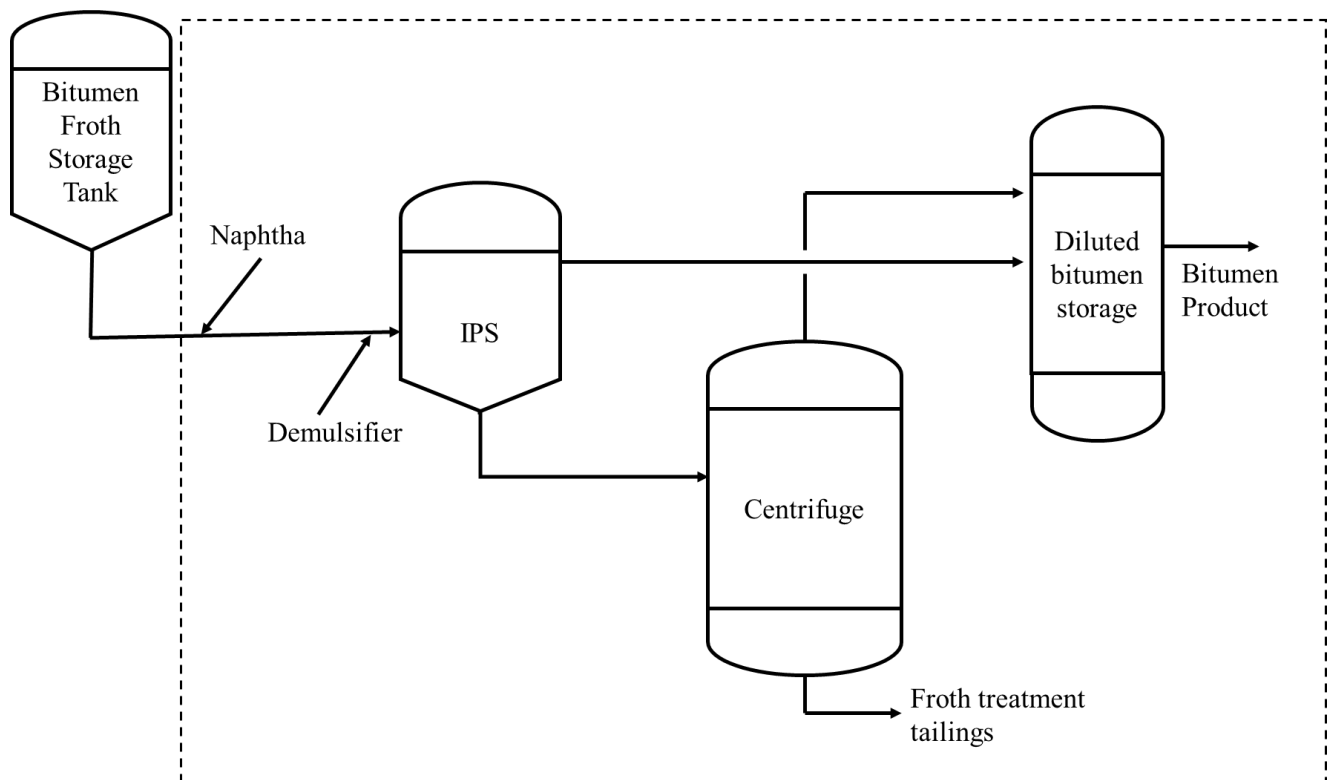
Figure 1.1 Simplified representation of typical naphthenic froth treatment process. Adapted from Rao. et al. [3].

As can be seen, bitumen froth is mixed with naphtha (solvent) and a demulsifier [2–4]. The addition of a demulsifier helps the droplets to grow in diameter either through coalescence or flocculation.

Coalescence is defined as droplets combining to become a large droplet, while flocculation is droplets coming together to form an agglomerate, as explained in Figure 1.2.
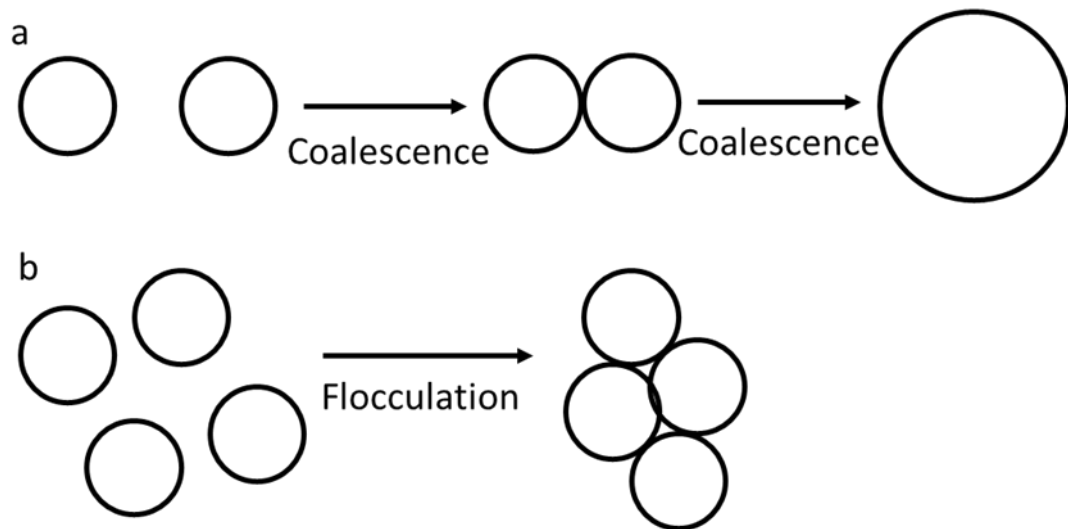
Figure 1.2 (a) Schematic illustrations of (a) coalescence and (b) flocculation.

The coalescence process effectively removes large water droplets, while flocculation removes small water droplets [5]. The mixture of naphtha-diluted bitumen and demulsifier is subsequently passed through a series of separating equipment such as Inclined Plate Settlers (IPS) and centrifuges [2–4]. An inclined plate setter is a gravity settler in which a stack of plates is inclined at a certain angle, as shown in Figure 1.3 [4,8]. As the naphtha-diluted bitumen flows through the plates, water droplets /solids settle on the lower plate and slide down, as shown in Figure 1.3 [8]. The underflow is sent to the centrifugation unit to further process the naphtha-diluted bitumen. The IPS overflow is sent to a storage tank and from there directly to upgrading facilities without further separation [2–4], as shown in Figure 1.1.
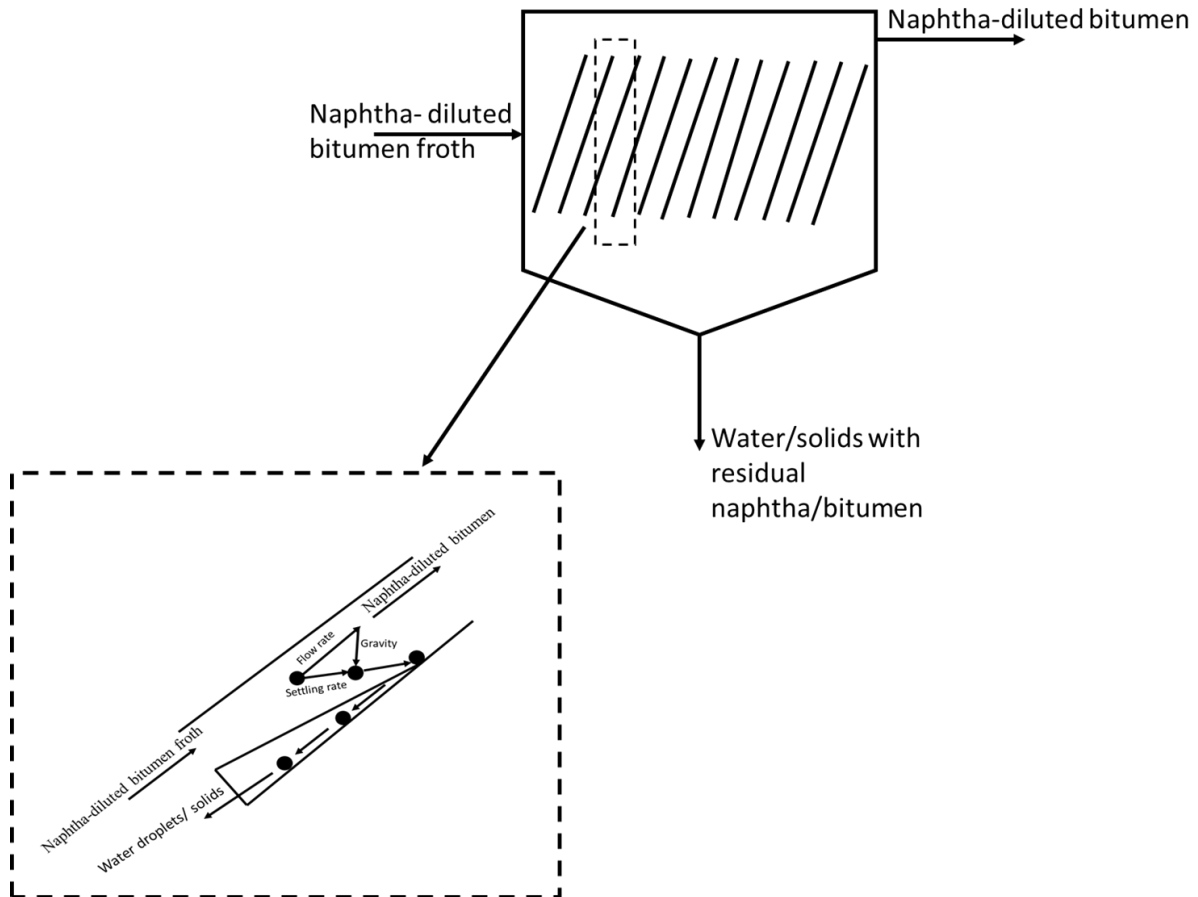
Figure 1.3 Simplified schematic of an Inclined Plate Settler and the settling mechanism between the parallel plates. Adapted from Bengston and Metchem webpage [9,10].

The diluted bitumen has a final water concentration of around 1.5 - 2.5 wt.% [2,4], as most of the water is separated in the IPS. This residual water forms a very stable emulsion (water-in-diluted bitumen) with droplet diameter in the range of 1-10 μm [2,4,11]. These small water droplets contain chloride ions that may be converted to hydrochloric acid during upgrading, leading to corrosion problems in the plants, therefore affecting the plant integrity and reliability [2,4–6]. Hence, it is imperative to have a final water concentration of less than 0.5 wt.% after froth treatment [2,4–6].

In the last half-century, numerous studies have been conducted to understand the factors responsible for the stability of water-in-bitumen emulsions [2,6,12–14]. It was discovered that stability is due to a rigid film enveloping the water droplets [2,6,12,14]. This rigid film comprises naturally occurring surfactants such as asphaltenes and fine solids [2,6,12,14] and exhibits resistance to coalescence equivalent to the centrifugal force of 10,000 G [3,5]. The settling of such small water droplets in the absence of induced flocculation will take several hours or days, exceeding the residence time of an IPS. Moreover, it is impractical to coalesce such highly stable small droplets in centrifuges as industrial multistage centrifuges are designed for centrifugal forces up to 2500G [3,4]. Therefore, the efficacy of froth treatment depends mainly on the performance of the IPS units, which depends on the combination of demulsifier injection/selection and IPS residence time.

The selection of demulsifier type and concentration relies on data collected from lab-scale bottle tests [2,4–6,15]. This test is often used to evaluate different demulsifiers and study the stability of the emulsion [2,4–6,15]. In this test, representative emulsion samples are transferred into a number of bottles or tubes. Then, a different demulsifier is added to each bottle at a specific concentration and mixed to ensure proper dispersion. After mixing, samples are left undisturbed to observe the phase separation over time. The main criteria for selecting the demulsifier and assessing the emulsion stability are measuring the amount of water separated in the time corresponding to the residence time of separating equipment [5,6,15]. This test is also used to estimate the retention time and optimal demulsifier dosage, which can be utilized to develop the design and operating conditions for separating equipment (IPS) [2,4–6,15]. However, these tests are carried out in a static environment and fail to account for the dynamic conditions experienced in the IPS unit [2,4–6,15].

This project uses analog water-in-oil emulsion with properties similar to the water-in-diluted bitumen due to complexities in working with bitumen as the quality of bitumen froth varies depending on the type of ore and processing conditions [16,17].

1.2 Problem Statement

On the industrial scale, the demulsifier is injected into the pipelines that feed the IPS unit, as shown in Figure 1.1, where turbulent conditions are encountered [18]. In the past, studies have been performed to develop a lab-scale methodology replicating industrial mixing conditions for demulsifier injection and dispersion in the pipelines [18]. However, as the diluted bitumen – demulsifier mixture enters the IPS, it experiences laminar shear. It is known from studies on surfactant stabilized oil-in-water emulsions that applying gentle shear has led to an increase in the rate of flocculation/coalescence of the dispersed phase [19–21]. The same principle of increased flocculation rate due to gentle shear rate can be applied to water-in-oil or water-in-bitumen emulsions. It is, therefore, vital to develop a robust lab-scale test/device that accounts for the shear experienced in separating equipment (IPS) by the dispersed water droplets. The increase in diameter of water droplets (dispersed phase) due to shear will increase their settling velocity, enhancing the settling and removal of the smaller water droplets. Thus, data from these tests will allow better control of the IPS units and improve bitumen quality.

1.3 Project Objectives

A comprehensive study of flocculation due to applied gentle shear rate (shear-induced flocculation) of water droplets can be invaluable to the ongoing effort to produce cleaner bitumen. Studies have been conducted in the past on oil-in-water emulsion or particulate suspension to understand the effect of shear on coalescence/flocculation of dispersed phase. However, to the author's best knowledge, no studies have been performed to investigate the effect of shear on the dispersed phase (water droplets) in a water-in-oil emulsion. Furthermore, there is a huge gap between the existing bottle test and the need to obtain more realistic information to optimize the operating conditions of the IPS units. The present study uses water-in-light mineral oil emulsion with density and viscosity similar to the water-in-bitumen emulsion.

The main objective of this project is to study the effect of shear on the flocculation of the dispersed phase (water) in a water-in-oil emulsion.

The major activities required to complete the project are as follows:

- Develop a procedure to consistently produce water-in-oil emulsions with a mean droplet size in the range of 1-10 μm.

- Determine the shear rate range experienced in the separating equipment (IPS).

- Design and construct a lab-scale shearing device suitable for replicating the shear rates experienced in separating equipment (IPS).

- Design the procedures to perform experiments in the lab-scale shearing device and analyze the results.

1.4   Thesis Outline

The thesis has five chapters, including the present chapter. The remaining chapters are described below:

- **Chapter 2: Literature Review** provides a detailed overview of the subjects relevant to the present study, such as the froth treatment process, emulsion stability, demulsification, flocculation, and lab-scale shearing devices. This chapter also identifies the knowledge gaps relevant to this research project.

- **Chapter 3: Experiments and Methods** includes detailed information on the materials and equipment used in the project. It also documents all the procedures/protocols followed in the project.

- **Chapter 4: Results and Analysis** discusses the results of experiments to produce the water-in-light mineral oil emulsion and shearing experiments conducted at various conditions. The repeatability of the experiments is also discussed in the chapter.

- **Chapter 5: Conclusions and Recommendations** summarizes the key findings of the project and proposes ideas to improve further and expand the current study.

1.5   Author contributions

In this project, the author has designed a lab-scale testing device to investigate the effect of shear on the flocculation of the dispersed phase in a water-in-light mineral oil emulsion. The device can be used to study the shear effect in similar systems in the future.

Prof. Sean Sanders and Dr. Marcio Machado made significant contributions in conceptualizing the project, offering guidance and advice at each stage.

The MATLAB script used to characterize the emulsion was modified by the author. It was first developed by Bach Vo and Dr. David Breakey. This script can be used to characterize different emulsions and spherical-particle systems.

The author has developed another MATLAB script to characterize the flocs observed during shearing experiments.

The safe work procedure for emulsion preparation, microscope image acquisition, and shearing experiments was developed by the author.

The procedure used for the silanization of microscope slides and needles was developed by Shaun Leo [22] and later rewritten by the author.

The equipment and materials necessary for the experiments are provided by the Pipeline Transport Process Research Group. Dr. Hongbo Zeng's research group provided the homogenizer for emulsion preparation and an optical microscope for emulsion characterization.

The findings from the study can lay the foundation for the future improvement of conventional bottle tests by accounting for the effect of shear and further optimizing the operating condition for

separating equipment (IPS) as the study has been conducted in the context of oil sands froth treatment.

Chapter 2 : Literature Review

2.1 Introduction

This chapter contains information on the relevant subjects that are essential for a better understanding of the project. This chapter begins with a discussion of froth treatment, its importance, different types, and their respective shortcomings in Section 2.2. The types of emulsions encountered in bitumen extraction, their stability, and the factors responsible for that stability are covered in Section 2.3. Section 2.4 explains the basics of the flocculation process and provides an overview of the chemical demulsification methods employed in bitumen froth treatment. The most commonly used lab-scale test to study the stability of the emulsion or in the selection of demulsifier, with its shortcomings, is introduced in Section 2.5. Section 2.6, summarizes the previous research done to replicate the industrial conditions for demulsifier mixing. A comparison of different lab scale shearing devices is provided in Section 2.7. Section 2.8 discusses the previous work done to understand the effect of laminar shearing on flocculation/ coalescence of dispersed phase (oil/solids) in oil-in-water emulsions/particulate suspensions. This section also highlights that there has not been any study to understand the effect of laminar shear rate on flocculation of dispersed phase (water droplets) in water-in-oil emulsions. Finally, Section 2.9 lists the detailed objectives of the project in connection with the contents of this chapter.

2.2   Froth Treatment

There are two methods for recovering bitumen from oil sands: open pit (surface) mining and steam-assisted gravity drainage [2]. The open-pit (surface) mining is applied to the shallow (less than 75 m below from the earth surface) oilsands deposits [2]. A general schematic of bitumen recovery in open pit (surface) mining is shown in Figure 2.1. As can be seen, oil sands are mined and crushed. The crushed ore is then mixed with hot water (60 - 90°C) and NaOH in slurry preparation equipment [2,3]. The resulting slurry is fed into hydrotransport pipelines where bitumen is attached to air bubbles [2,3]. The slurry from the hydrotransport pipeline is fed to the Primary Separating Vessel (PSV), where bitumen is recovered through gravity separation as bitumen froth [2,3].
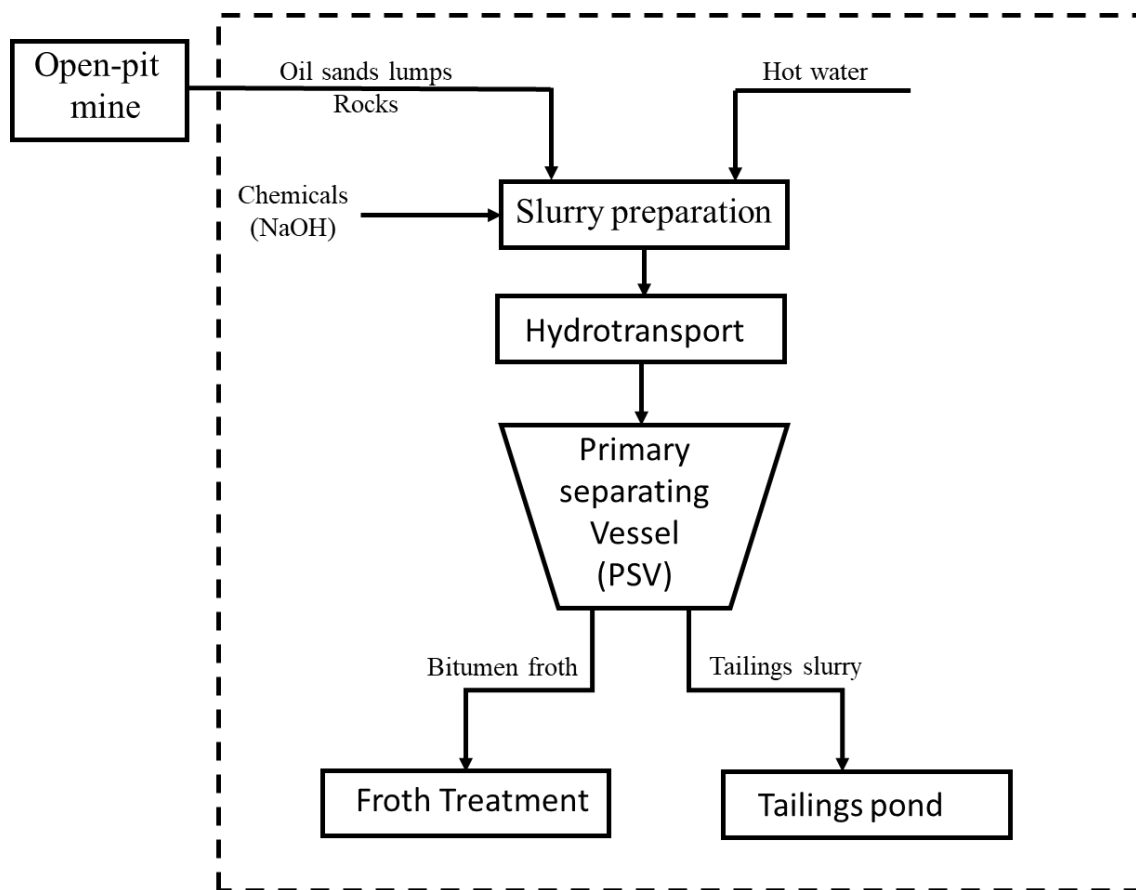
Figure 2.1 Schematic for bitumen recovery through surface mining. Adapted from Masliyah et al. [2].

Bitumen froth is a mixture of bitumen, water (small and large droplets), and solids (coarse and fine). It has a composition of about 60 wt.% bitumen, 30 wt.% water, and 10 wt.% solids [2–5], although the composition can vary with the ore quality, process temperature, and the operating condition of the extraction plant [16,17]. Water and solids are detrimental to pipeline transport, upgrading, and refining facilities. Salts in water can lead to severe corrosion problems, while solids can cause equipment/pipeline wear and plug the downstream equipment, resulting in increased operating and maintenance costs [2,4,6]. It is, therefore, crucial to remove water and solids from bitumen before feeding it to upgrading facilities.

The removal of water and solids can be accomplished by passing the bitumen froth through separating equipment in a process known as froth treatment, where water droplets and solids are removed by gravity settling or centrifugation. However, bitumen has a high viscosity and density comparable to water, making it difficult to separate water through gravity/centrifugation-based operations [2,4]. Therefore, the primary step in the froth treatment process is adding solvent/diluent to induce a density difference and to lower the continuous phase viscosity to facilitate the separation [2,4].

The two types of commercial froth treatment methods used in the Alberta oilsands industry are Paraffinic Froth Treatment (PFT) and Naphthenic Froth Treatment (NFT). In Paraffinic Froth Treatment (PFT), an aliphatic/paraffinic solvent is added to the bitumen froth at a solvent to bitumen ratio greater than 2 [2,4]. The mixture is passed through a series of gravity-settling vessels in counter-current arrangement [2,4]. The addition of solvent begins the precipitation of asphaltenes to form large flocs [2,4]. These large asphaltene flocs entrap small solids, and water droplets exit at the bottom of the settling equipment, leaving clean diluted bitumen as overflow [2,4]. The diluted bitumen recovered in PFT has a negligible water and solids contents, thus meeting the criteria for upgrading facilities, i.e., solids and water content less than 0.5 wt.% [2,4].

However, it is expensive as the diluent used is costly, and the high solvent to bitumen ratio necessitates larger equipment, further raising the capital and operating costs [2] . It also is only used in newer operations.

The older froth treatment method is Naphthenic Froth Treatment (NFT) which uses a naphthenic solvent. A typical schematic of NFT is shown in Figure 1.1. In the process, naphtha and bitumen are mixed at a ratio (naphtha to bitumen) roughly in the range of 0.5 to 0.7 (weight basis), at a temperature of 80 °C [2,4,23]. Following this step, the demulsifier is injected to improve the separation by inducing flocculation/coalescence of water droplets [2,4,23]. In flocculation, droplets combine to form flocs, whereas, in coalescence, they combine to form larger droplets, as described by Figure 1.2. The naphtha diluted bitumen and demulsifier mixture is processed through Inclined Plate Settlers (IPS) and centrifuges shown in Figure 1.1[2–4].

An inclined plate settler is a gravity settler that consists of a stack of parallel plates inclined at a certain angle [4,8], as shown in Figure 2.2. It has traditionally been used for water clarification in water treatment and thickening operations in mineral industries [4]. However, since 1984, IPS has been used in the NFT process as primary separating equipment [4].
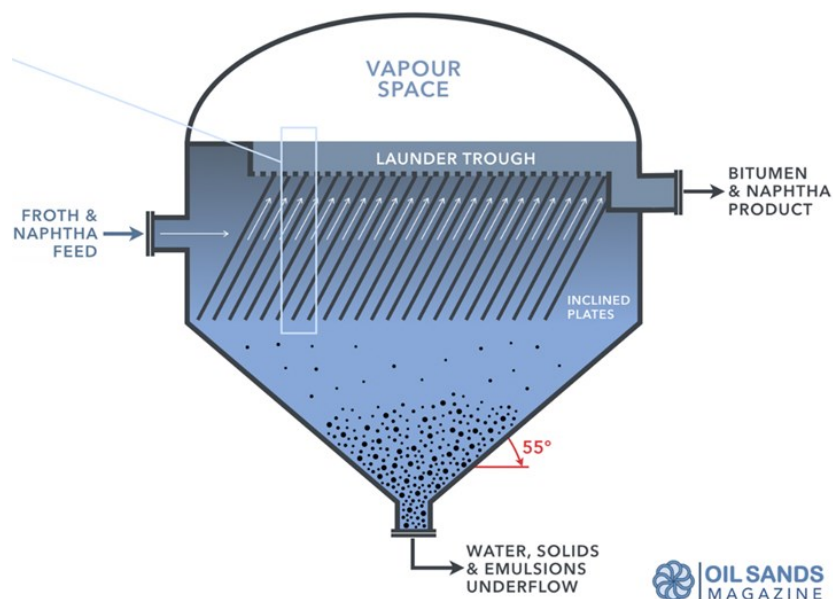
Figure 2.2 Inclined plate settler used in NFT. Taken from Oilsands Magazine [8].

This arrangement of plates reduces the projected settling distance, resulting in faster settling of flocs/droplets/solids than in vertical gravity settlers, and thus enhancing the separation efficiency [4,24]. The increased horizontal projected area makes the unit compact and capable of handling larger volumes [4]. This IPS feature makes it suitable for froth treatment that involves processing approximately 0.375 million barrels of diluted bitumen froth per day [2,4]. The most important requirement for the effective performance of the IPS is to maintain a laminar flow between the plates, implying Reynolds number should be less than 500 [25–27] as defined:

$$Re = \frac{\rho_l * v * D_h}{\mu_l} \qquad\qquad 2.1$$

where ρ_l is the fluid density, v is the average fluid velocity, D_h is the hydraulic diameter, and μ_l is the fluid viscosity.

As the bitumen froth flows between the parallel plates in the IPS unit, the large water droplets/ flocs along with solids settle on the lower plate and slide down to the underflow, as explained in Figure 1.3. The underflow is routed through rotary equipment such as centrifuges to further process the diluted bitumen, whereas overflow from the IPS is sent directly to a storage tank [2–4]. Most of the water separates within the IPS (residence time less than 20 minutes)[25]; nonetheless, the diluted bitumen obtained as IPS overflow has roughly 1.5 - 2.5 wt.% and 0.5 wt. % solids. It has a density and kinematic viscosity of 860 kg/m^3 and 6.1 mm^2/s at 80 °C, respectively [28].

It is known that some fraction of the dispersed water is difficult to remove in an IPS. This water is present as a stable water-in-diluted bitumen emulsion and can lead to corrosion problems in the upgrading facilities. It is, therefore, crucial to understand factors responsible for the stability of water droplets in diluted bitumen.

2.3   Emulsion stability

An emulsion is a colloidal mixture of two immiscible liquids with one phase stably dispersed as droplets in another [5,6]. The stability of the emulsion is described as the ease of separating with time [6]. Emulsions are typically classified based on the size of the dispersed phase, i.e., microemulsions and macroemulsions. Microemulsions have dispersed droplets of less than $0.1\mu m$, whereas macroemulsions have dispersed droplets in size range of 0.1-100 µm [6,29]. Microemulsions are beyond the scope of this project as water droplets dispersed in diluted bitumen have sizes greater than 0.1 µm [2,4,11].

Macroemulsions are thermodynamically unstable but kinetically stable systems [5,6,29]. This implies that a macroemulsion is stable over a period but tends to separate to minimize the interfacial area/energy [5,6,29]. Stabilizing agents, such as surfactants, can impart kinetic stability to emulsions. Surfactants are chemicals with both hydrophilic and hydrophobic parts that adsorb at the interface to form an interfacial film [6,29]. The formation of an interfacial film stabilizes the emulsion by decreasing the Interfacial Film Tension (IFT). The adsorption of surfactants also increases the rigidity of the interfacial film. The increase of rigidity of the film prevents the droplet coalescence by increasing the film drainage and rupture time [6,29]

The water droplets in diluted bitumen froth can be divided into three categories based on their size [11]:

- Emulsified water with droplets sizes less than 10 µm. It is challenging to remove emulsified water droplets within one IPS residence time unless induced coalescence/flocculation occurs [11].
- Dispersed water with droplets diameter in the range of 10 - 60µm that can be removed. These settle faster than emulsified droplets but require sufficient residence time and or additional help of external acceleration forces such as centrifugation [11].

15

- Free water with droplets/water pockets greater than 60 μm in diameter. This fraction can be removed quickly without any assistance as these water droplets start settling as soon as the solvent is added to the bitumen froth [11].

The diluted bitumen recovered as IPS overflow contains stable emulsified water, i.e., droplets with diameters of less than 10 microns [2,4,11]. It was discovered that the stability of these water droplets is due to the formation of a rigid film enveloping the water droplets, as shown in Figure 2.3 [4]. The rigid film comprises naturally occurring surfactants such as asphaltenes and resins, fine solids, organic acids, and bases [2–4,12–14].
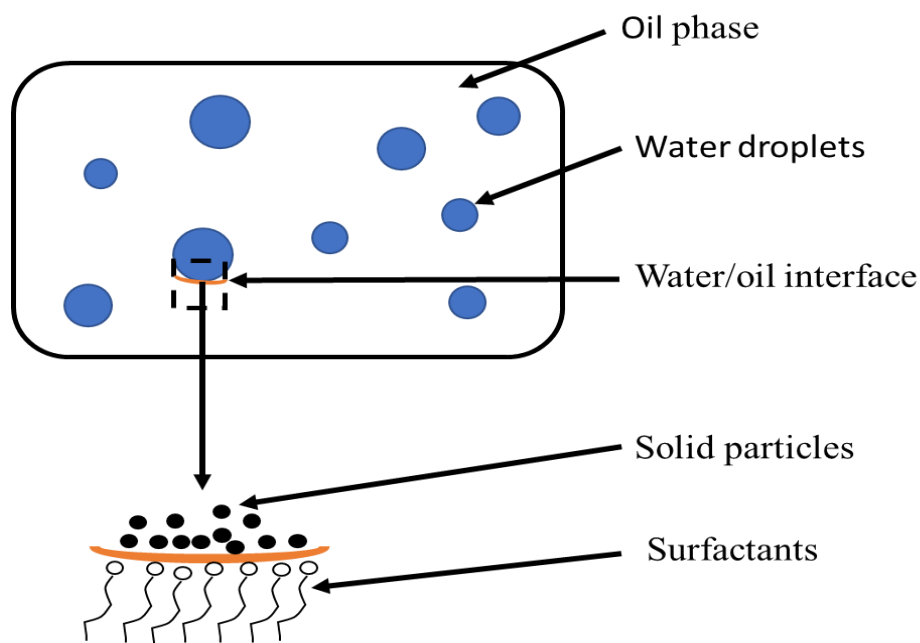
Figure 2.3 Schematic representation of surfactant adsorption at water/oil interface. Reproduced from Rao et al.[3].

The interfacial film around emulsified water droplets in diluted bitumen can be 8 - 40 nanometres thick [13,23]. It has a resistance to coalescence equivalent to the centrifugal force of 10,000 G [3]. It is impossible to separate these water droplets through coalescence as industrial centrifuges are not designed for such a high G value. Gravity settling of such small water droplets in separating equipment like the IPS would take many hours or days, i.e., far beyond the IPS residence time.

Thus, the effectiveness of water removal depends on the extent of flocculation/coalescence of water droplets in (or upstream of) IPS.

2.4 Demulsification

The process of separating an emulsion into its constituent phases is known as demulsification [5,6,29]. It typically involves a sequence of steps, including flocculation, coalescence, sedimentation, and phase separation [5,6,29].

Figure 2.4 is a representation of the typical steps involved in the demulsification of a water-in-diluted bitumen emulsion.
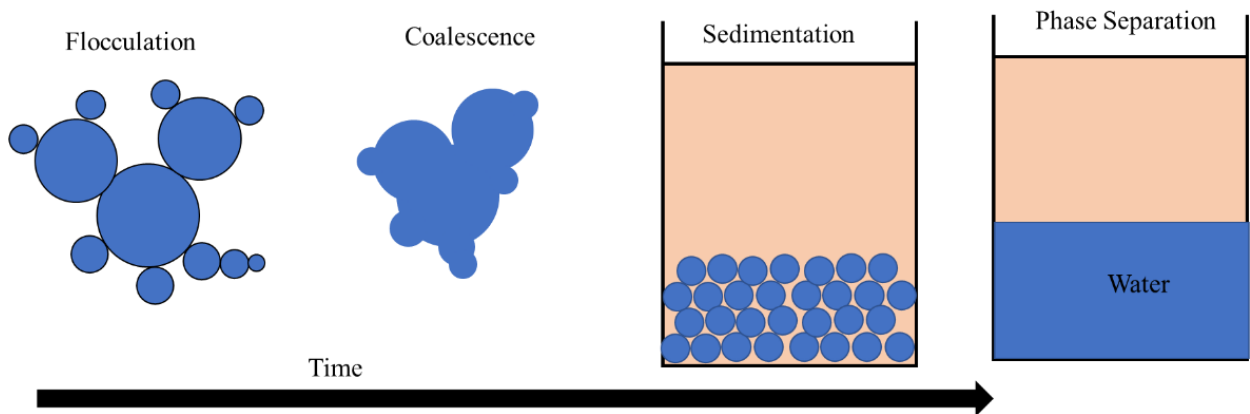
Figure 2.4 Steps involved in the separation of a water-in-oil emulsion. Adapted from Goodarzi et al. [29].

There are three types of demulsification: chemical, mechanical, and electrical [5,6], but the focus of the project is flocculation and chemical demulsification.

2.4.1 Flocculation

Flocculation is defined as a process of fine droplets/particles approaching each other to form large agglomerates known as flocs [2,30–32]. The process consists of two basic steps: transport and attachment:

1. Transport brings the droplets/particles close to each other and resulting in a collision [31]. The hydrodynamics of the system, such as variations in the fluid or dispersed phase velocity [30–32], govern their transport.

2. Attachment is adhering of the droplets/particles to stay as a single entity. The attachment between them is governed by the colloidal forces present in the system [30–32].

The two steps can be characterized analytically as a rate of successful collisions between particles of size i and j, or rate of flocculation [31,32]:

$$\text{Rate of flocculation} = \alpha * \beta(i,j) * n_i * n_j \qquad\qquad 2.2$$

where α is the collision efficiency, n_i, n_j are the concentration of droplets/particles of size i and j, respectively, and $\beta(i,j)$ is the collision frequency between droplets/particles of size i and j.

Collision efficiency (α) represents the percentage of collisions that lead to attachment, and its value ranges from $0 - 1$ [30,32]. The collision frequency (β) is a measure of transport efficiency leading to collisions and is a function of transport mechanics [28,30].There are three types of flocculation based on the mode of transport [30–32]:

   i.   Perikinetic flocculation:

      Flocculation is controlled predominantly by the random thermal motion of particles known as Brownian motion [2,30,32]. This process is limited to particles with a diameter less than 0.1 µm [2,32] and completes within a few seconds. Figure 2.5 shows a schematic of the perikinetic flocculation.

Perikinetic flocculation is out of scope for this project, as the focus here is on water-in-oil emulsions with droplet diameters in the range of 10 µm.
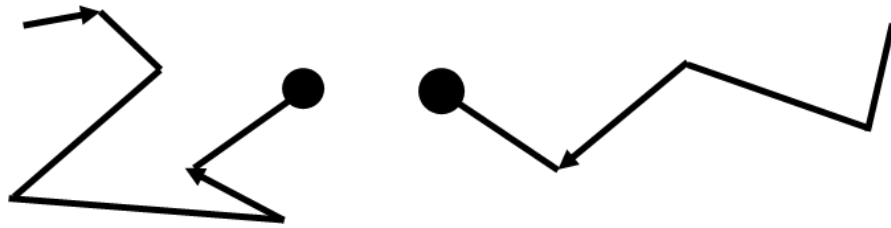
Figure 2.5 Schematic representation of perikinetic flocculation.

ii.   Orthokinetic flocculation:

In orthokinetic flocculation, floc formation results from the induced velocity gradient in the fluid either due to fluid flow or mechanical mixing [2,30–32], as shown in Figure 2.6. The induced velocity gradient or shear rate forces droplets/particles to come in contact with each other, thus increasing the number of collisions in a given time and promoting floc formation [28–31].
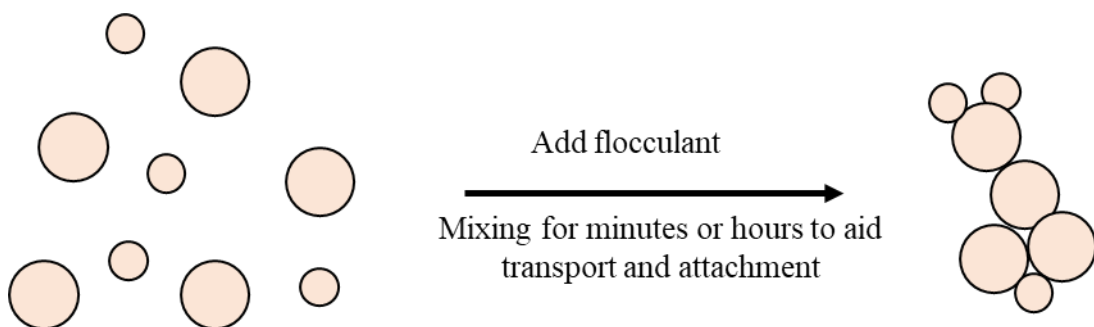
Figure 2.6 Schematic representation of orthokinetic flocculation.

In laminar shear, the rate of orthokinetic flocculation between droplets/particles of size i and j is described mathematically [30,32,33] by:

$$r_{orthokinetic} = \frac{1}{6}\left(\frac{du}{dy}\right)\left(d_i + d_j\right)^3 * \alpha * n_i * n_j \qquad 2.3$$

where (du/dy) is velocity gradient or shear rate, di and dj are the diameters of colliding droplets/particles i and j, respectively, α is the collision efficiency, n_i is the concentration of ith droplets /particles, and n_j is the concentration j^{th} droplets/particles.

Equation 2.3 accounts only for the floc formation and suggests that as the shear rate increases, floc formation increases. However, flocs do not keep growing for a given shear but as the shear rate increases, the flocs become more prone to breakage and erosion. Thus, at shear rates beyond some limiting values, the final floc diameter should decrease with increasing shear rate [33,34].

iii.   Sweep flocculation:

Floc formation resulting from the collision due to differences in the terminal settling velocities of flocs/particles/droplets is known as sweep flocculation [30]. The rate of sweep flocculation can be defined as [28]:

$$r_{Differential\ Settling} = \frac{\pi g\ (\rho_p - \rho_l)*(d_i - d_j)*(d_i + d_j)^3 *\alpha*\ n_i*n_j}{72\mu_l} \qquad 2.4$$

where ρ_p is the droplet/particle density, ρ_l is the fluid density, μ_l is the fluid viscosity, and d_i, d_j are the diameters of the colliding droplets/particles i and j, respectively.

The probability of collision of flocs/ droplets/particles with the same terminal velocity is low, as demonstrated through Equation 2.4. This flocculation mechanism can be predominant in systems with broader size distributions [30].

The floc growth in sweep flocculation is due to the sweeping of small flocs/droplet/particle by larger floc/droplets/particles while settling [34], as shown in Figure 2.7 and Figure 2.8.
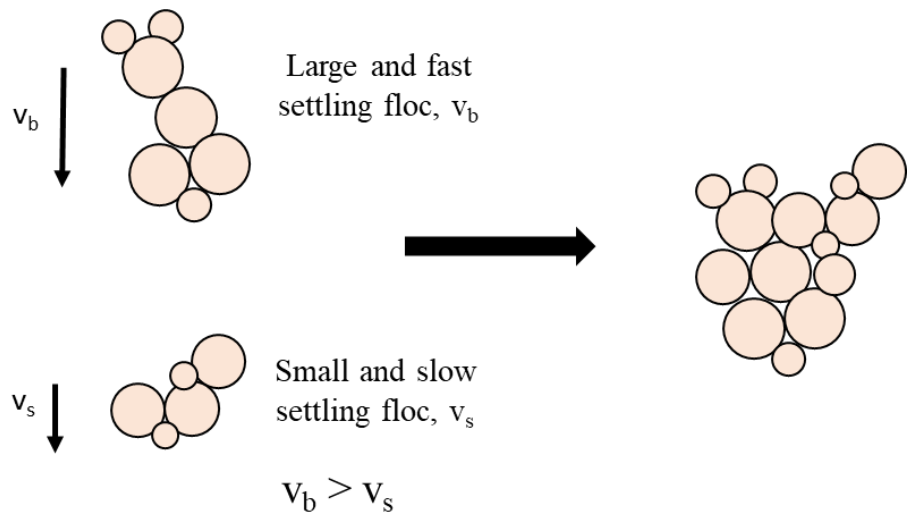
Figure 2.7 Schematic representation of floc formation due to sweep flocculation. The larger is sweeping the smaller floc.
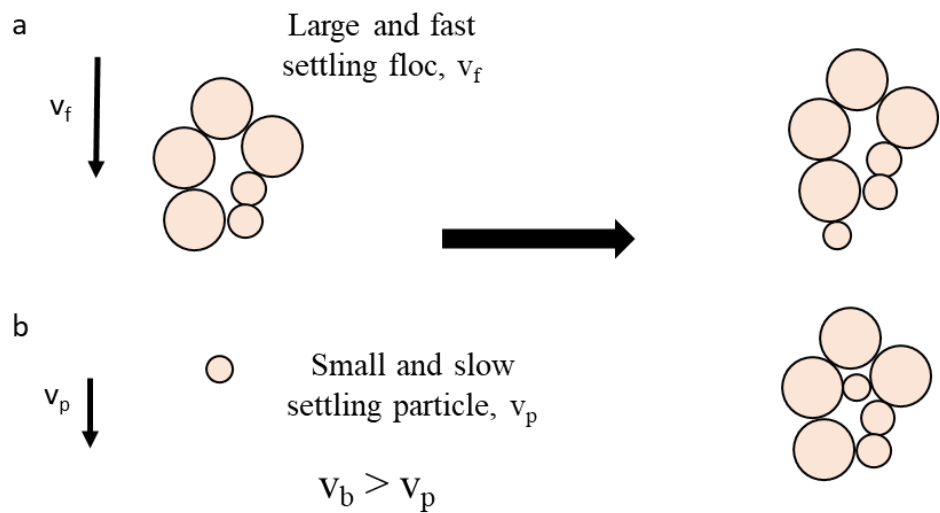
Figure 2.8 Schematic representation of floc formation due to sweep flocculation. The larger floc sweeps the smaller droplet/particle. (a) Droplet/particle attaching to the floc surface. (b) Droplet/particle falling inside the floc cavity.

When a larger floc sweeps the smaller droplet/particle, it can either stick to the floc surface or can fall inside the cavity [34], as shown in Figure 2.8. Sweep flocculation induces faster removal of smaller droplets/particles that otherwise would take a long time to settle or remove.

The settling velocities of droplets/particles play a vital role in sweep flocculation. There are several types of settling based on droplet/particle concentration and morphology:

i. Discrete settling

ii. Flocculant settling

iii. Hindered settling

iv. Compression settling

Discrete and flocculant settling are defined for dilute systems, while hindered and compression settling are observed in the concentrated system. Flocculant settling is similar to sweep flocculation, which was described above.

In discrete settling, droplets/particles do not interfere with each other [2]. The most straightforward settling equation is derived based on the assumptions of Newtonian fluid, rigid spherical particles, no wall effects and for a particle settling in Stokes' regime [2], is described by:

$$v_{p\infty} = \frac{g * d^2 * (\rho_p - \rho_l)}{18 * \mu_l} \qquad\qquad 2.5$$

where $v_{p\infty}$ is the settling velocity of a single particle/droplet, d is the diameter of the droplet/particle, ρ_p is the droplet/particle density, ρ_l is the fluid density, and μ_l is the fluid viscosity.

2.4.2   Chemical Demulsification

In the chemical demulsification process, chemicals known as demulsifiers are added to the emulsion. The addition of a demulsifier may promote coalescence of water droplets by weakening the rigid film or induce flocculation of the water droplets by connecting emulsified droplets, or both

may occur [2,5,6]. Coalescence or flocculation can be rate controlling in demulsification[6]. The flocculation/coalescence helps droplets grow, increase their settling velocities, and improve the efficiency of the separation process.

The literature from the early 20th century, i.e., before 1939, suggests using simple organic salts as demulsifiers while the present-day demulsifiers are surface-active polymers or polymer mixtures [2]. The most common classification of demulsifiers is done based on their molecular weight. Polymers/ blends of polymers with molecular weight less than 3000 Da promote coalescence of water droplets [5,35]. They are known as water droppers [35] and are responsible for removing large fractions of water from bitumen [6].

Polymers with a molecular weight greater than 10,000 Da act as flocculants. They effectively remove the emulsified and widely distributed water droplets but act slowly compared to coalescence-inducing demulsifiers [4,5]. These polymers are integrated into the gaps between the droplets, allowing them to form three-dimensional structures known as flocs [5]. The other essential characteristics of flocculants are their highly branched structure [5,36], strong affinity towards water droplets [5], and solubility in both oil and water phases [37].

Studies have been carried out to develop a scientific way of selecting a demulsifier by linking its properties with its performance or crude oil properties. Berger et al. [36] tried to relate the properties of around 2400 crude oil samples. However, they could not find any relation between demulsifier properties, crude oil properties, and demulsifier performance [36]. Wu et al. [38] tried to link the molecular weight of around 52 demulsifiers with their performance in dewatering water-in bitumen emulsion. They observed that increasing the molecular weight enhances the dewatering performance of the demulsifier [38]. A similar trend was observed by both Kailey et al. and Chen et al. [39,40]; the increase in molecular weight of the polymer increases its tendency to flocculate droplets, which enhanced the dewatering performance [39,40]. However, Shetty et al. observed that

the performance of the demulsifier decreases with increasing molecular weight [41]. Industries often use a blend of polymers as a very site-specific demulsifier, and its composition is unavailable in the public domain.

It can be concluded that there is no reliable methodology developed to date to select demulsifiers. The selection of the suitable demulsifier is typically based on the trial-and-error method carried out in a simple lab-scale bottle or jar test.

2.5   Bottle or Jar Test

The bottle test or jar test is commonly used to screen demulsifiers in the laboratory. The test involves adding a different demulsifier at a specific concentration to emulsion samples placed in several bottles [2,4–6,15]. The emulsion samples are mixed to disperse the demulsifier and left undisturbed in the bottle to observe the phase separation over time. Demulsifier selection depends on the percentage of water separated during a given period. Once the screening process is complete, additional bottle tests are performed to determine the optimal concentration of the demulsifier [2]. The selected demulsifier at different concentrations is added to the emulsion samples in several bottles, and phase separation is observed over time. The concentration at which maximum phase separation occurs is considered optimal.

These tests guide the design and selection of operating conditions for separating equipment such as the IPS [2,4–6,15]. However, the tests are performed at static conditions and fail to account for shear/flow experienced in the field [2,4–6,15]. The flow/shear rate conditions experienced in the field can help enhance the flocculation/coalescence of the dispersed phase, which can lead to faster phase separation [19–21]. Hence, neglecting the effect of shear conditions in bottle tests can significantly impact the estimation of operating conditions such as optimal demulsifier dosage for separating equipment [2].

2.6 Replicating industrial conditions

In the context of the NFT process, the demulsifier is mixed with naphtha–diluted bitumen by injecting it in the pipeline feeding to the IPS. Several studies have been conducted to design a lab-scale device to replicate the pipeline conditions for mixing demulsifiers. Machado et al. developed a Confined Impeller Stirred Tank (CIST) that provides the turbulent mixing conditions experienced in the pipeline during demulsifier injection [18]. Laplante et al.[42] conducted experiments in CIST to study demulsifier performance at different mixing conditions in diluted bitumen. It was observed that favourable mixing conditions could enhance the demulsifier performance and reduce the optimal demulsifier dosage by 50 % [42]. Arora followed the experiment protocol of Laplante et al. to determine the dominant settling mechanism in bitumen froth and the effect of mixing conditions on the dominant settling mechanism [28]. It was observed that the dominant settling mechanism for water droplets and solids in diluted bitumen is sweep flocculation. Mixing conditions did not change the dominant mechanism, but favourable mixing conditions accelerated floc growth and improved water and solid removal [28].

Overall, to the author's best knowledge, there is a lack of literature on developing a lab-scale shearing device imitating the laminar shear rate experienced in the IPS. Additionally, the effect of laminar shear rate on the settling mechanism has not been investigated.

2.7 Lab shearing devices

Many devices such as mixing tanks, paddle mixers, Couette cells, and oscillating grids have been employed to study the flocculation of particle suspensions and emulsions [19–21,43–46]. These devices generate mostly turbulent and non – homogenous conditions [43]. In tanks and mixers, the fluid in regions closer to impellers experience high shear rates, leading to floc breakage [43].

Serra et al.[43] performed a study to compare the aggregation/flocculation of latex particles in water over the same range of shear rate using three different devices (paddle mixer, oscillating grids, Couette cell). The maximum floc size for a fixed shear rate value was observed for the Couette cell compared to the paddle mixer and oscillating grids [43]. Therefore, Couette cells, as shown in Figure 2.9, are the best choice for floc formation studies as they provide conditions where flocs are less susceptible to breakage.
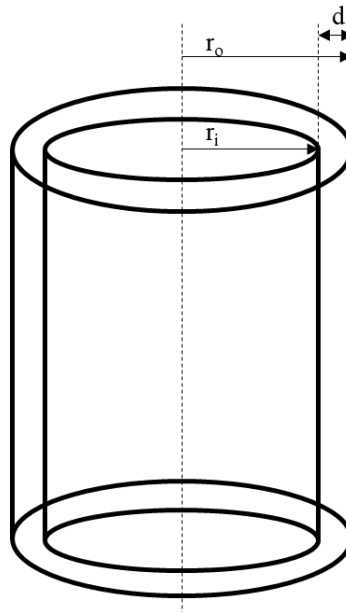
Figure 2.9 Schematic of the Couette cell.

A Couette cell consists of two concentric cylinders; either one can be rotating. The Couette cell will have a shear profile similar to parallel plates when the ratio of the gap between the cylinders to the outer cylinder radius ratio) is less than 0.05 [47]. This is because the curvature in the shear rate profile can be neglected at such a small ratio (gap to outer cylinder radius) [47], as shown in Figure 2.10. Therefore, a Couette cell with a gap to outer radius ratio less than 0.05 is suitable for imitating the shear rate experienced across the parallel plates in an IPS unit.
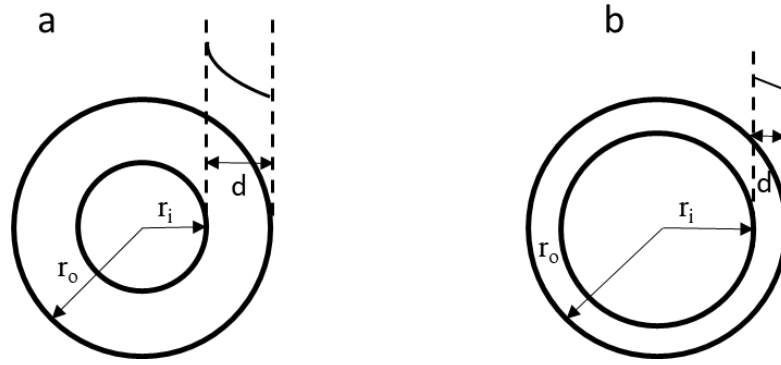
Figure 2.10 The shear rate profile across the gap in a Couette cell for (a) d/r_o > 0.05 (b) d/r_o < 0.05.

2.8   Shear-induced flocculation /coalescence

In the past, no studies have been conducted to understand the effect of laminar shear on coalescence/flocculation of water-in-oil emulsions. Several studies were conducted to understand the effect of laminar shear conditions on coalescence/flocculation in oil-in-water emulsions and suspensions. For example, Rahmani et al. [46] studied the impact of laminar shear rate on the flocculation of asphaltenes in heptane-diluted bitumen. It was observed that the floc size distribution shifted towards the smaller diameters at higher shear rates due to floc breakage [48]. Meenakshi et al. [21] studied the effect of shear on the coalescence of the dispersed phase in neutrally buoyant surfactant stabilized oil-in-water emulsions. The emulsion had an initial volume mean diameter (d_{43}) of 4µm, where d_{43} is defined as:

$$d_{43} = \frac{\sum n_i * d^4_i}{\sum n_i * d^3_i}$$

2.6

where, n_i is the number of ith particles, and d_i is the diameter of the ith particle.

The emulsion was sheared in the inner cylinder rotating Couette cell over a shear rate range 10 - 20s[1]. It was observed that the average volume mean diameter of the emulsion increases with increasing shear rates, as the momentum of colliding droplets increases [21]. In a study by Mishra

et al. [49], the effect of shear rate on coalescence was studied for oil-in-water emulsions with a volume mean diameter in the range of 5 - 7 µm over a shear rate range of 55-213 s^{-1} [49].

A similar observation was made: the coalescence rate increases with shear rate, and the maximum coalescence rate was observed for 213 s^{-1}. Furthermore, Schokker et al. [19] studied the effect of shear rate on flocculation for an oil-in-water emulsion in a Couette Cell [19]. It was pointed out that the volume-weighted mean diameter of emulsion experiencing shear is greater than the emulsion at quiescent conditions due to increased droplet collisions [19].

In contrast, Nandi et al. [18] noticed some exciting results for an oil-in-water emulsion with an initial volume-weighted mean diameter of around 8 µm [20]. The emulsion was sheared in a Couette cell over a shear rate range 10.8-43 s^{-1}[20]. They observed that the coalescence rate decreases with increasing shear rate, and the maximum value was achieved at the lowest shear rate.

It can be concluded that applying a laminar shear can increase the flocculation rate or coalescence rate in an oil-in-water emulsion or particulate suspension. Additionally, the aforementioned studies did not provide microphotographs to confirm coalescence in oil-in-water emulsions [17–19], or flocculation of asphaltenes in heptane-diluted bitumen [48].

The literature primarily discusses the effect of laminar shear on the coalescence of oil droplets in oil-in-water emulsions and flocculation in particulate suspensions. There is a dearth of literature on the effect of laminar shear rate on the flocculation of water droplets in a water-in-oil emulsion.

2.9   Scope of the project

The literature review presented above highlights the connection between laminar shear and coalescence/flocculation rate in oil-in-water emulsions and suspensions. The rate of coalescence/ flocculation increases as the laminar shear rate is applied but only up to a particular shear rate value; beyond that, floc breakage occurs. The details of IPS unit, where laminar shear rate conditions are

experienced in froth treatment, and the laboratory scale bottle or jar test used as a guide to the design and selection of operating conditions for the IPS were discussed. The Couette cell has been shown to be capable of emulating the shear rate experienced between the parallel plates of an IPS.

Moreover, this review highlights a few shortcomings in the existing literature where further exploration is required:

- The bottle or jar tests used as a guide to design separating equipment (IPS) do not account for the flow/shear experienced in the field. It is true that some work has been done to design a laboratory-scale device that replicates the demulsifier mixing conditions in the pipelines feeding an IPS; however, no work has been done to design a laboratory-scale device replicating the shear rate conditions experienced in the plates of the IPS.
- There has been insufficient focus on understanding the effect of laminar shear rate on the water-in-oil emulsion and further understanding of flocs settling is needed.

The work on understanding the effect of shear on flocculation in water-in-oil emulsion projects can play a crucial role in modifying the current bottle or jar test. An improved bottle test that incorporates shear can help to determine the optimal operating conditions for an IPS unit in the NFT process.

Thus, the objectives of this project are:

- To identify the shear rate range for floc formation and floc breakage in a water-in-light mineral oil emulsion.
- To understand the settling of flocs formed and establish that sweep flocculation is a dominant settling mechanism for faster settling of water flocs/droplets.
- To confirm the formation of flocs in water-in-light mineral oil emulsion by providing microphotographs.

Chapter 3 : Experiments

3.1   Introduction

The purpose in this project is to investigate the effect of shear rate on water droplet flocculation and subsequent settling. The experimental procedure consists of three different steps. A flow chart shown in Figure 3.1 depicts the experimental procedure. The first step involves preparing a water-in-light mineral oil emulsion with a desired mean droplet size. The second step is the addition of flocculant to the emulsion, and the final step is shearing the emulsion in the Couette cell at different shear rates.

Sections 3.2 and 3.3 provide details of the materials and equipment used in the experiments. All the procedures such as emulsion preparation, shearing the emulsion in Couette Cell, microscopy, and image analysis are discussed in detail in Section 3.4, and Safe Work Procedures (SWPs) are provided in Appendix B.
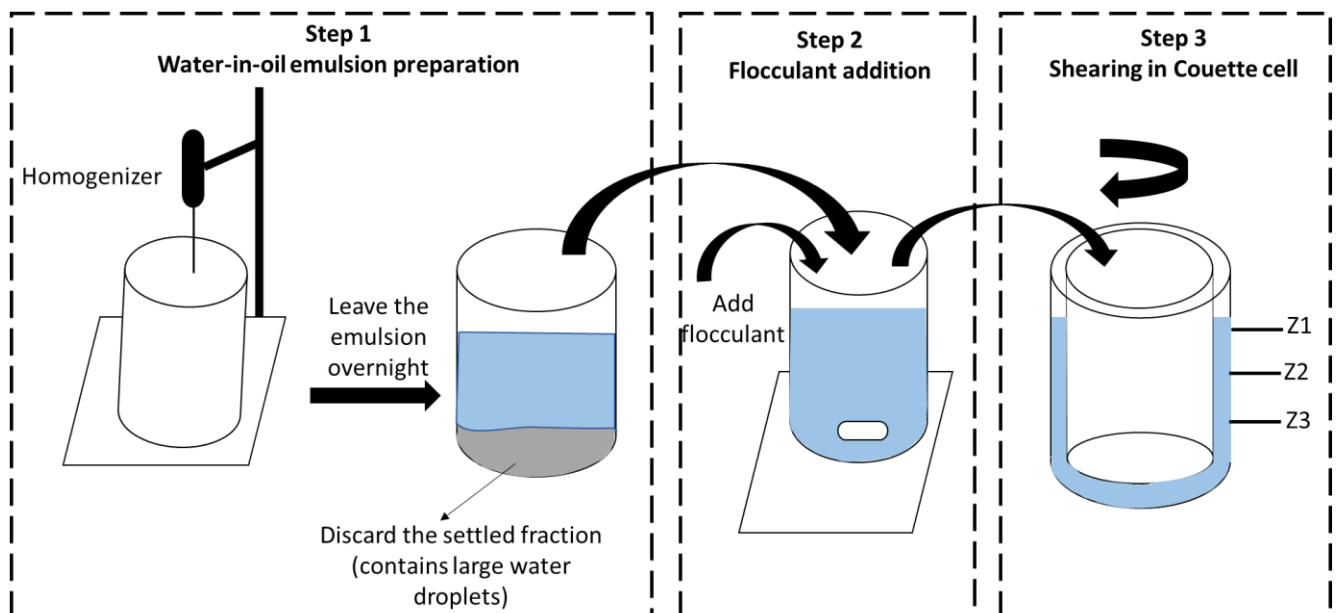
Figure 3.1 An overview of the experimental procedure.

3.2   Materials

This section provides a detailed description of the materials used in each step of the experimental procedure.

3.2.1 Mineral oil

This project uses water-in-light mineral oil emulsions as analogs to the water-in bitumen emulsion. Hence, selecting an oil with properties comparable to diluted bitumen (Density – 860 kg/m^3 and kinematic viscosity – 6.1 mm^2/s at 80 °C) is essential [28]. The light mineral oil with a density of 846 kg/m^3 at room temperature and kinematic viscosity 15 mm^2/s at 40°C from Sigma Aldrich was used for the emulsion preparation. The maximum droplet size of the dispersed phase is a function of continuous phase density [50], as explained:

$$d_{max} = \Pi^{-2/5} * \sigma^{3/5} * \rho_c^{-1/3}$$ 3. 1

where Π is the power per unit volume, σ is the surface tension and ρ_c is continuous phase density.

Therefore, an oil with a density similar to diluted viscosity was selected to have similar water droplet size distribution. The dynamic viscosity of the mineral oil at room temperature, measured using a viscometer, is 28.3 mPa.s (kinematic viscosity 33.3 mm^2/s). The viscosity of the light mineral oil is of the same order of magnitude as diluted bitumen. However, the light mineral oil viscosity is around 5 times greater than that of diluted bitumen; this higher viscosity will slow the gravity settling and provide a larger time window for settling experiments. Furthermore, this increased viscosity of light mineral oil will also slow the coalescence of the water droplets by increasing the droplet rupture/drainage time. Thus, helping to stabilize the water-in-light mineral against coalescence [50].

3.2.2 Surfactant

Emulsions are kinetically unstable systems and separate into two phases over time to reduce interfacial energy [5]. Surfactants are required to stabilize the dispersed phase against coalescence and eventual phase separation, as discussed in Section 2.2. For these tests, SPAN 80 (Sigma Aldrich) was selected because it has similar surface activity as asphaltenes, which are primarily responsible for the stability of water-in-bitumen emulsion [51]. The Hydrophilic Lipophilic Balance (HLB) of SPAN 80 is around 4.3, which is ideal to prepare a water-in-oil emulsion [2]. Moreover, SPAN 80 has been used in past to prepare water-in-oil emulsions [51], and has provided stability against coalescence of water droplets.

3.2.3 Deionized water

Deionized water from Millipore Elix Advantage 5 was used to prepare water-in-light mineral oil emulsions. This unit is available in the Pipeline Transport Processes (PTP) laboratory.

3.2.4 Flocculant

The scope of the project is limited to the flocculation of water droplets, i.e., the focus is on the droplet flocculation and not coalescence. Therefore, polymers with a molecular weight greater than 10,000 Da and a highly branched structure, as discussed in Section 2.4.2, are an appropriate choice for this study.

There is limited ability to select flocculants a priori, as their use and effectiveness is highly case-specific. Here, highly branched Polyethyleneimine (PEI) with molecular weight 70,000 Da from Polysciences is used as a flocculant. Due to its high molecular weight and branched structure, it performs more slowly than commercially available demulsifiers, which is advantageous for the project. The slower performance will delay flocculation-induced coalescence and provide a sufficient time window to study the effect of shear on the flocculation of water droplets.

3.3   Equipment

3.3.1 Homogenizer

The emulsions were prepared using VWR 250 homogenizer with a saw tooth probe having dimensions 11.5 x 1 cm. It is a high-speed dispersing device with a speed range of 10,000 - 30,000 RPM used to homogenize, emulsify, and mix liquid/liquid dispersions [52].

3.3.2 Microscope

Microphotographs presented in this thesis were taken using a QICAM FAST Color 12-bit camera mounted on an AXIOSKOP – 40 optical microscope. The microphotographs were captured in Step-1 and Step -3 of the experimental procedures. A 20x objective lens was used to view the emulsion droplets and to capture all the microphotographs. The resolution of the microphotographs is 1376 x 1024 pixels.

3.3.3 Couette cell

The effect of shear rate on the flocculation of water droplets was studied using a custom-built Couette cell.

The apparatus consists of a solid inner (rotating) cylinder of radius 68.43 mm and a hollow outer shell with a radius of 71.43 mm, thereby ensuring a gap of 3 mm. The inner cylinder and outer cylinder are made from Teflon and transparent Acrylic, respectively. The gap to outer cylinder radius ratio is less than 0.05 to generate a constant shear rate in the annular region. The length to the gap ratio is greater than 20 to avoid longitudinal instabilities and end effects [53]. The total volume of the Couette cell is approximately 176 cm^3. The outer cylinder has three equidistant sampling ports, Z1, Z2, and Z3, as shown in Figure 3.2 and Figure 3.3. The distance between each port is 35 mm, which is identical to the spacing of plates of a standard Inclined Plate Settler.

Figure 3.2 The Couette cell used in this research project.
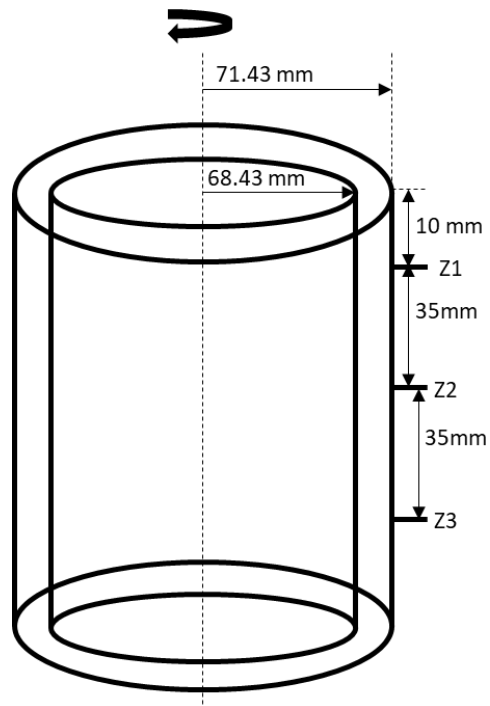
Figure 3.3 Drawing of the Couette cell used in the project.

The inner cylinder is connected to a DC motor and set of gears with a high reduction ratio to achieve the maximum operating speed of 20 RPM. The shear rate range for the experiments was decided based on the shear rate experienced between the parallel plates in the IPS (Appendix A). The Couette cell can produce a maximum shear rate of around $50s^{-1}$. The rotating speed of the inner cylinder corresponding to the average shear rate value was determined by:

$$G = \frac{2*\omega*R_i*R_o}{(R_o^2 - R_i^2)} \qquad\qquad 3.2$$

where G is the average shear rate, ω is the angular speed, R_i is the radius of the inner cylinder, and R_o is the radius of the outer cylinder. All experiments were conducted in laminar shear flow conditions as the Taylor number (around 2) is less than the critical Taylor number of 41 [53].

The mathematical expression to calculate Taylor number is given by:

$$Ta = \frac{\rho_l*\omega*(R_o - R_i)^{\frac{3}{2}}*(R_i)^{1/2}}{\mu_l} \qquad\qquad 3.3$$

where Ta is Taylor number, ρ_l is the density of the fluid, ω is the angular speed, R_i is the radius of the inner cylinder, R_o is the radius of the outer cylinder, and μ_l is the viscosity of the fluid.

3.4   Procedures

All the steps of experimental procedure were performed at room temperature (~20˚C).

3.4.1 Emulsion preparation

A number of 200 ml batches of 7 vol % analog emulsion (water-in-light mineral oil) were prepared with the high-speed homogenizer. The preparation of emulsion involves the following steps:

1. Place a 250 mL beaker, pipette, graduated cylinder, a bottle of light mineral oil, and surfactant inside the fume hood.

2. Measure the desired amount of light mineral oil (186 mL) with the graduated cylinder and pour it into the 250 mL beaker.

3. Use a separate graduated cylinder to measure the desired amount of de-ionized water (14mL) and pour it into a 20 mL glass vial.

4. Measure the amount of the surfactant SPAN 80 (147 µL, which is 3.2 times its CMC value) using a graduated pipette. The CMC value for SPAN 80 is 0.025 wt./v % (weight of surfactant by total volume) [51].

5. Add the surfactant to the light mineral oil in the beaker and gently stir it with a glass rod.

6. Cover the beaker containing the light mineral oil and surfactant with parafilm.

7. Bring the beaker, glass vial with deionized water, and 3-mL plastic pipette to the homogenizer that was located in another lab.

8. Place the beaker (containing the light mineral oil) on a jack under the homogenizer; then slowly raise the jack such that the probe tip is entirely inside the mixture.

9. Plug in the homogenizer and set its rotating speed to 22000 RPM. This speed was decided after performing certain trial to obtain the emulsion with desired droplet size range.

10. Turn on the homogenizer and mix the light mineral oil and surfactant mixture for 1 minute.

11. After mixing for 1 minute, using the plastic pipette, add the deionized water in dropwise fashion to the mixture while continuing to mix. This step should take 4 minutes.

12. Leave the mixture to homogenize for another 5 minutes. This additional shearing time will generate smaller water droplets and improve aqueous phase dispersion.

13. Turn off the homogenizer after the shearing period is complete and carefully lower the jack to remove the beaker containing the prepared water-in-light mineral oil emulsion.

14. Overnight leave the prepared 7 vol % water-in-light mineral oil emulsion undisturbed.

15. Collect the supernatant the next day in a 400 mL beaker and safely discard the settled component that contains large water droplets.

The overall emulsion preparation time is thus 10 minutes: 1 minute of surfactant mixing, 4 minutes of water addition, and another 5 minutes for homogenization. Samples were taken from the top and bottom of the supernatant when it was first collected and again after 4 hours, using a plastic pipette. The emulsion was shaken gently before withdrawing each sample to attempt to ensure homogeneity and to break any flocs that might have formed. The samples were collected to determine the droplet size and emulsion stability using microscopy.

The water-in-light mineral oil emulsion with small water droplets recovered (supernatant) is used in the next steps of the experimental procedure as shown in Figure 3.1.

3.4.2 Flocculant addition

Step - 2 of the experimental setup, as shown in Figure 3.1, involves the addition of flocculant to the recovered water-in-light mineral oil emulsion through the following steps:

1. Place the 400 ml beaker with water-in-light mineral oil emulsion on the magnetic stirrer and carefully drop the magnetic stir bar into the beaker.
2. Measure the specified amount of flocculant solution PEI (272μL) using a 1 mL syringe.
3. Plug in the magnetic stirrer and set the speed to 1500 RPM.
4. Turn on the magnetic stirrer and start adding dropwise the flocculant PEI solution to the emulsion.
5. Turn off the magnetic stirrer after 5 minutes of mixing.

3.4.3 Shearing in Couette cell

In the final step, Step – 3 of the experimental setup, the emulsion flocculant mixture is sheared in the Couette cell following these steps:

1. Fill the Couette cell with emulsion flocculant mixture until the Z1 sampling port is covered (see Figure 3.2).

2. Plug in the Couette cell motor and set the desired rotating speed.

3. Turn on the Couette cell and shear the emulsion flocculant mixture for 15 minutes. The shearing time was selected based on the residence time of the commercial IPS unit, which is around 10-20 minutes.

4. After 15 minutes, turn off the Couette cell and allow the emulsion flocculant mixture to settle for one hour.

5. Every 20 minutes, collect the samples in glass vials from the Z2 sampling port using a silanized needle attached to the 10 mL.

During the one hour of settling, a total of four 1-millimeter samples were collected in the glass vial, and microscopy was performed on the collected samples.

The needle used to collect the samples and microscope slides used in microscopy were silanized to make them hydrophobic so that water droplets did attach to the surface and undergo coalescence. A detailed procedure to silanize the needles and microscope slides is provided in Appendix B.

3.4.4 Microscopy

The water droplet size measurements of Step - 1 and floc size determination of Step - 3 were achieved using microphotographs of the corresponding samples captured using microscopy. The following steps were carried out for the microscopy work:

1. Put a drop of the emulsion sample on a salinized microscope slide using a plastic pipette.

2. Cover the emulsion sample on the microscope slide gently using an unsilanized coverslip. Allow the emulsion sample to expand in the gap between the slide and coverslip.

3. Place the prepared microscope slide on the microscope bench.

4. Turn on the microscope and camera mounted on it and set it to dark field operation.

5. Capture the microphotographs with a 20x objective lens at different positions by sweeping the microscope across the slide. Take around 90 – 150 images per sample for emulsion samples collected in Step-1 of the experimental procedure and around 90 – 100 microphotographs per sample for the collected samples in Step-3 of the experimental setup.

The Safe Work Procedure (SWP) in Appendix B has more details of the microscopy procedure.

3.4.5 Analysis

Two MATLAB scripts were used to analyze the microphotographs captured in Step-1 and Step-3 of the experimental procedure. The scripts are provided in Appendix C.

The microphotographs captured in Step-1 to determine the water droplet size and emulsion stability against coalescence were analyzed with MATLAB Script-1. This script detects the droplets as hollow objects and encircles the edges of the droplets, as shown in Figure 3.4. The diameter values corresponding to the encircled droplets were used to obtain the droplet size distributions. Figure 3.4 is just a representation of how the script detects droplets; the diameter range should be adjusted based on trial and error to include all the droplets present, except for the blurred droplets present in flocs. Around 10 000 droplets per sample were considered to plot the droplet size distribution.
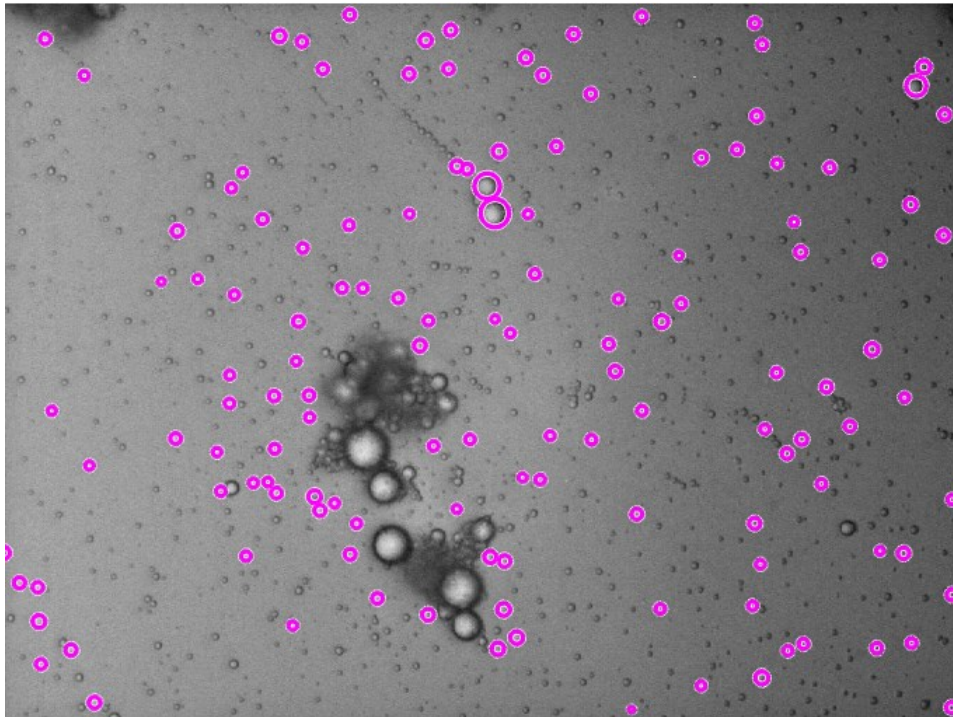
Figure 3.4 Representative processed image of the water-in-light mineral oil emulsion sample

MATLAB Script-2 was used to obtain floc size distributions from the microphotographs captured in Step-3 of the experimental procedure. The first script converts the colored image into a grayscale image. Thresholding was then done on the greyscale image to identify white-colored aggregates from the black background. The sensitivity parameter in the thresholding was set to 0.68 based on trial and error to ensure that all the flocs present in microphotographs could be detected. The script calculates the area-based diameter of the flocs. All the connected flocs, out-of-focus flocs, and single droplets were manually removed from the microphotographs to eliminate these from the subsequent analysis of flocs, as shown in Figure 3.5 and Figure 3.6. From the total microphotographs collected for each sample around 350 – 2500 flocs were considered to plot the floc size distribution.

Figure 3.5 Processing of a sample microphotograph collected in Step – 3 (for a 5 RPM run)

(a) Original image. (b) Processed image.

Figure 3.6 Processing of a sample microphotograph collected in Step – 3 (for a 5 RPM run)
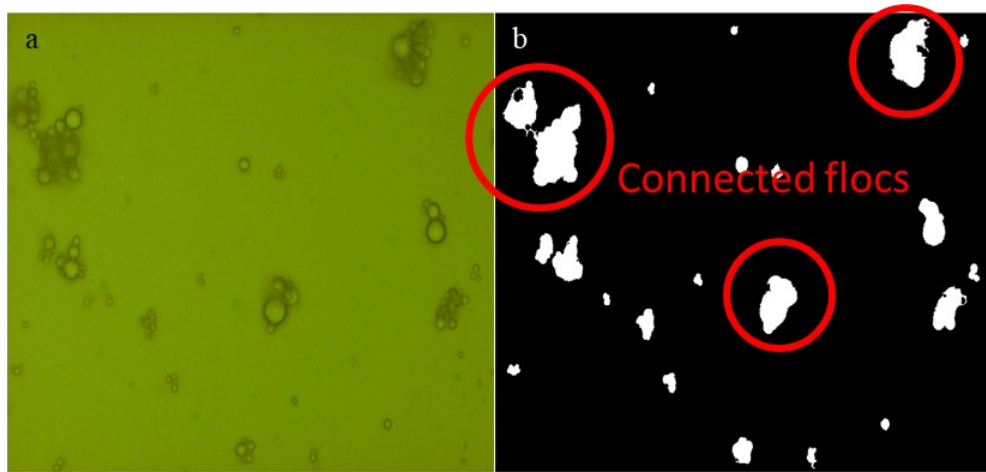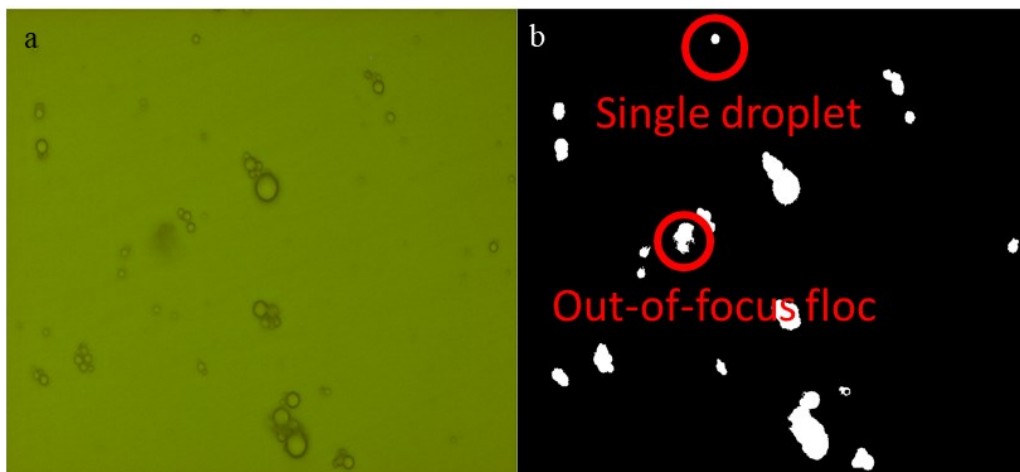
(a) Original image. (b) Processed image.

Chapter 4 : Results and Analysis

4.1   Introduction

The chapter discusses the test results obtained during this research, which indicate the effect of shear on the flocculation of water droplets and the subsequent settling of flocs. The results and analysis have been divided into five sections, including the present section. Section 4.2 discusses the results related to the formulation of stable water droplets in light mineral oil corresponding to Step -1 of the experimental setup (Refer to Figure 3.1). Sections 4.3 and 4.4 interpret the experiments performed in Step - 3 of the experimental setup. In Step -3 of the experimental setup, the emulsion was sheared for 15 minutes and allowed to settle for another 60 minutes in the Couette cell. Section 4.3 discusses the effect of different shear rates on the flocculation of water droplets to establish a connection between shear rate and orthokinetic flocculation. Section 4.4 investigates the effect of shear rate on the settling of water flocs formed by orthokinetic flocculation. Different analysis approaches have been used to justify sweep flocculation as the primary mechanism responsible for settling water droplets and flocs. Section 4.5 provides the details of the methodology used to determine the repeatability of the experiments performed at different shear rates and summarizes the results.

4.2   Preparation of water-in-light mineral oil emulsions:

The first step towards fulfilling the project objective is the formulation of a water-in-oil emulsion with a similar mean diameter as the more stable (small droplet) water-in bitumen emulsions found in the naphthenic froth treatment process. A 7 vol% water-in-light mineral oil emulsion was prepared following the procedure described in Chapter-3. The emulsion was left undisturbed for roughly 21 hours after preparation to allow larger droplets to settle. After 21 hours, the supernatant (emulsion containing small droplets) was recovered and transferred to another beaker.

Samples were collected from the top and bottom of the beaker immediately after recovering the supernatant (t = 0 hours) and after 4 hours (t = 4 hours). Microphotographs of the samples were acquired using the camera and microscope setup described in the previous chapter. Around 100 – 150 images per sample were taken. Figure 4.1 shows representative (typical) microphotographs of the water-in-light mineral oil samples withdrawn from the beaker bottom and top at t = 0 and t = 4 hours, respectively.
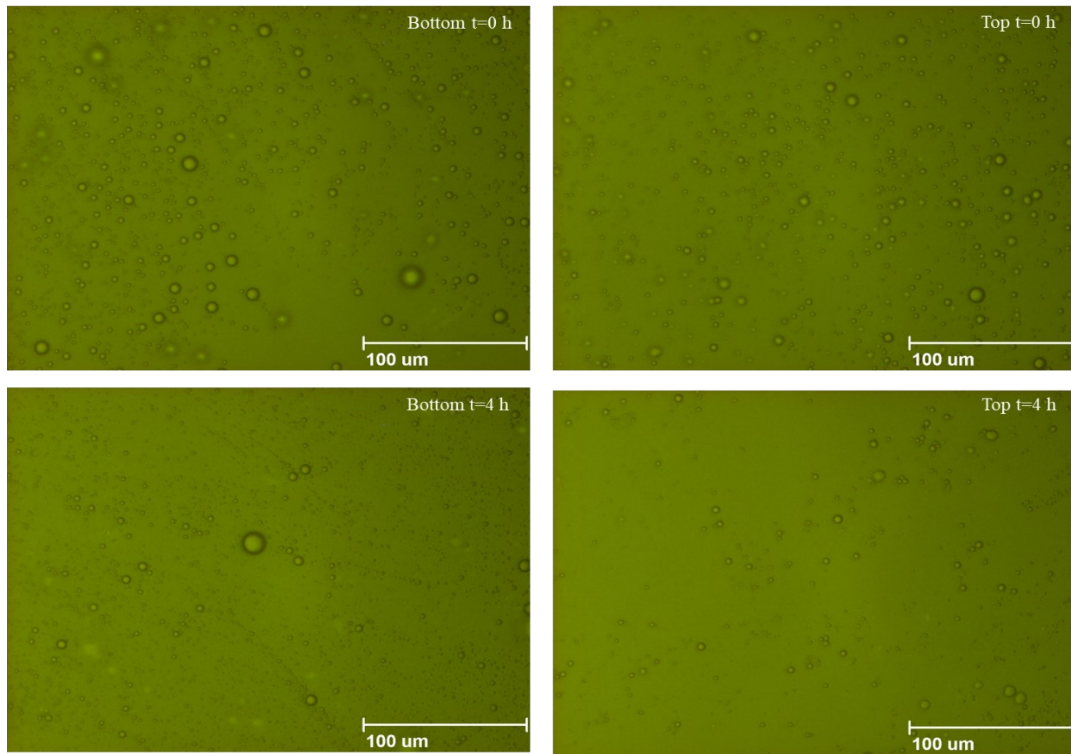
Figure 4.1 Representative microphotographs of the small droplet water-in-light mineral oil emulsion samples withdrawn from the bottom and top of the beaker at t = 0 h and t = 4h.

As qualitatively observed in the microphotographs displayed in Figure 4.1, there is no immediately appreciable difference in the droplet diameters for samples collected from the bottom and top of the beaker at t = 0 and t = 4 hours. There are no larger droplet present in the microphotographs of samples collected after 4 hours, implying that the droplet size did not significantly grow. These observations suggest that the emulsion can withstand coalescence for four hours once the largest droplets have been removed.

As part of a more quantitative analysis of droplet stability, the droplet sizes were extracted from the microphotographs to plot the volume-based distribution using the MATLAB script-1 (see Appendix C). The volume-based droplet size distribution (DSD) of the samples obtained from the bottom and top of the beaker at time t = 0 h and t = 4 h are shown in Figure 4.2. The abscissa represents the droplet diameter, and the ordinate denotes the volume-based differential frequency. The volume-

based differential frequency is defined as the ratio of the volume fraction of a bin to its respective

bin size.
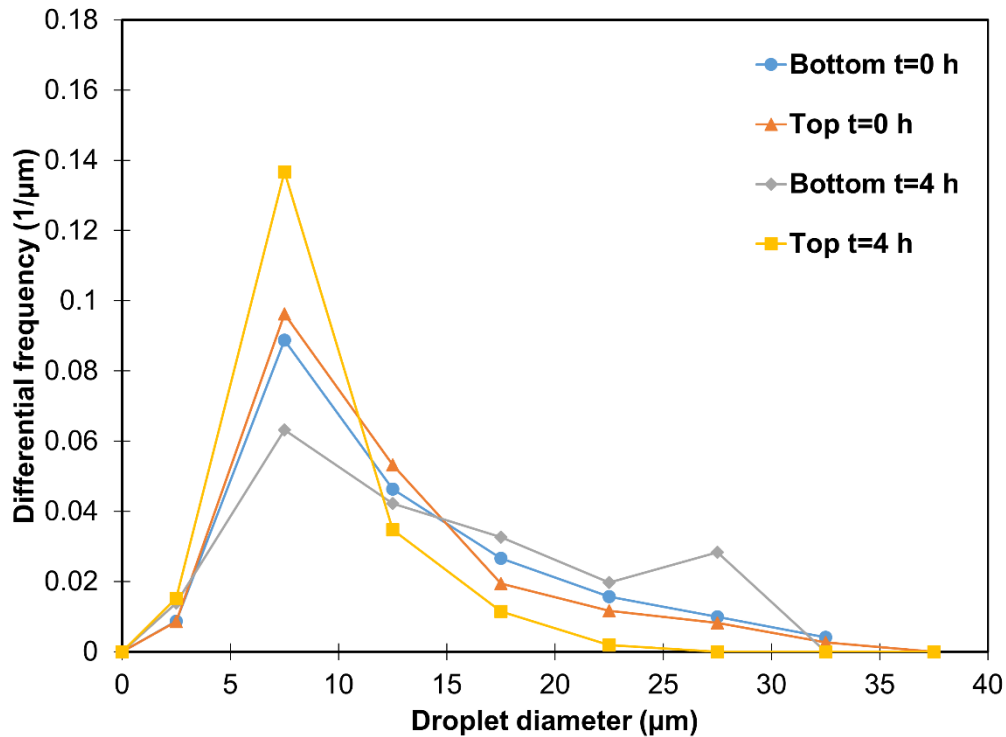
Figure 4.2 Time evolution volume base droplet size distribution of emulsion samples withdrawn from bottom and top of the beaker.

The DSDs of the emulsion samples (collected from the bottom and top of the beaker at the interval of 4 hours) indicate no significant change in the droplet size range (0-35 microns), implying that the droplets do not coalesce over the four-hour period. There is a slight increase in droplet volume fraction in the size range of 5-10 microns for the top sample after 4 hours. This increase is probably due to the settling of droplets in the size range of 15 - 30 μm, as reflected by the increase in the volume fraction of the larger droplets (15 - 30 μm) for the bottom sample after 4 hours. Hence, it can be established that emulsion is stable against coalescence for four hours, which is significantly longer than the total duration of an experiment which takes approximately one and half hours.

The Sauter mean diameter d_{32}, volume-weighted mean diameter d_{43}, and number mean diameter d_{10} are calculated to describe the emulsion droplet size distribution (DSD). The Sauter mean diameter

(d_{32}) and volume-mean diameter (d_{43}) are more sensitive to large droplets and can indicate coalescence in the system [21]. The Sauter mean diameter (d_{32}) is defined as:

$$d_{32} = \frac{\sum n_i * d^3{}_i}{\sum n_i * d^2{}_i}$$
<div align="right">4.1</div>

where, n_i is the number of ith particles, and d_i is the diameter of the ith particle.

Table 4.1 lists the values of d_{32}, d_{43}, d_{10} for samples withdrawn at time t = 0 h and t = 4 h. There are minor changes in the values of Sauter mean diameter (d_{32}) and volume-weighted mean diameter (d_{43}) for samples withdrawn from the bottom and top of the beaker at time t = 0 and t = 4 h.

Table 4.1 Different mean diameters calculated for a water-in-light mineral oil emulsion.

Diameters (µm)						
	Bottom			Top		
Sampling time (hours)	d_{10}	d_{32}	d_{43}	d_{10}	d_{32}	d_{43}
t = 0	4.7	8.3	11.7	4.8	8.0	11.0
t = 4	4.0	8.4	12.9	4.3	6.4	7.9

The results suggest that the water-in-light mineral oil emulsion recovered as supernatant after 21h of settling is stable against coalescence for at least 4 hours. The emulsion has a number mean diameter, d_{10}, of around 5 µm, similar to that reported for stable water-in-bitumen emulsions [2]. Therefore, it seems to be acceptable to use the emulsion produced here in Step - 3 of the experimental procedure to study the effect of shear rate on the flocculation of water droplets.

Repeats tests were performed to check the droplet size and stability of the emulsion. Table 4.2 lists the value of d_{32}, d_{43}, d_{10} for the sample withdrawn at time t = 0 h and t = 4 h for the repeat.

Table 4.2 Different mean diameters calculated for a water-in-light mineral oil emulsion, repeat test.

Diameters (µm)						
	Bottom			Top		
Sampling time (hours)	d_{10}	d_{32}	d_{43}	d_{10}	d_{32}	d_{43}
t = 0	4.9	7.7	10.5	5.1	8.6	11.1
t = 4	3.9	5.2	7.4	4.0	7.2	10.1

The calculated diameter values for the repeat are similar those of Table 4.1. The similarity in the mean diameters suggests the repeatability of the emulsion preparation procedure. More details regarding the repeat test are given in Appendix D.

4.3   Effect of shear rate on flocculation

Water-in-light mineral oil emulsions, like those described in the previous section, were mixed with a flocculant (PEI) using a magnetic stirrer for 5 minutes. The emulsion was then sheared in the Couette cell for 15 minutes. Values of shear rate similar to those experienced by water droplets passing through the plates in the IPS during naphthenic froth treatment were selected. Table 4.3 lists the shear rates explored in the study and the corresponding cylinder rotating speeds.

Table 4.3 Shear rates value corresponding to the different rotating speeds of the Couette cell.

Serial No.	Couette cell rotating speed (RPM)	Shear rate (s^{-1})
1	5	12.2
2	8	19.5
3	12	29.3

After shearing the emulsion for 15 minutes, the Couette cell was stopped, and a sample was collected immediately (t = 0 minutes) from the Z2 sampling port, as shown in Figure 3.2. The sample was analyzed using an optical microscope, following the procedure described in Section 3.4.4. Around 100 microphotographs per sample were captured and analyzed using the MATLAB script- 2, which is provided in Appendix C. The script determines the area-based diameter of flocs. Recall that all the single droplets, out of focus or connected flocs, were excluded from the floc size distribution (FSD), as explained using earlier Figure 3.5 and Figure 3.6.

The effect of shear rate on the flocculation of water droplets is investigated through variations in the volume-based floc size distribution (FSD). Figure 4.3 (a) presents the volume-based floc size distribution (FSD) obtained for different rotational speeds/shear rates at time t = 0 minutes, and Figure 4.3 (b) shows volume distribution at each rotational speeds/shear rate relative to that of the unsheared emulsion, i.e., 0 RPM / 0s^{-1}. The horizontal axis of the distributions denotes the area-based diameter of the flocs, and the vertical axis represents volume-based differential frequency.

As seen in Figure 4.3, there are more flocs in the size range of 5 - 25 µm for all rotating speed/shear rates than there are at 0 RPM / 0 s^{-1}. The increase is an indicator of floc formation due to an induced velocity gradient known as orthokinetic flocculation. The induced velocity gradient forces droplets or flocs to come in contact, increasing the number of collisions between droplets or flocs and thus promoting floc formation, as discussed in Chapter 2. This observation is in agreement with the studies conducted in the past, where the rate of coalescence increases with increasing the shear rate for oil-in-water emulsions [17, 18, 19]. In Figure 4.3 (b), the horizontal axis represents the area-based diameter of the flocs, and the vertical axis represents the difference between the differential frequency of flocs for emulsion sheared at different rotating speeds and unsheared emulsion (that is, 0 RPM). A positive number on the y-axis represents the presence of more flocs in that size range, and a negative value on the y-axis represents the absence of flocs in that size range. It can be seen there is a greater number of larger flocs (25 - 45 µm) for emulsion sheared at 8 RPM as compared

to 5 PM, but then at 12 RPM, the results show a decrease in larger flocs. This decrease at 12 RPM is believed to be related to the continuous breakage of larger flocs into smaller flocs at the higher shear rate, whereas the decrease at 5 RPM could be due to the insufficient shearing time for flocs to grow. A similar trend was observed in a previous study conducted to understand the effect of shear rate on asphaltene aggregates [48].
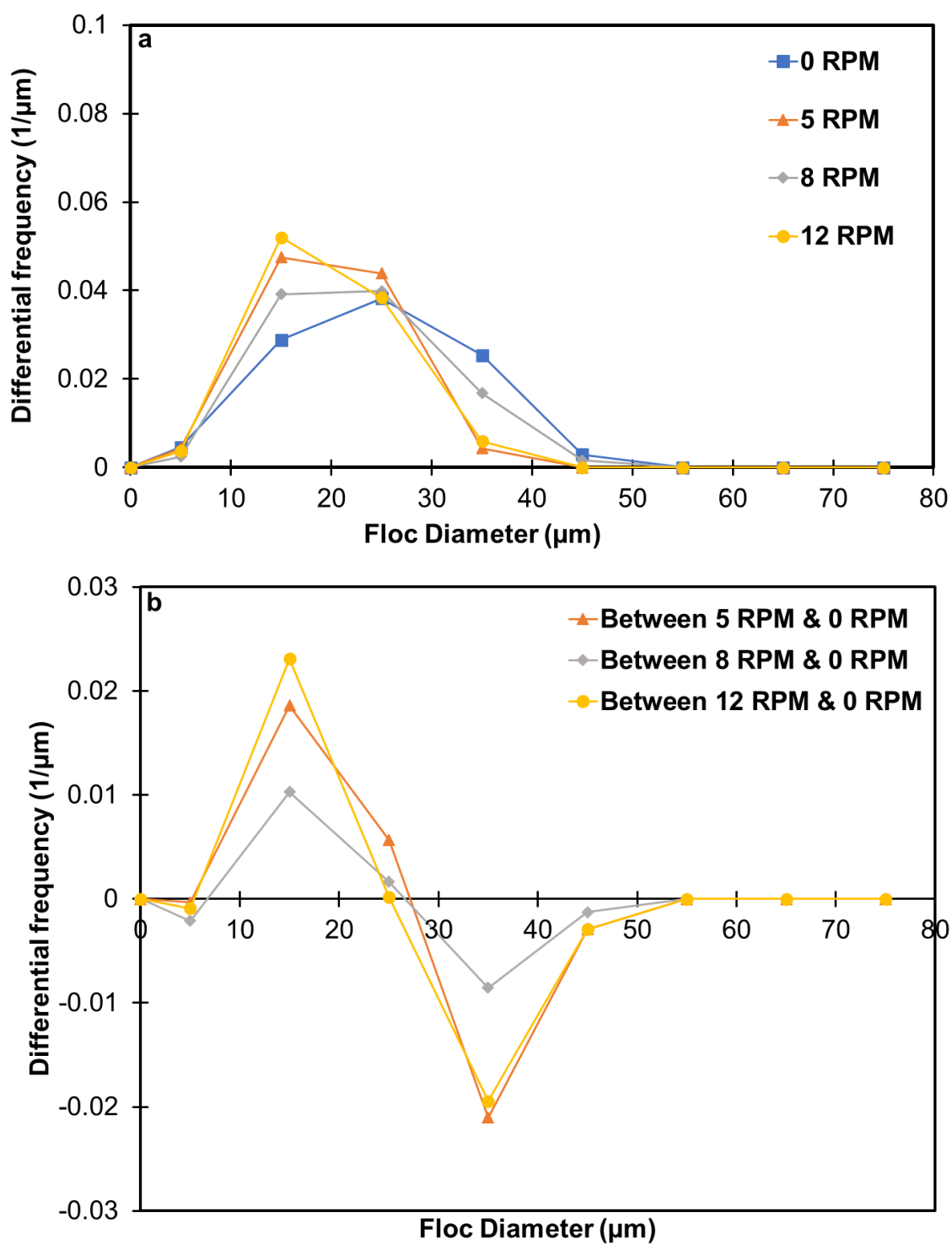
Figure 4.3(a) Volume-based floc size distribution at different shear rates. (b) The difference between volume-based floc size distribution of sheared and unsheared emulsion.

The floc size distributions can also be characterized by calculating the Sauter mean diameter (d_{32}). Table 4.4 lists Sauter mean diameter (d_{32}) values corresponding to different rotating speeds/shear rates. As can be seen, the calculated Sauter mean diameter (d_{32}) value is the greatest for 8 RPM/19.2 s^{-1} and minimum for 12 RPM / 29.3 s^{-1}. This implies Sauter mean diameter increases with rotating speed/shear rate until a particular value, after which it starts to decrease. The decrease in Sauter mean diameter (d_{32}) at higher rotating speeds suggests the breakage of larger flocs into smaller ones. A similar observation can be made from Figure 4.3(a-b), that suggests that 8 RPM produces larger flocs than 12 RPM and 5 RPM. This could be a reason for higher value of Sauter mean diameter (d_{32}) at 8 RPM compared to other rotating speeds.

These results suggest that a relatively low shear rate (up to 29.3 s^{-1}) promotes floc formation and growth. However, there is an optimal shear rate value; at values greater than that, floc breakage becomes dominant.

Table 4.4 Sauter mean diameter calculated at different rotating speed/shear rates.

Couette Cell Rotating Speed (RPM)	Shear rate (s^{-1})	Sauter mean diameter, d_{32} (μm)
5	12.2	16.4
8	19.5	17.7
12	29.3	15.5

4.4 Effect of shear rate on settling

Once the shearing test was completed, the Couette cell was stopped (i.e., set to 0 RPM), and the emulsion was allowed to settle for one hour. During the one-hour settling period, samples were withdrawn from the Z2 sampling port (see Figure 3.2) immediately after stopping the Couette cell (t = 0 minutes) then in 20-minute intervals (t =20 minutes, t = 40 minutes, and t = 60 minutes). Approximately 100 microphotographs were taken for each sample withdrawn, and then the images were processed to extract area-based floc diameter distributions using the MATLAB script-2

(Appendix C). Photographs of the bottom of the Couette cell were also taken, as shown in Figure 4.4. The effect of shear rate on the settling of flocs could be better understood by analyzing the information gathered (images of the bottom of Couette cell microphotographs, floc diameter) using different approaches.

In the first approach, images of the bottom of the Couette Cell and microphotographs captured at different shear conditions were analyzed. Figure 4.4 (a) shows the image of the bottom of the Couette cell for the unsheared emulsion, and Figure 4.4(b) represents the bottom of the Couette cell for an emulsion sheared at a fixed rotating speed/shear rate.
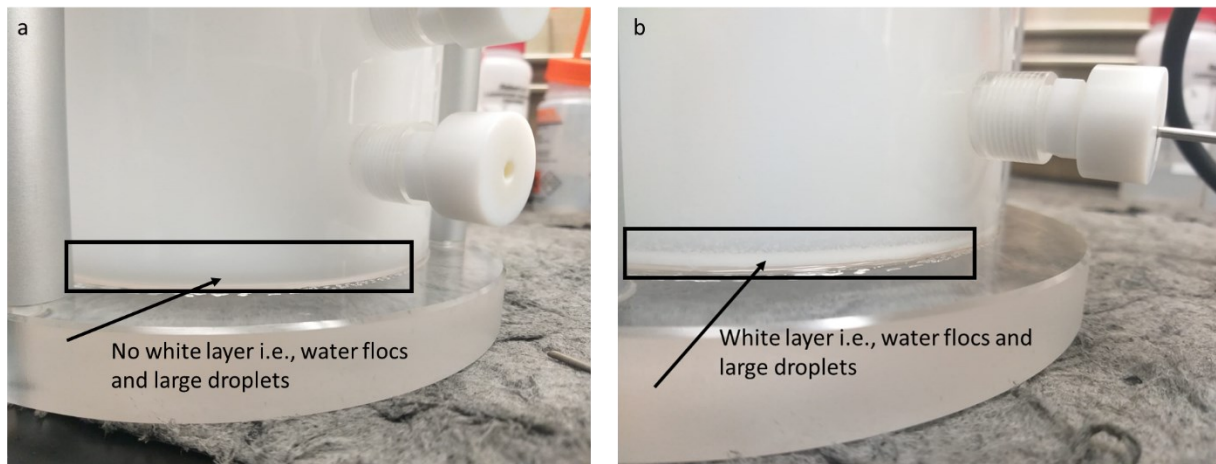

Figure 4.4 (a) Image of the bottom of the Couette cell for the unsheared emulsion. (b). Image of the bottom of the Couette cell sheared at 5 RPM.
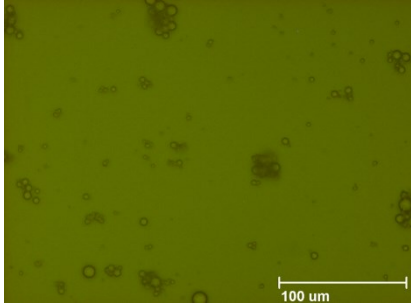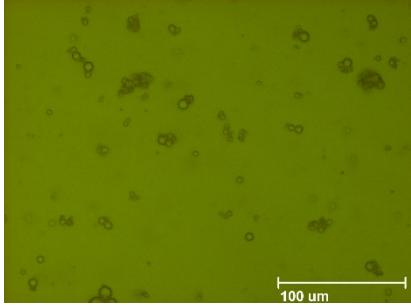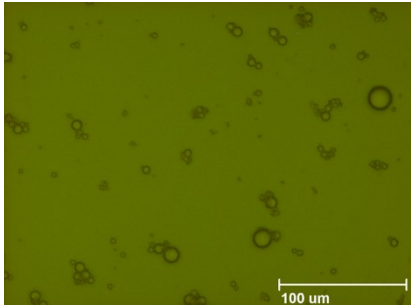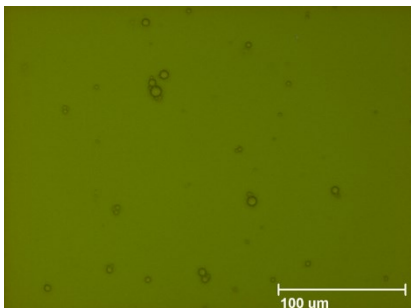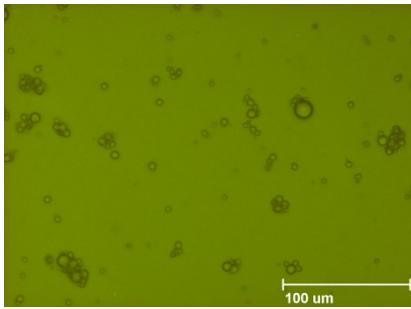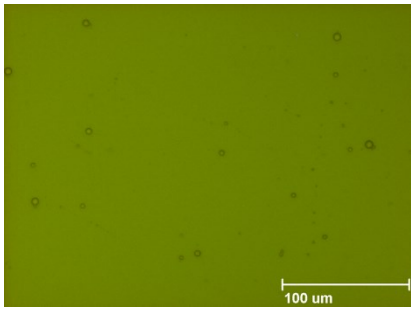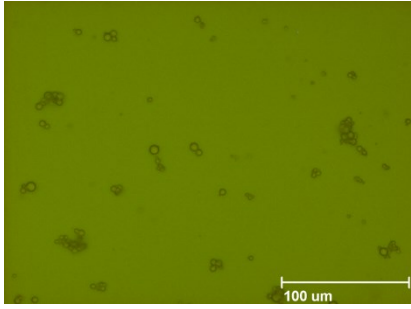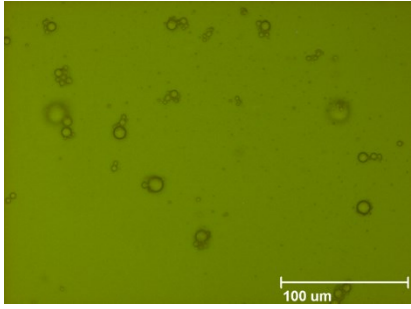
It can be seen in Figure 4.4 (b) that the shear produces a white layer at the bottom of the Couette cell, while this sediment is not found when the emulsion was not sheared, as can be seen in Figure 4.4 (a). The white layer consists of settled water flocs and large water droplets formed due to flocculation-induced coalescence. The presence of the white layer indicates that the rate of settling of water flocs can be increased by applying shear. It should be noted, though, that the time required for the formation of the white layer varies with rotating speed. It took around 60 minutes to form the settled emulsion layer at 5 RPM, 40 minutes at 8 RPM, and around 80-90 minutes at 12 RPM. There was no sediment/ emulsion at the bottom of the Couette cell even after 6 hours for the

unsheared emulsion. This finding again suggests that there should be an optimal shear rate value to promote rapid floc settling.

In another analysis approach, microphotographs were acquired for the samples withdrawn from the Z2 sampling port at time t = 0 and t = 60 minutes. Table 4.5 shows the representative microphotographs at time t = 0 minutes and t = 60 minutes for all the rotating speed/shear rates investigated in the study. As can be seen, the microphotographs of sheared emulsions show fewer water flocs/droplets than microphotographs of the unsheared emulsion after 60 minutes of settling. The observed trend could be due to the sweeping of smaller flocs/droplets by the faster settling flocs, which implies faster (large) settling flocs will attach to the small flocs/droplets on their way. This will increase the size, further enhancing the settling velocity and decreasing the time required to cross the Z2 sampling point, leaving behind cleaner oil. Therefore, microphotographs of sheared emulsion have fewer flocs/droplets.

Closer observation of the microphotographs suggests that the emulsion sheared at 8 RPM has the smallest fraction of flocs/water droplets after 60 minutes of settling compared with results obtained at the other rotating speeds. This finding again indicates that the 8 RPM / 19.5 s^{-1} is optimal for producing more rapidly settling water flocs/ droplets. It should be noted that this optimum may not translate to other systems: it is limited to the conditions of the present study.

Table 4.5 Microphotographs of samples withdrawn from the Z2 sampling port at time t = 0 and t = 60 minutes for all rotating speed/shear rates and unsheared emulsion.

Settling time (min) / Rotating speed (RPM)	t = 0	t = 60
0		
5		
8		
12		

In a subsequent analysis, microphotographs of the samples withdrawn from the Z2 sampling port at different time intervals were analyzed to extract area-based floc diameters, and floc size distributions (FSD) were then plotted. The variations in the FSD will help understand the reasons why the sheared emulsion settles more quickly than the unsheared emulsion. Figure 4.5 presents the time evolution of volume-based floc size distribution for emulsions sheared at different rotating speeds/shear rates along with the FSDs for the unsheared emulsion. The horizontal axis of the distribution represents the area-based floc diameter, while the vertical axis shows the volume-based differential frequency. There are some common trends for the results obtained at different rotating speeds: the distributions shift significantly towards smaller values over time; and the tail of each distribution lengthens with time. However, these trends are not quite as clear for the unsheared emulsion. The shift and lengthening of the tail in the distribution could be because of the settling of flocs overtime. The large flocs (formed due to shearing of emulsion) at t = 0 minute while settling attach to other slower settling flocs on their way and sweep them away from the Z2 sampling port. Moreover, as discussed earlier, the unsheared emulsion has fewer large flocs compared to the sheared emulsion, therefore, less sweeping of smaller flocs/droplets and less evident shifts in distributions.

The emulsion sheared at 8 RPM has fewer smaller flocs and a more significant number of larger flocs compared to the emulsions sheared at other rotating speeds, as shown in Figure 4.3(b). Consequently, the emulsion sheared at 8 RPM has the widest floc size distribution, which is the ideal condition for the dominance of sweep flocculation in any system, as described by Equation 2.4. These results help explain why the 8 RPM condition provides more rapid settling of water droplets/flocs, resulting in producing a cleaner oil "product."
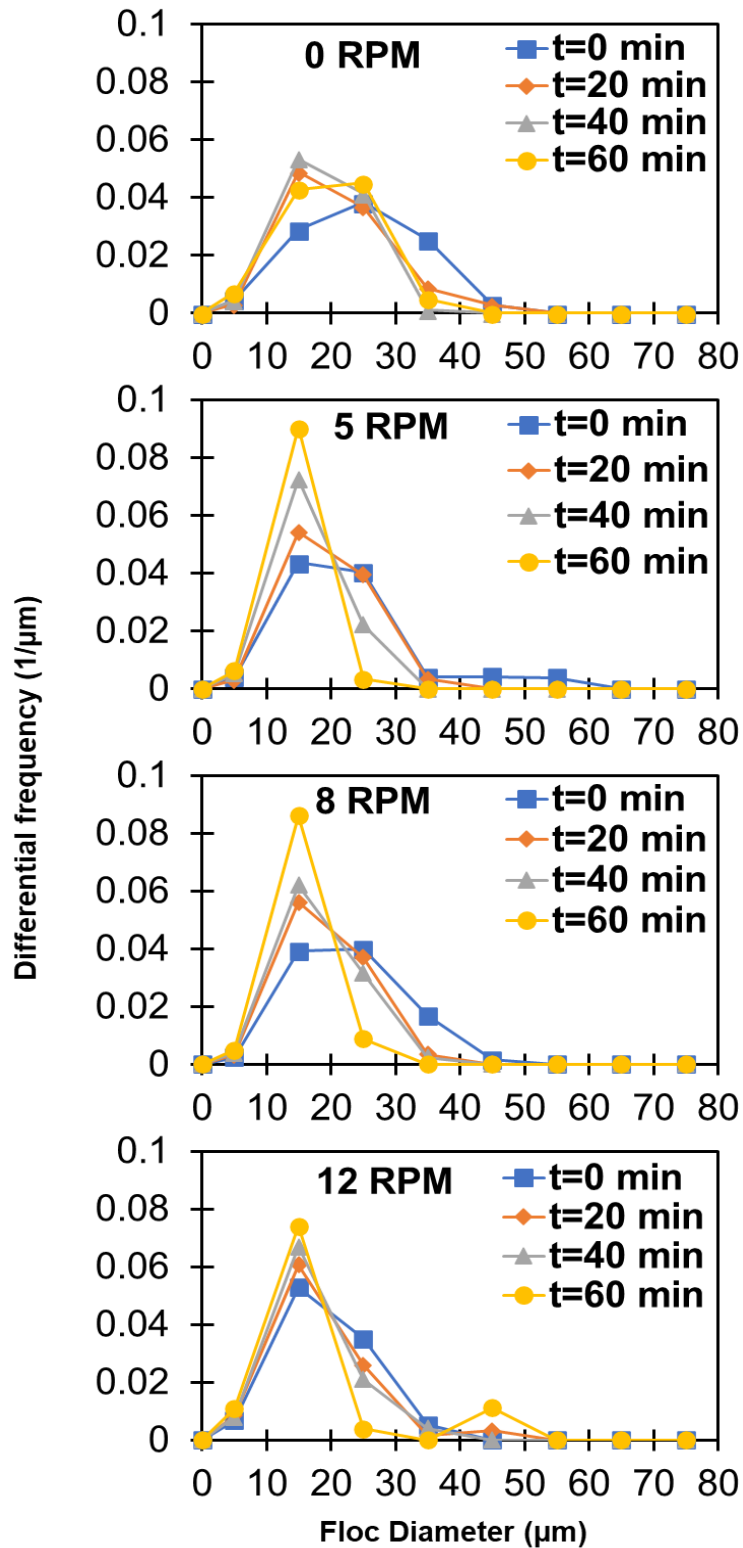
Figure 4.5 Volume-based floc size distributions of the samples withdrawn from Z2 sampling port at different rotating speeds/ shear rates.

The floc settling time to cross Z2 sampling port based on Stokes' law was also compared with the estimated time a floc would take to disappear from the volume-based floc size distribution shown in Figure 4.5. The settling velocity of a droplet of size range 35 to 50 µm was calculated using Stokes' law to determine the time it should take to travel to a distance of 3.5 cm. The droplet size range of 35 – 50 µm was selected because the maximum floc size observed in the FSDs falls in this range. Table 4.6 lists the settling calculated settling time for a single droplet of size 35 – 50 µm (using the size increment of 5 µm). These settling times are compared with the conservative estimates of the time the flocs in size range of 35 - 50 µm would take to disappear from FSD shown in Figure 4.5. It can be seen from the distributions in Figure 4.5 that flocs greater than 35µm in size were not present at the Z2 sampling port (3.5 cm from the top of the Couette cell) after 20 minutes. Compared to the value listed in Table 4.6, the time taken by flocs of diameter greater than 35 microns to travel 3.5 cm is around 4 - 8 times less than the value calculated based on Stokes' law.

Table 4.6 Settling time calculated based on Stokes's law for different water droplet diameters

Serial No.	Water droplet Diameter (µm)	Time to travel 3.5 cm (min)
1	35	161
2	40	122.5
3	45	98
4	50	77

The significant difference in the settling time suggests that larger flocs are attaching to smaller flocs, forming even larger flocs, and as a result, increasing their settling velocity and reducing the settling time. This again suggests the importance of sweep flocculation in the sheared emulsion systems.

In a fourth approach to the analysis, the temporal differences in the Sauter Mean diameter (d_{32}) were evaluated to understand the effect of shear rate on floc formation and settling. Figure 4.6 shows the time variation in the normalized Sauter Mean diameter (d_{32}) at different rotating speed/shear rates,

where the Sauter Mean diameter ($d_{32,t}$) at time 't' is normalized by the initial Sauter mean diameter ($d_{32,0}$) of the respective distribution. The abscissa represents the settling time, and the represents the normalized Sauter mean diameter ($d_{32,t} / d_{32,0}$). The rate of decrease in normalized diameter over time is the lowest for 0 RPM and the highest for 8 RPM. This trend could be because there are fewer number of flocs for unsheared emulsion compared to sheared emulsion. Therefore, more sweeping of smaller flocs/droplets for the sheared emulsion and more change in Sauter Mean Diameter. Furthermore, emulsion sheared at 8 RPM has the widest size distribution as discussed earlier, which are the ideal conditions to sweep flocculation. Consequently, 8 RPM has the highest change in normalized Sauter mean diameter. These results suggest that shearing the emulsion can improve the settling of the dispersed phase. The shear rate applied to the emulsion forced droplets to come together and form flocs. The formed flocs have settling velocities greater than an individual droplet. The fast-moving flocs sweep the smaller flocs/ droplets on their way, causing them to grow in size and decreasing the settling time. This result also suggests that sweep flocculation is a primary mechanism in cleaning the oil.

The reduction in Sauter mean diameter (d_{32}) with settling time was further quantified by calculating the percentage change for each shear rate after 60 minutes of settling. Figure 4.7 represents the percent change in the Sauter mean diameter (d_{32}) from time t = 0 to t = 60 minutes for all the shear rates investigated. The abscissa of the graph is the rotating speed of the inner cylinder of the Couette cell, and the ordinate represents the percentage change in the Sauter mean diameter at time t = 0 and t = 60 minutes. Figure 4.7 shows that the percentage change in Sauter mean diameter (d_{32}) is more significant for all the sheared emulsions compared to the unsheared emulsion. This trend suggests that fast settling large flocs are attaching to slowly settling flocs/droplets, removing them and leaving behind fewer smaller flocs/droplets. Additionally, the change in the normalized Sauter mean diameter reaches a maximum, i.e., approximately 32% for 8 RPM and the smallest change (around 23 %) is observed for 12 RPM. Thus, advocating for 8 RPM/19.5 s^{-1} is the best condition

for effective water removal for the studied system. This finding agrees with the analysis done in the previous sections, for example, microphotographs after 60 minutes of settling has the least number of flocs/droplets, the white layer (settled flocs/ large water droplets) at the bottom of Couette cell formed fastest (within 40 minutes) .
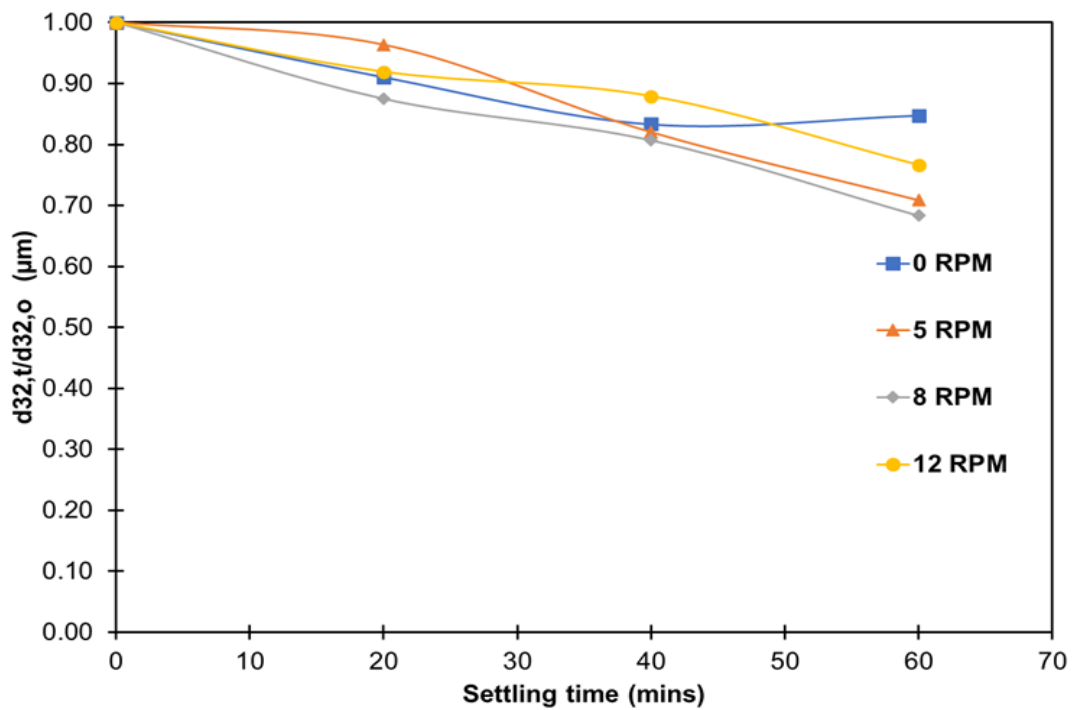

Figure 4.6 Variation in normalized floc Sauter mean diameters at different rotating speeds/shear rates.
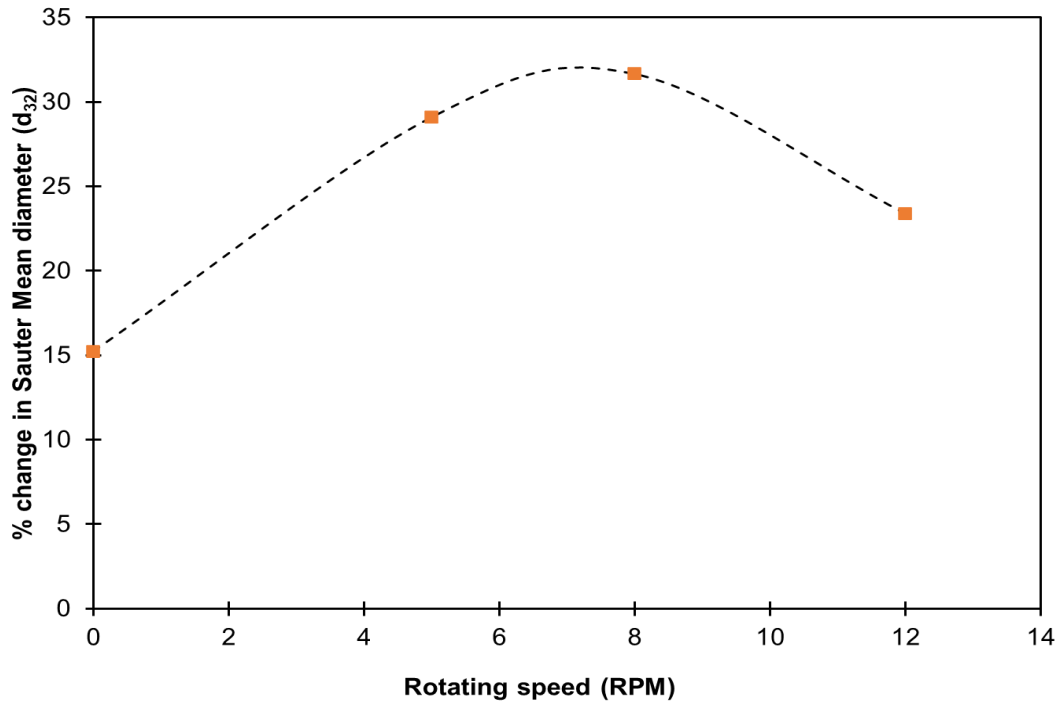
Figure 4.7 Percentage change in floc Sauter mean diameters at different rotating speeds/shear rates, for 60 minutes of settling.

It is clearly evident from the results that shearing the emulsion accelerates the settling of water droplets, and it seems that sweep flocculation is the likely primary mechanism behind it. Shearing the emulsion helps form larger flocs with a settling velocity greater than an individual droplet. These fast-settling flocs will attach to the small flocs/droplets, becoming even larger and speeding their removal by increasing the settling velocity. This way, sweep flocculation will help remove the smaller droplets from the oil that otherwise would take many hours or days to remove/settle.

4.5   Methodology for Studying Repeatability

This section discusses the repeatability of the experiments performed at different shear rates. In the previous section, the effect of shear rate on the flocculation and settling of water droplets was studied by considering only the flocs present in the microphotographs. The MATLAB script that was used to extract the floc area-based diameter detects both droplets and flocs present in the

microphotographs. As a result, single droplets were removed manually from each image. The process of removing the single droplets is exhaustive and time-consuming. For example, it takes around 6 – 8 hours to remove the droplets from the microphotographs of just one sample. This new approach to the analysis, described here, can help expedite the image analysis for future experiments.

In this new approach, single water droplets were included in the floc size distributions. The volume-based distribution of flocs alone and flocs with droplets were then compared. Figure 4.8 represents the time evolution of the volume-based size distribution of flocs alone and flocs with single droplets for an emulsion sheared at 5 RPM or 12.2 s^{-1}

Both distributions are similar and follow a similar trend, as can be seen in Figure 4.8 (a-b); however, there is a slight increase in the differential frequency of droplets that are 5 µm in size due to the inclusion of the single droplets present in the analysis.
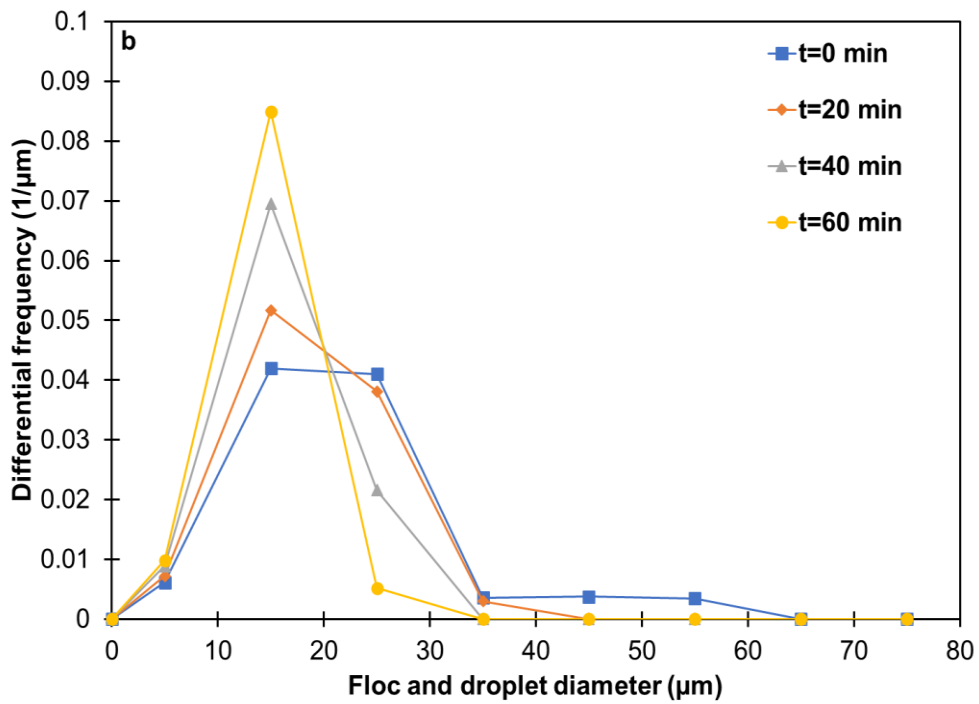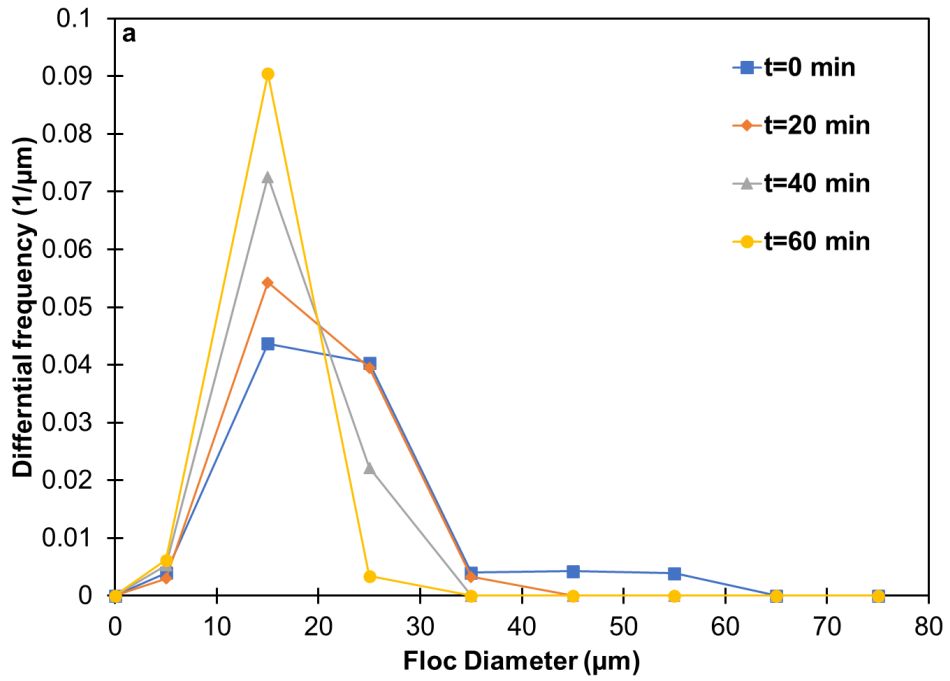
Figure 4.8 (a) Volume-based distribution of flocs (original methodology). (b) Volume-based distribution of flocs with single droplets included (new methodology).

The Sauter mean diameter (d_{32}) was also calculated to characterize both distributions, and the values are reported in Table 4.7

Table 4.7 Sauter mean diameter values for flocs alone and flocs with single droplets included, respectively

Sampling time (min)	Sauter mean diameter (d_{32}) (µm)	
	Only flocs	**Flocs and Droplets**
0	16.4	15.8
20	15.8	14.8
40	13.5	12.7
60	9.3	11.6

There is a slight decrease in the Sauter mean diameter (d_{32}) values when the single water droplets are included, but the difference is not significant enough to consider that the two distributions are different. It can therefore be stated that volume-based distributions obtained when including single droplets provide nearly identical results to the more time-consuming approach involving the manual subtraction of individual droplets from the FSDs. This new approach was thus used to evaluate the repeatability of the shearing experiments. Figure 4.9 (a-b) shows the time evolution of volume-based size distribution for two repeats performed for an emulsion sheared at 5 RPM/ $12.2s^{-1}$. It can be seen that a similar trend of distribution shifting towards the smaller diameters with time is observed for both repeats. Thus, some limited confirmation of the repeatability of the experiments is provided. The volume-based distributions of repeats for the emulsions sheared at 8 and 12 RPM are provided in Appendix D.
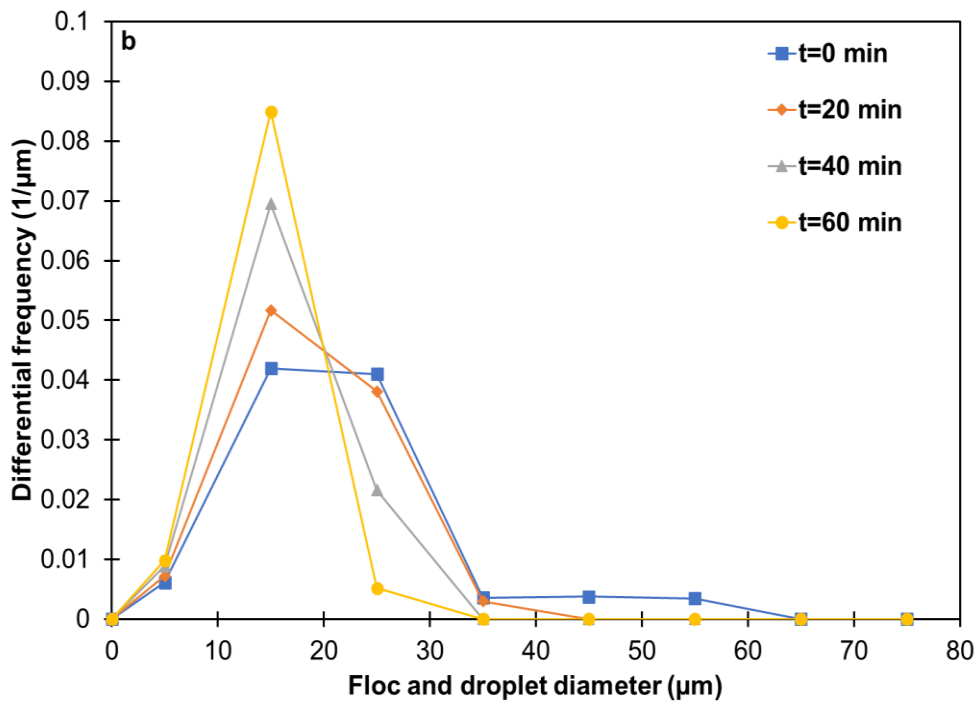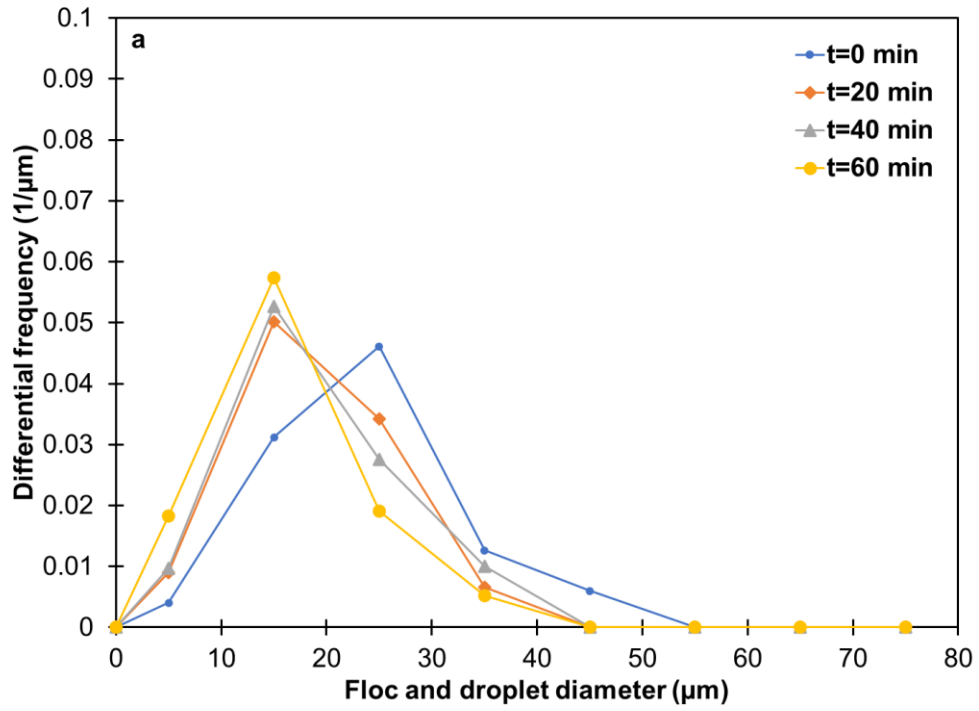
Figure 4.9 (a) Volume-based distribution of flocs and single droplets for repeat-1. (b) Volume-based distribution of flocs with single droplets for repeat-2.

4.6   Summary

The results presented in this chapter indicate that the application of shear rates in the range of 12.2 – 29.3s^{-1} increase the flocculation of water droplets. The formation of larger/more flocs seems to promote sweep flocculation. Sweep flocculation results in the faster and more effective removal of water droplets from the oil. However, it appears that an optimal shear rate will produce the maximum flocculation and the cleanest oil. The increase in shear rates beyond that optimal value causes larger flocs to break into smaller flocs, reducing their settling velocity and increasing the time required for their removal. The optimal shear rate value observed in the present study was 19.5 s^{-1} (8 RPM).

Chapter 5 : Conclusions and Recommendations

5.1 Conclusions

The primary objective of this project, as outlined in Section 1.3, was to study the effect of shear rate on the flocculation and improved settling of small stable water droplets in a light mineral oil continuous phase. This system was chosen to be an idealized version of a water-in-diluted bitumen emulsion. The investigations to understand the effect of shear rate on flocculation of water droplets and improved settling were carried out using a Couette cell. Different analysis approaches were used during this study to gather evidence on settling rates and floc size distributions to understand the effect of shear rate and to identify the mechanism(s) producing small droplet settling.

The key findings can be summarized as follows:

- Experiments indicate that induced shear promotes orthokinetic flocculation in the emulsion. The most likely explanation is that shearing (velocity gradient) has forced droplets/ flocs to come in contact with each other, thus promoting floc formation.

- The Sauter mean diameter (d_{32}) initially increases with the increasing rotating speed of the Couette cell but decreases after a specific value. The decrease in d_{32} is possibly due to the breakage of bigger flocs into smaller fragments.

- Faster removal of water droplets was observed for emulsions subjected to shear in the Couette cell. As the shear rate increases, more flocs are formed, and they have much higher settling velocities than an individual droplet. These rapidly settling flocs likely entrap the smaller droplets in their path; the flocs grow in diameter, which increases the settling velocity and reduces settling time.

- The comparison of results obtained at different shear rates shows that there is an optimal value of the shear rate to achieve the most effective removal of the dispersed phase. The

optimal shear rate for the present study is 19.5 s^{-1}. It is important to note that this value is system-specific and is unlikely to apply directly to any other system.

- The effect of shear rate on flocculation and settling was studied by only considering the flocs present in the microphotographs; implying single water droplets were not included. However, the process of droplet subtraction was completely manual and time consuming. Therefore, a new approach of including the single droplets was suggested for future. The volume-based distributions for flocs and flocs with single droplets included were similar. More importantly, floc distributions that included single droplets were significantly less time-consuming to produce as it was done automatically by the MATLAB script. This new approach can expedite the image analysis process for future experiments.

5.2   Novel contribution of this research

A broad base of information is available in the literature to understand the effect of shear rate on the orthokinetic flocculation of oil-in-water emulsions and solid particle suspensions. Very few studies have been conducted to understand and quantify sweep flocculation. To the author's knowledge, no study has been done to investigate the effect of shear rate on flocculation (orthokinetic/sweep) in water-in-oil emulsions.

The current research establishes a connection between shear rate and orthokinetic flocculation in a water-in-oil emulsion and indicates that sweep flocculation can promote the removal of small stable water droplets. In this research, various methods for analyzing and quantifying sweep flocculation in the system have been described. Moreover, the lab-scale shearing device (Couette cell) employed in the shearing experiments has a shear rate profile similar to that of an Inclined Plate Setter (IPS) and the water-in-light mineral oil emulsions used in the experiments had mean water droplet size, density, and a viscosity similar to the water-in-bitumen emulsion encountered in Naphthenic Froth Treatment (NFT). Therefore, findings from the present study can lay a foundation for improving

the conventional lab-based demulsifier tests used in the industry by accounting for the effect of shear rate and optimizing the operating condition for the effective removal of smaller water droplets from diluted bitumen froth in Inclined Plate Settler (IPS) in Naphthenic Froth Treatment (NFT).

5.3   Recommendations for Future Work

- The experiments conducted in the present study used an idealized water-in-oil emulsion to gain insight into the effect of shear rate on the flocculation of water droplets. Similar experiments conducted with the water-in-bitumen emulsions that are encountered in the froth treatment process should be completed to study and optimize the actual process conditions.

- In the present study, a sampling and microscopy technique has been used to analyze the emulsion sheared in the Couette cell. Sampling can lead to the breakage and formation of new flocs. Therefore, analysis of sheared emulsions in Couette cell should be performed using in-situ measurement techniques such as Smart Online Particle Analysis Technology (SOPAT) probe or Particle Video Microscope (PVM) probe to have more accurate results and provide an improved understanding of orthokinetic and sweep flocculation.

- The MATLAB script that issued to determine floc size distributions from microphotographs cannot automatically remove single water droplets from the distributions. The inefficiency of scripts used here provides an excellent opportunity to develop a more robust analysis that automatically differentiates between single water droplets and water flocs.

- In the future, a few shearing experiments should be performed without the addition of flocculant to the emulsion. These experiments will help to understand just the effect of shear on the floc formation and their subsequent settling.

- Laboratory bottle tests used to determine the optimal concentration of the demulsifiers used for industrial application are performed under static conditions, as discussed in Chapter 1.

Hence, new experimental methods should be developed using the Couette cell designed for this study, as it better represents the industrial shear conditions. This new protocol could be used to determine the optimal demulsifier concentration. There is a possibility of a decrease in the optimal demulsifier concentration needed due to the induced shear rate. This decrease can help industries save on operating costs and further optimize the operating conditions.

- The experiments performed in the present study used a flocculant that acts very slowly compared to the demulsifiers used in industry. In the future, similar shearing experiments should be done using different industrial demulsifiers to understand their effect under shearing conditions.

- In the future, more repeats of the experiments at one shear rate should be done to ensure reproducibility and determine the error margins before including the shear to modify the current lab-scale bottle or jar test.

- The experiments of the present study have used the same batch of mineral oil to prepare emulsions. The properties of mineral oil, especially viscosity, vary with the batch number from the supplier. Therefore, the oil with the same batch number should always be used to prepare the emulsion. Moreover, same homogenizer should always be used to prepare the batches of emulsion as changing the homogenizer can impact the droplet size distribution in the emulsions.

References

1.   Regulator, A.E. *Alberta Energy Outlook 2021*; 2021.

2.   Masliyah, Jacob H., Jan Czarnecki, and Z.X. *Handbook on Theory and Practice of Bitumen Recovery from Athabasca Oil Sands Volume I*; 2011.

3.   Rao, F.; Liu, Q. Froth Treatment in Athabasca Oil Sands Bitumen Recovery Process: A Review. *Energy and Fuels* **2013**, *27*, 7199–7207, doi:10.1021/ef4016697.

4.   Masliyah, Jacob H., Jan Czarnecki, and Z.X. *Handbook on Theory and Practice of Bitumen Recovery from Athabasca Oil Sands Volume II*; 2013.

5.   Sjoblom, J. *Encyclopedic Handbook of Emulsion Technology*; 2001.

6.   Kokal, S. Crude-Oil Emulsions: A State-of-the-Art Review. *SPE Production and Facilities* **2005**, *20*, 5–12, doi:10.2118/77497-pa.

7.   Oilsands magazine Naphthenic Froth Treatment Available online: https://www.oilsandsmagazine.com/technical/mining/froth-treatment/naphthenic.

8.   Oilsands magazine Inclined Plate Separators Available online: https://www.oilsandsmagazine.com/technical/mining/froth-treatment/naphthenic/ips-inclined-plate-separator#:~:text=Mar 6 Inclined Plate Separators&text=Inclined plate separators (IPS) are,commonly used for water treatment.

9.   Bengtson, H. No Title Available online: https://www.engineeringexcelspreadsheets.com/2020/05/lamella-inclined-plate-clarifier-design-spreadsheet/.

10.   No Title Available online: https://metchem.com/new-clarifiers-manufactured-by-met-chem/.

11. Mullins,O.C.; Sheu, E.Y.;Hammami, A.; Marshall, A.G. *Asphalthenes, Heavy Oils, and Petroleomics*; Springer: New York, 2007.

12. Gafonova, O. v.; Yarranton, H.W. The Stabilization of Water-in-Hydrocarbon Emulsions by Asphaltenes and Resins. *Journal of Colloid and Interface Science* **2001**, *241*, 469–478, doi:10.1006/jcis.2001.7731.

13. Kilpatrick, P.K. Water-in-Crude Oil Emulsion Stabilization: Review and Unanswered Questions. *Energy and Fuels* **2012**, *26*, 4017–4026, doi:10.1021/ef3003262.

14. Yarranton, H.W.; Hussein, H.; Masliyah, J.H. Water-in-Hydrocarbon Emulsions Stabilized by Asphaltenes at Low Concentrations. *Journal of Colloid and Interface Science* **2000**, *228*, 52–63, doi:10.1006/jcis.2000.6938.

15. Raynel, G.; Salomon Marques, D.; Al-Khabaz, S.; Al-Thabet, M.; Oshinowo, L. A New Method to Select Demulsifiers and Optimize Dosage at Wet Crude Oil Separation Facilities. *Oil and Gas Science and Technology* **2021**, *76*, doi:10.2516/ogst/2020096.

16. Romanova, U.G.; Yarranton, H.W.; Schramm, L.L.; Shelfantook, W.E. Investigation of Oil Sands Froth Treatment. *Canadian Journal of Chemical Engineering* **2004**, *82*, doi:10.1002/cjce.5450820410.

17. Romanova, U.G.; Valinasab, M.; Stasiuk, E.N.; Yarranton, H.W.; Schramm, L.L.; Shelfantook, W.E. The Effect of Oil Sands Bitumen Extraction Conditions on Froth Treatment Performance. *Journal of Canadian Petroleum Technology* **2006**, *45*, doi:10.2118/06-09-03.

18. Machado, M.B.; Kresta, S.M. The Confined Impeller Stirred Tank (CIST): A Bench Scale Testing Device for Specification of Local Mixing Conditions Required in Large Scale

Vessels. *Chemical Engineering Research and Design* **2013**, *91*, doi:10.1016/j.cherd.2013.06.025.

19.   Schokker, E.P.; Dalgleish, D.G. The Shear-Induced Destabilization of Oil-in-Water Emulsions Using Caseinate as Emulsifier. *Colloids and Surfaces A: Physicochemical and Engineering Aspects* **1998**, *145*, doi:10.1016/S0927-7757(98)00667-0.

20.   Nandi, A.; Khakhar, D. v.; Mehra, A. Coalescence in Surfactant-Stabilized Emulsions Subjected to Shear Flow. *Langmuir* **2001**, *17*, doi:10.1021/la001473m.

21.   Mazumdar, M.; Jammoria, A.S.; Roy, S. Effective Rates of Coalescence in Oil–Water Dispersions under Constant Shear. *Chemical Engineering Science* **2017**, *157*, doi:10.1016/j.ces.2015.11.037.

22.   Leo, S.S. Measurement and Analysis of Drop Size Distribution during Bitumen Clarification Using Image Analysis, University of Alberta, 2013.

23.   Shelfantook, W.E. A Perspective on the Selection of Froth Treatment Processes. *Canadian Journal of Chemical Engineering* 2004, *82*.

24.   Al-Dulaimi, S.M.S.; Racoviteanu, G. Performance of the Tube Settler Clarification at Different Inclination Angles and Variable Flow Rate. *Mathematical Modelling in Civil Engineering* **2018**, *14*, doi:10.2478/mmce-2018-0004.

25.   Lytra, M. Hydraulics of Lamella Sedimentation, Lund University, 2019.

26.   Poh, P.H. Development of Design Methods for Lamella Separators, Loughborough University, 1984.

27.   Cheremisinoff, N.P. *Pollution Control Handbook*; 2016.

28. Arora Nitin Mechanisms of Aggregation and Separation of Water and Solids from Bitumen Froth Using Cluster Size Distribution, University of Alberta,2016.

29. Goodarzi, F.; Zendehboudi, S. A Comprehensive Review on Emulsions and Emulsion Stability in Chemical and Energy Industries. **2019**, *97*, 281–309, doi:10.1002/cjce.23336.

30. Crittenden, John C., et al. *MWH's Water Treatment: Principles and Design*; 2012.

31. SA Parsons, B.J. *Introduction to Potable Water Treatment Processes*; 2006.

32. Thomas, D.N.; Judd, S.J.; Fawcett, N. Flocculation Modelling: A Review. *Water Research* 1999, *33*.

33. Bratby, J. Coagulation and Flocculation: With an Emphasis on Water and Wastewater Treatment. **1980**, doi:10.1016/0300-9467(81)80062-7.

34. Huang, H. Fractal Properties of Flocs Formed by Fluid Shear and Differential Settling. *Physics of Fluids* **1994**, *6*, doi:10.1063/1.868055.

35. Peña, A.A.; Hirasaki, G.J.; Miller, C.A. Chemically Induced Destabilization of Water-in-Crude Oil Emulsions. *Industrial and Engineering Chemistry Research* **2005**, *44*, doi:10.1021/ie049666i.

36. Berger, P.D.; Hsu, C.; Arendell, J.P. Designing and Selecting Demulsifiers for Optimum Field Performance on the Basis of Production Fluid Characteristics. *SPE Production Engineering* **1988**, *3*, doi:10.2118/16285-PA.

37. Kim, Y.H.; Wasan, D.T. Effect of Demulsifier Partitioning on the Destabilization of Water-in-Oil Emulsions. *Industrial and Engineering Chemistry Research* **1996**, *35*, doi:10.1021/ie950372u.

38.   Wu, J.; Xu, Y.; Dabros, T.; Hamza, H. Effect of Demulsifier Properties on Destabilization of Water-in-Oil Emulsion. *Energy and Fuels* **2003**, *17*, doi:10.1021/ef030113e.

39.   Kailey, I.; Feng, X. In Fl Uence of Structural Variations of Demulsi Fi Ers on Their Performance. **2013**.

40.   Chen, Z.; Peng, J.; Ge, L.; Xu, Z. Demulsifying Water-in-Oil Emulsions by Ethyl Cellulose Demulsifiers Studied Using Focused Beam Reflectance Measurement. *Chemical Engineering Science* **2015**, *130*, doi:10.1016/j.ces.2015.03.014.

41.   Bhattacharyya, B.R.; Nikolov, A.D.; Wasan, D.T. Demulsification of Water in Oil Emulsions Using Water Soluble Demulsifiers. *Journal of Dispersion Science and Technology* **1992**, *13*, 121–133, doi:10.1080/01932699208943302.

42.   Laplante, P.; Machado, M.B.; Bhattacharya, S.; Ng, S.; Kresta, S.M. Demulsifier Performance in Froth Treatment: Untangling the Effects of Mixing, Bulk Concentration and Injection Concentration Using a Standardized Mixing Test Cell (CIST). *Fuel Processing Technology* **2015**, *138*, doi:10.1016/j.fuproc.2015.05.028.

43.   Serra, T.; Colomer, J.; Logan, B.E. Efficiency of Different Shear Devices on Flocculation. *Water Research* **2008**, *42*, doi:10.1016/j.watres.2007.08.027.

44.   Rahmani, N.H.G.; Dabros, T.; Masliyah, J.H. Online Optical Monitoring of Asphaltene Aggregation. *Industrial and Engineering Chemistry Research* **2005**, *44*, 75–84, doi:10.1021/ie049689x.

45.   Rahmani, N.H.G.; Masliyah, J.H.; Dabros, T. Characterization of Asphaltenes Aggregation and Fragmentation in a Shear Field. *AIChE Journal* **2003**, *49*, doi:10.1002/aic.690490705.

46. Sinnreich, H. Baluty Market: A S Tudy of a F Ood S Pace. *Food, Culture & Society: An International Journal of Multidisciplinary Research* **2007**, *10*, 73–84, doi:10.2752/155280107780154079.

47. Ives, K.J. *The Scientific Basis of Flocculation*; Sijthoff & Noordhoff International Publishers, 1978.

48. Rahmani, N.H.G.; Dabros, T.; Masliyah, J.H. Evolution of Asphaltene Floc Size Distribution in Organic Solvents under Shear. *Chemical Engineering Science* **2004**, *59*, doi:10.1016/j.ces.2003.10.017.

49. Mishra, V.; Kresta, S.M.; Masliyah, J.H. Self-Preservation of the Drop Size Distribution Function and Variation in the Stability Ratio for Rapid Coalescence of a Polydisperse Emulsion in a Simple Shear Field. *Journal of Colloid and Interface Science* **1998**, doi:10.1006/jcis.1997.5217.

50. Berg, John.C. *An Introduction to Interfaces &Colloids*; 2009.

51. Lachance, J.W.; Dendy Sloan, E.; Koh, C.A. Effect of Hydrate Formation/Dissociation on Emulsion Stability Using DSC and Visual Techniques. *Chemical Engineering Science* **2008**, *63*, doi:10.1016/j.ces.2008.04.049.

52. *VWR, Homogenizer Models VWR 200 and VWR 250: Operator's Manual*.

53. Snyder, H.A. Stability of Rotating Couette Flow. II. Comparison with Numerical Results. *Physics of Fluids* **1968**, *11*, 1599–1605, doi:10.1063/1.1692167.

54. Burgess, D.J.; Yoon, J.K. Influence of Interfacial Properties of Lipophilic Surfactants on Water-in-Oil Emulsion Stability. *Colloids and Surfaces B: Biointerfaces* **1995**, *4*, 297–308.

55. Shelfantook, William.E., Hyndman, Alexander W., Hackman, Larry P., Inventors. Purification process for bitumen froth. US Patent US4859317A.

Appendix A: Sample calculation for Shear rate between parallel plates in IPS

Assumptions made for calculation are:

1. Steady state
2. Single-phase flow
3. Laminar regime
4. Newtonian fluid

Dimensions of IPS [55]

Gap between parallel plates, b; m	0.035
Length of plates, l; m	1.524
Width of plate, w; m	0.3048
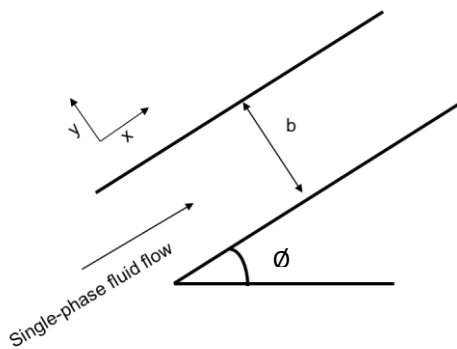
The average shear value between parallel plates of IPS was calculated after solving the Navier-Stokes equation based on the assumption mentioned in x- direction:

$$v_x = v(y), v_y = 0$$

$$g_x = -g \sin \emptyset$$

$$\rho \left(\mu * \frac{dv_x}{dx} + v_y * \frac{dv_x}{dy} \right) = \frac{-dp}{dx} + \rho g_x + \mu \left(\frac{d^2u}{dx^2} + \frac{d^2u}{dy^2} \right)$$

Simplifying the above-mentioned equation and integrating, the value of shear rate across the plate (G) can be calculated as:

$$G = \frac{3 * v_x}{b}$$

where v is the average fluid velocity in x – direction and b is gap between the parallel plates. The shear rate values are then calculated corresponding to different Reynolds number between the parallel plates of the IPS. Figure A1 shows the shear rate value corresponding to different Reynolds number for water-in-light mineral oil emulsion and diluted bitumen froth.
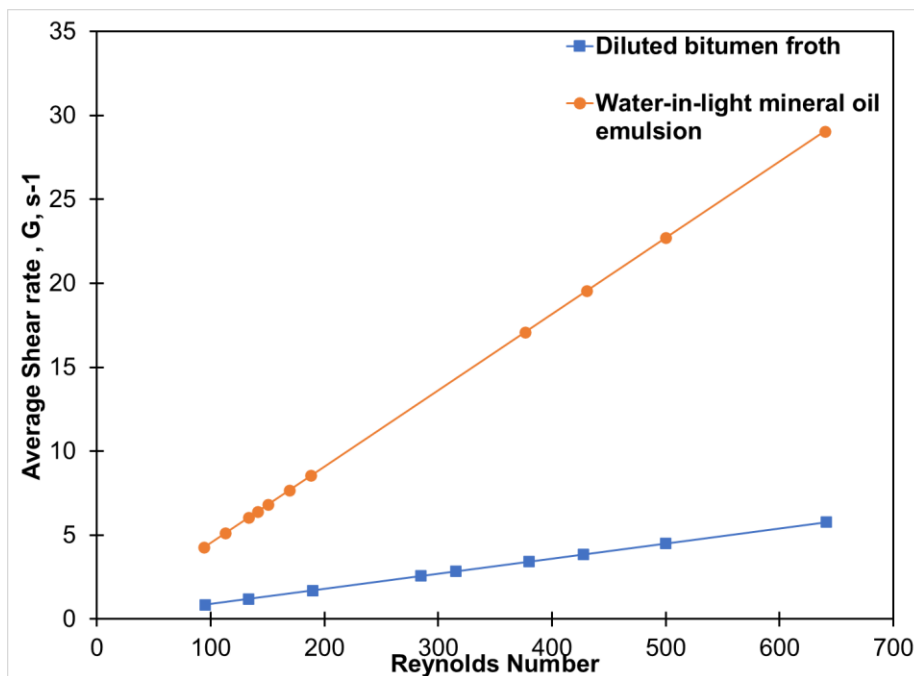
Figure A1 The value of the average shear rate corresponds to the Reynold numbers.

As can be seen in the figure, the shear rate value to keep the Reynolds number around 500 for water-in-light mineral oil emulsion is around 22s^{-1}.

Appendix B: Safe work procedures

B1: Safe Work Procedure for microscopy

Job title: **Bitumen Froth Droplet Flocculation Study**	Date: 13th December 2019
Written by: Aakanksha Bhargava	Conducted by: Aakanksha Bhargava
Required Protective Equipment: Lab coat, closed-toe shoes, full length pants, full coverage safety glasses.	
First Aid Measures: First aid kit.	

Number	Sequence of safe work procedure steps	Potential hazards
	Startup • Turn on the microscope, halogen lamp, camera, and computer. • Start the Eclipse software from the desktop of the connected computer. • Select digital focus option from the top menu bar. **Microscopy** • Draw liquid from vial using a plastic pipette and place a drop on the slide. • Place the cover slip (slide) to protect the sample from dust. • Place the prepared slide on the mechanical stage. • Select the appropriate objective lens (20x) by rotating the nosepiece. Ensuring its click into place. • Move the bench with stage control (x and y direction) to get the desired position.	Cuts due to the sharp edges of microscopy slides and cover slips. First aid kit should be handy.

• Raise the mechanical stage to the maximum height. Be careful to prevent bumping of slide to the lens. • Stop when desired focus is achieved and then sharpen the image by turning the fine focus. • Once suitable contrast and focus is achieved in the picture, exit the digital focus. • Lower the stage and remove the slide. **Image Analysis** • Choose the save option from the top menu bar and save the image. • Calibrate the image by choosing the calibration distance tool from the menu. • After calibration, put the distance stamp using calibration linear bar from the menu. **Shut down** • Turn off the microscope, halogen lamp and microscope. • Shutdown the computer. • Cover the microscope with its dust cover.	

Once the experiment is complete, clean the counter. Also, make sure that all the microscopic slides are put in the appropriate waste disposal area.

B2: Safe Work Procedure for Silanization of Needles and Microscope slides

Job title: **Bitumen Froth Droplet Flocculation Study** **Silanization of needles and microscope slides**	Date: 18th November 2019
Written by: Aakanksha Bhargava	Conducted by: Aakanksha Bhargava

Required Protective Equipment:

Lab coat, closed-toe shoes, full length pants (to provide protection against splashes), nitrile gloves, full coverage safety glasses, and approved and fitted respiratory mask.

First Aid Measures:

In case of skin contact, wash off with soap and plenty of water.

In case of eye contact, flush eyes with water. Don't forget to remove the contact lens if present.

If swallowed, rinse mouth with water. Don't induce vomiting.

If inhaled, move into the fresh air.

For more details see MSDS

Number	Sequence of safe work procedure steps	Potential hazards
	Perform all the steps inside a fumehood • Immerse slides, needles, and glass pipettes in silanization solution (5% dimethyldicholrosilane in heptane) for 5 mins. • Remove them and allow to air dry. • Dip the dried slides in toluene up and down 5 times. For needles and pipettes, draw the toluene in and out five times using an auto pipette. • Allow them to air dry. • Repeat the above step (2nd step) with acetone.	Silanization solution is highly corrosive to the skin and respiratory tract. Ensure to wear the properly fitted respirator mask and 2 -3 layers of nitrile gloves.

Once the experiment is complete, clean the counter inside the fume hood. Also, make sure that all the bottles of chemicals used are put in the appropriate storage area.

Appendix C: MATLAB Scripts

C1: MATLAB script -1 for determining droplet size in the emulsion

```matlab
clc
clear
close all
NewImage  = dir('*.tif');
nfiles = length(NewImage);
diameters=zeros (1,10000);
diameters = array2table(diameters);
all_diameters1 = {};
excel_filename = 'all_diameters'
for i = 1 : 2
    image_i.filename = NewImage(i).name;
    x = imread(image_i.filename);
    y = rgb2gray(x);
    figure(1)
    imshowpair(y,x,'montage')
    [centersDarksmaller, radiiDarksmaller, metricDarksmaller] =
imfindcircles(y,[3 10], ...
        'ObjectPolarity','dark','Sensitivity',0.83,'EdgeThreshold',0.05);
    hDarksmaller = viscircles(centersDarksmaller,
radiiDarksmaller,'Color','r');
    [centersDarksmall, radiiDarksmall, metricDarksmall] =
imfindcircles(y,[11,28], ...
        'ObjectPolarity','dark','Sensitivity',0.89,'EdgeThreshold',0.05);
    hDarksmall = viscircles(centersDarksmall, radiiDarksmall,'Color','b');
    [centersDarkbig, radiiDarkbig, metricDarkbig] = imfindcircles(y,[29, 100],
...
        'ObjectPolarity','dark','Sensitivity',0.9,'EdgeThreshold',0.05);
    hDarkbig = viscircles(centersDarkbig, radiiDarkbig,'Color','g');
    n = numel(radiiDarksmall)+ numel(radiiDarkbig)+numel(radiiDarksmaller); %
Number of droplet detected
    All_centers = [centersDarkbig;centersDarksmall;centersDarksmaller];
    combinedradius_pixels = [radiiDarkbig;radiiDarksmall;radiiDarksmaller];
    mkdir newcode
    fname = 'A:\31032021bottomt=4\newcode';
    saveas(gcf,fullfile (fname , strcat('new_',image_i.filename)))
for j= 1: n
    s=j+1;
    for k=s:n
        d_ij=sqrt((All_centers(j,1)-All_centers(k,1)).^2+(All_centers(j,2)-
All_centers(k,2)).^2);
        k=combinedradius_pixels(j)-combinedradius_pixels(k);
         if d_ij <abs(k)+20
             All_centers(j,1)=0;
             All_centers(j,2)=0;
            combinedradius_pixels(j)=0;
         end
    end
end
Newallcenters = All_centers;
Newallradius =combinedradius_pixels;
```

```matlab
combinedradius_microns = Newallradius ./4.3;
figure(2)
imshowpair(y,x,'montage')
hnewcircles = viscircles(Newallcenters,Newallradius,'Color','m');
mkdir corrected
 fname1 ='A:\31032021bottomt=4\corrected' ;
 saveas(gcf,fullfile (fname1 , strcat('corrected_',image_i.filename)))
    image_i.diameter = nonzeros(combinedradius_microns .*2);
    all_diameters1{end+1} = image_i;
     diameters = all_diameters1{i}.diameter;
    xlswrite(excel_filename
,{all_diameters1{i}.filename},'Sheet1',char(strcat(xlsColNum2Str(i),'1')));
    xlswrite(excel_filename ,image_i.diameter
,'Sheet1',char(strcat(xlsColNum2Str(i),'2')));
end
```

C2: MATLAB script -2 for determining the diameter of the flocs

```matlab
clc
clear
close all
NewImage  = dir('*.tif');
nfiles = length(NewImage);
diameters=zeros (1,5000);
diameters = array2table(diameters);
all_floc_diameters1 = {};
excel_filename = 'all_floc_diameters'
mkdir flocs-1
for i = 1:nfiles
    image_i.filename = NewImage(i).name;
    x = imread(image_i.filename);
y = rgb2gray(x);
BW =
imbinarize(y,'adaptive','ForegroundPolarity','bright','Sensitivity',0.68);
se = strel('disk',20);
Ie = imerode(BW,se);
BW = imreconstruct(Ie,BW);
BW = 1-BW;
BW = imclearborder(BW);
BW =bwareaopen(BW,100);
BW = imfill(BW,'holes');
figure
imshowpair(BW,x,'montage');
fname = 'E:\8RPM\29062021_8RPM\z2t=0\flocs-1';
saveas(gcf,fullfile (fname , strcat('new_',image_i.filename)));
A = cell2mat(struct2cell(regionprops(logical(BW),'area')));
A_microns = A./(4.3^2);
A_final = reshape(A_microns,[],1);
diameter_final = sqrt((A_final.*4)./3.14);
image_i.diameter = diameter_final;
    all_floc_diameters1{end+1} = image_i;
     diameters = all_floc_diameters1{i}.diameter;
 xlswrite(excel_filename
,{all_floc_diameters1{i}.filename},'Sheet1',char(strcat(xlsColNum2Str(i),'1'))
);
 xlswrite(excel_filename ,image_i.diameter
,'Sheet1',char(strcat(xlsColNum2Str(i),'2')));
end
```

Appendix D: Repeats of experiments

D1: Results of repeats of water-in-light mineral oil emulsion preparation
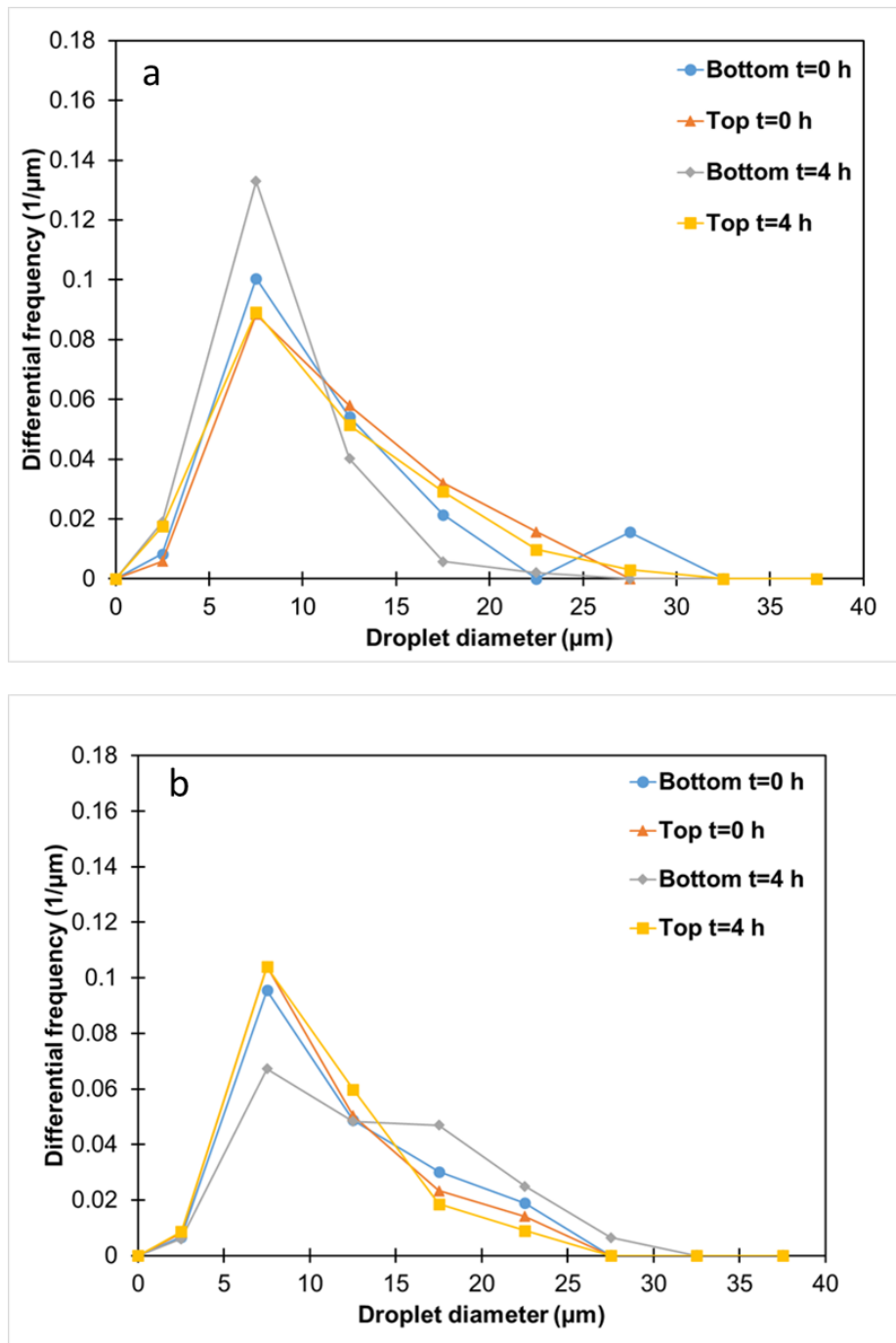
Figure D1.1 (a) Volume-based droplet size distribution for Repeat-1. (b) Volume-based droplet size distribution for Repeat-2.

Table D1.1 Different mean diameters calculated for water-in-light mineral oil emulsion (Repeat-2)

Diameters (µm)						
	Bottom			Top		
Sampling time (hours)	d_{10}	d_{32}	d_{43}	d_{10}	d_{32}	d_{43}
t = 0	4.8	8.4	11.0	4.6	7.7	10.4
t = 4	4.8	9.4	12.8	4.7	7.4	9.5

D2: Repeats of shearing experiments in Couette cell at 8 RPM and 12 RPM
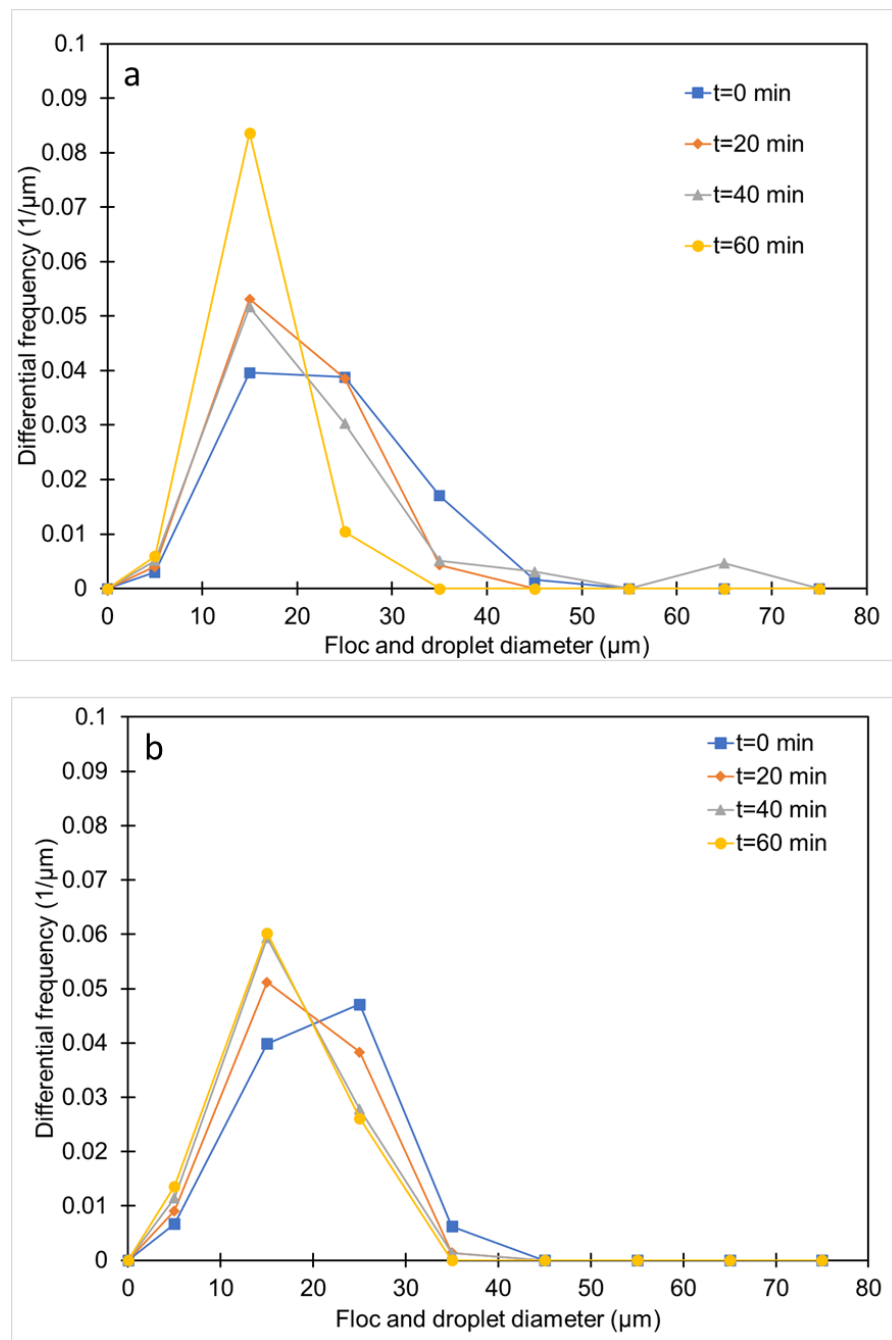
Figure D2.1 (a) Volume base floc and single droplet size distribution for Repeat-1at 8 RPM.

(b) Volume base floc and single droplet size distribution for Repeat-2 at 8RPM.
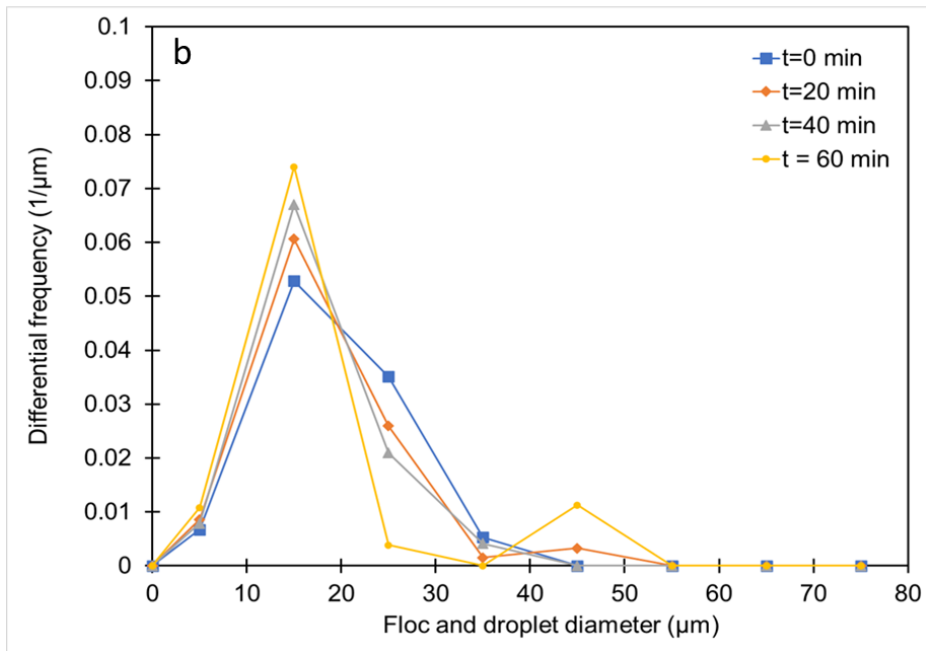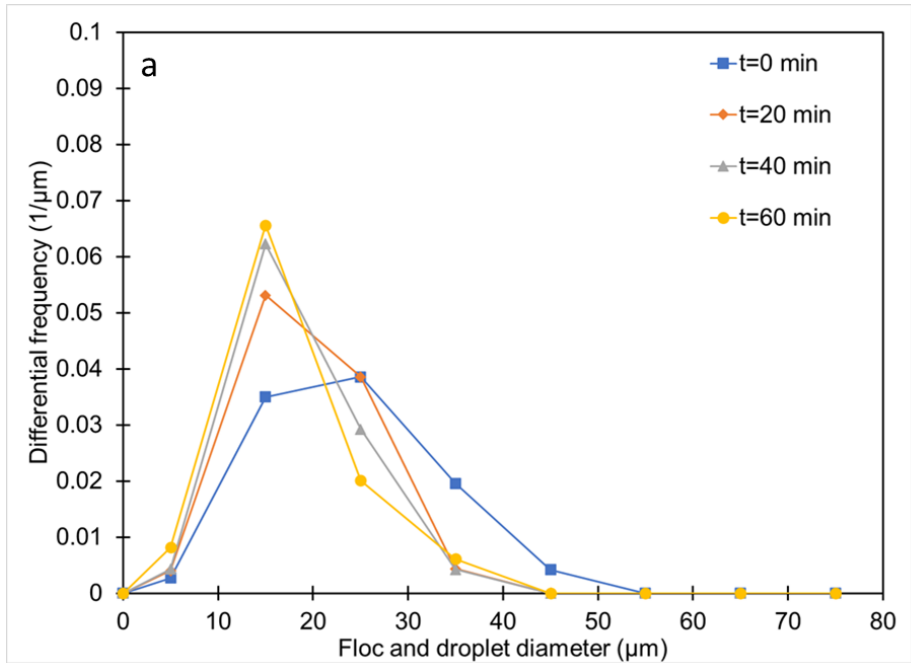
Figure D2.2 (a) Volume base floc and single droplet size distribution for Repeat-1at 12 RPM.

(b) Volume base floc and single droplet size distribution for Repeat-2 at 12 RPM.

Appendix E: Microphotographs

E1: Water-in-light mineral oil emulsion preparation
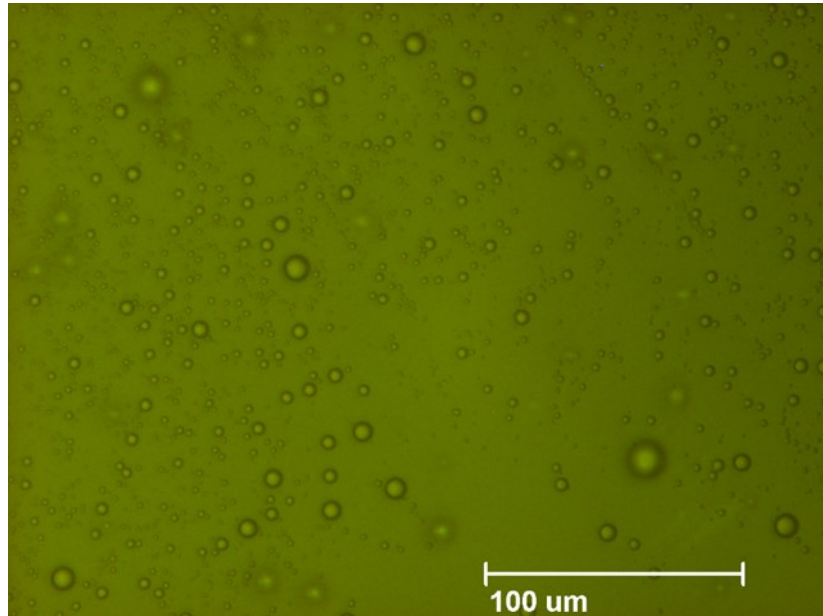
Figure E1.1 Representative microphotograph of the emulsion sample collected from the bottom of beaker at time t =0 h.
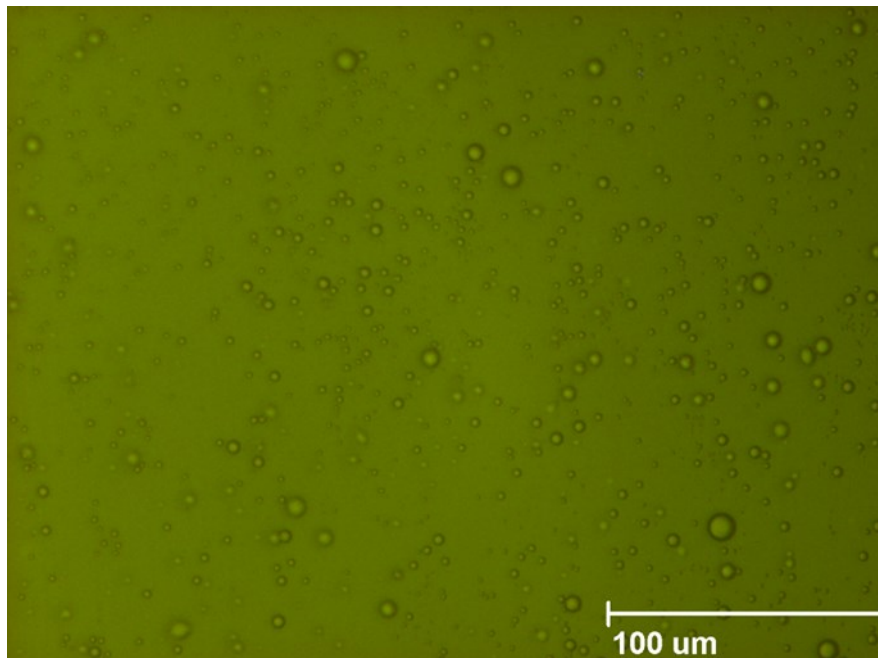
Figure E1.2 Representative microphotograph of the emulsion sample collected from the top of beaker at time t =0 h.
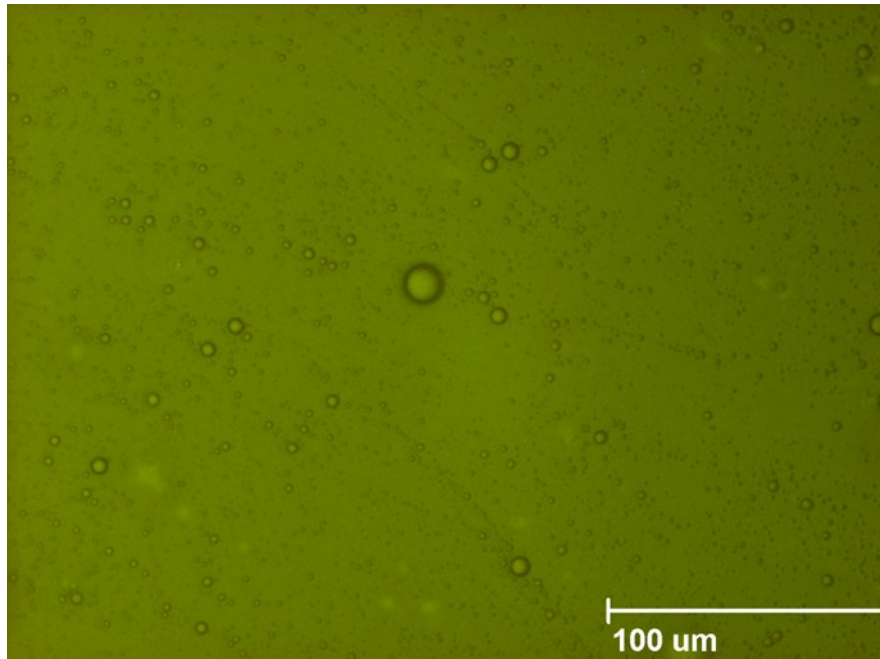
Figure E1.3 Representative microphotograph of the emulsion sample collected from the bottom of beaker at time t =4 h.
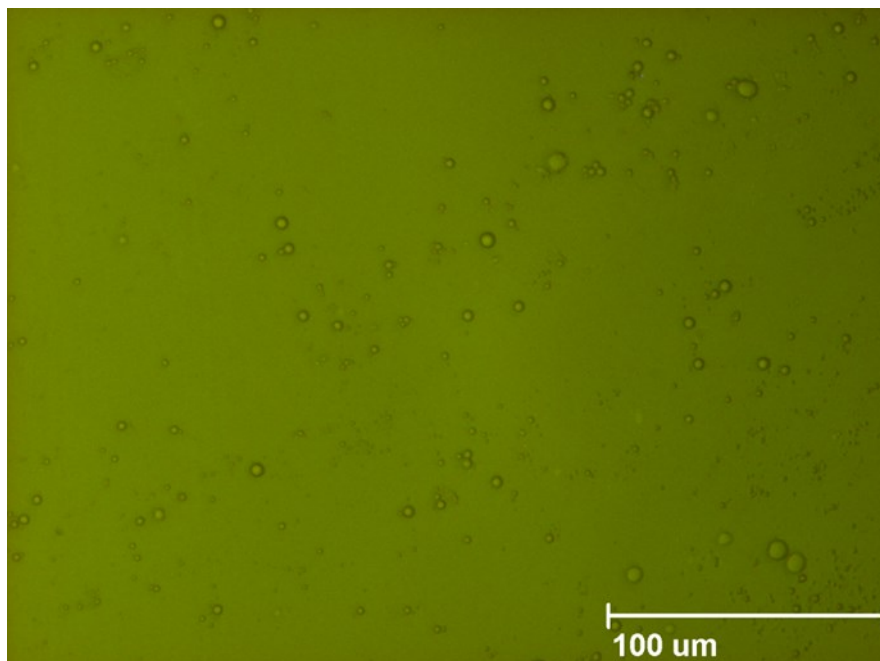
Figure E1.4 Representative microphotograph of the emulsion sample collected from the bottom of beaker at time t =4 h.

E2: Shearing of emulsion in the Couette cell
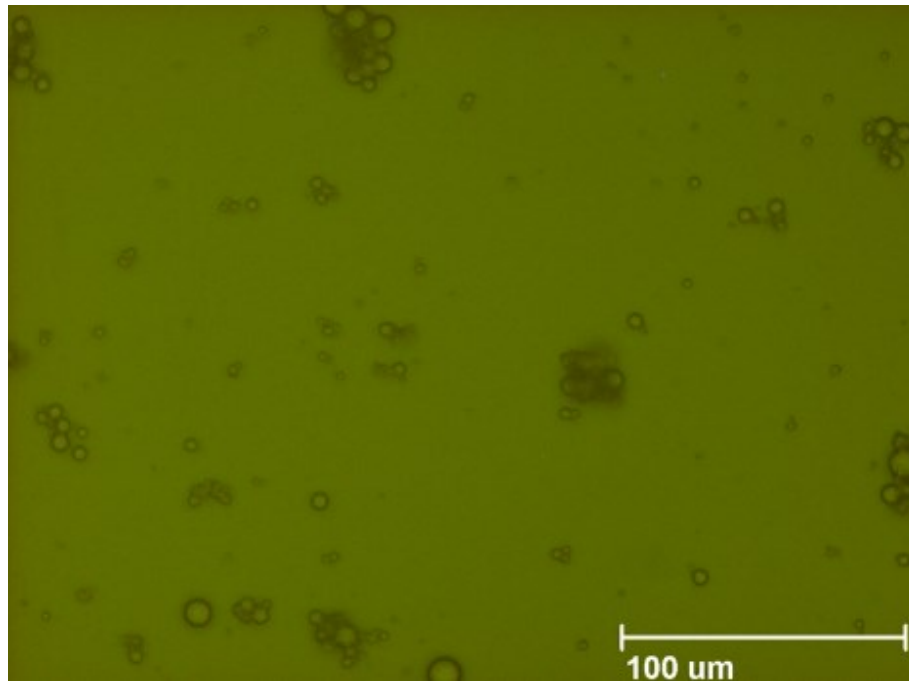
Figure E2.1 Representative microphotograph of the emulsion sample collected at = 0 min of settling for unsheared emulsion.
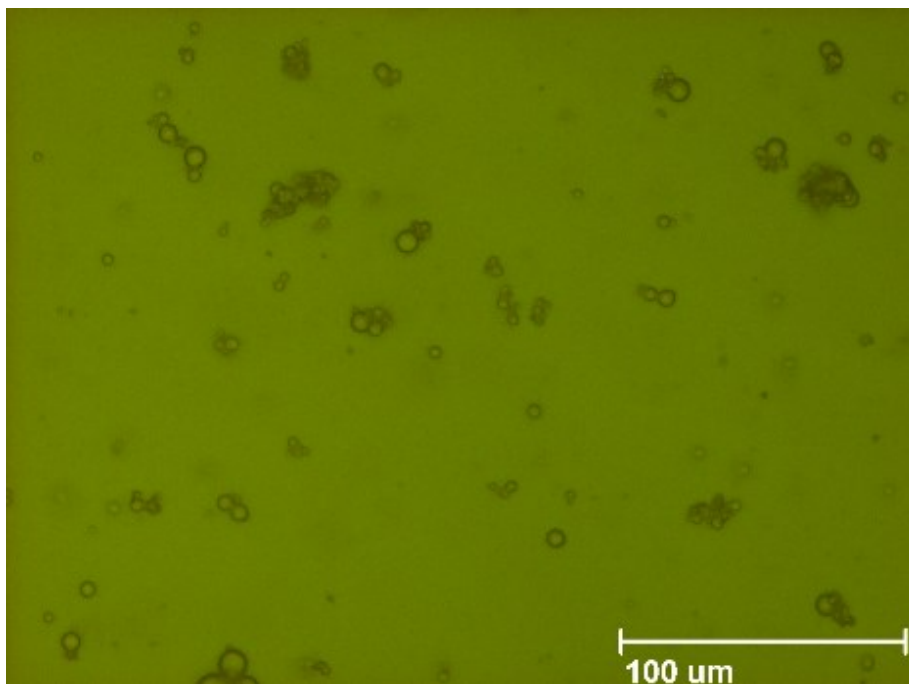
Figure E2.1 Representative microphotograph of the emulsion sample collected at = 60 min of settling for unsheared emulsion.
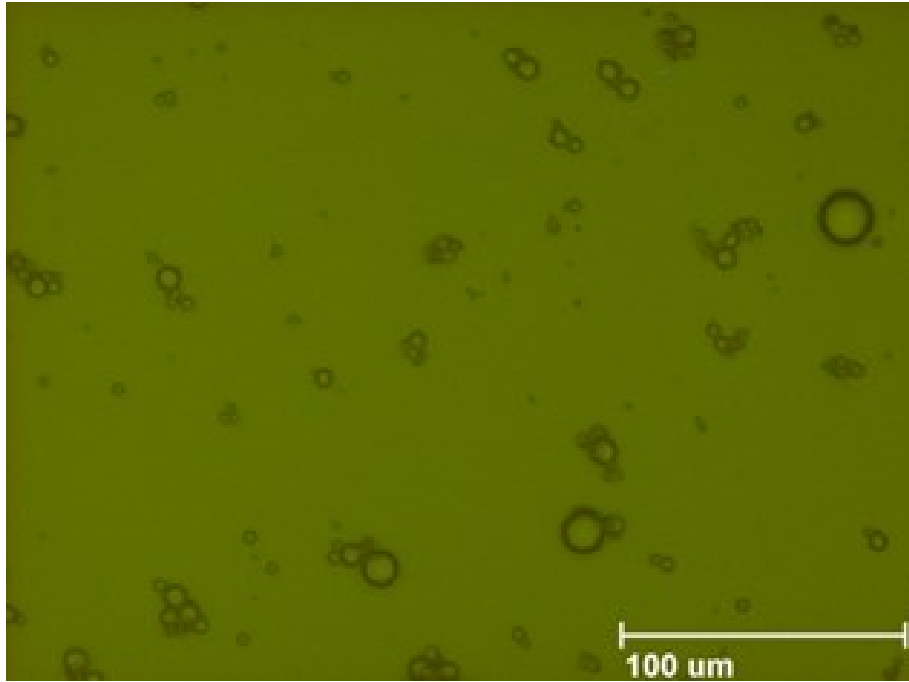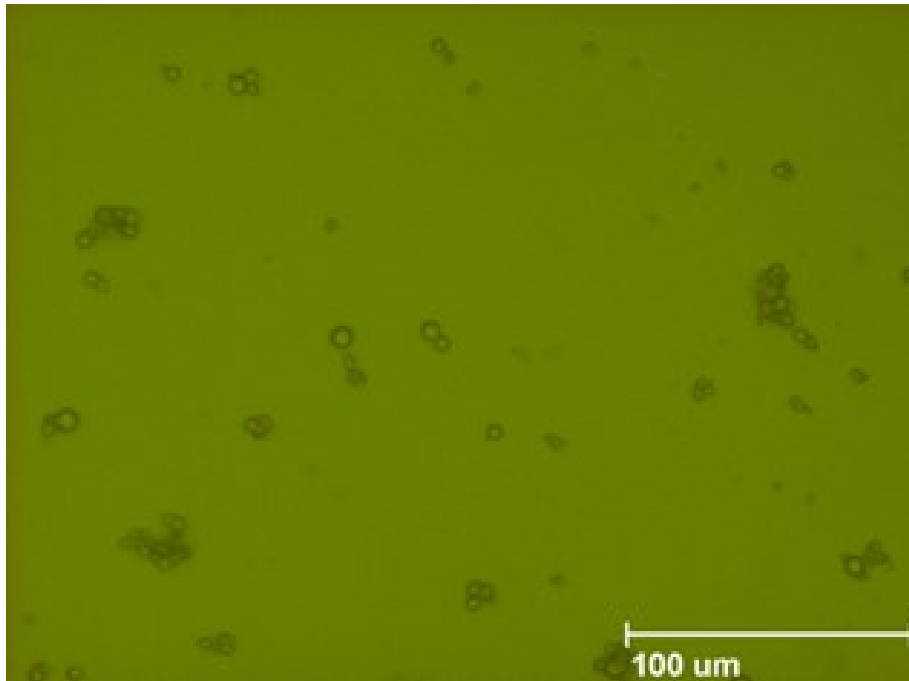
Figure E2.3 Representative microphotograph of the emulsion sample collected at = 0 min of settling for emulsion sheared at 5 RPM.
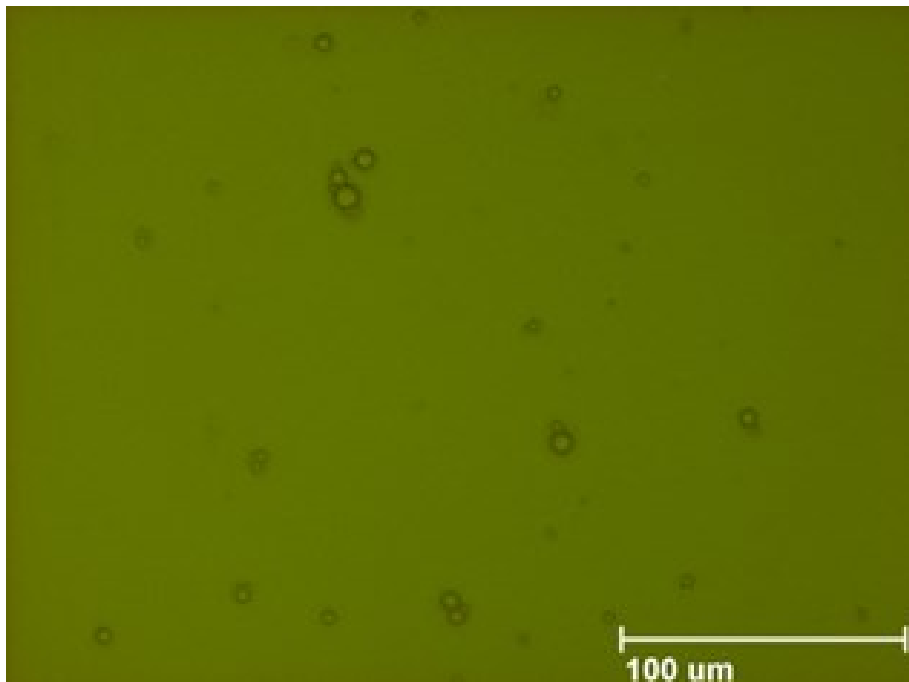
Figure E2.4 Representative microphotograph of the emulsion sample collected at = 60 min of settling for emulsion sheared at 5 RPM.
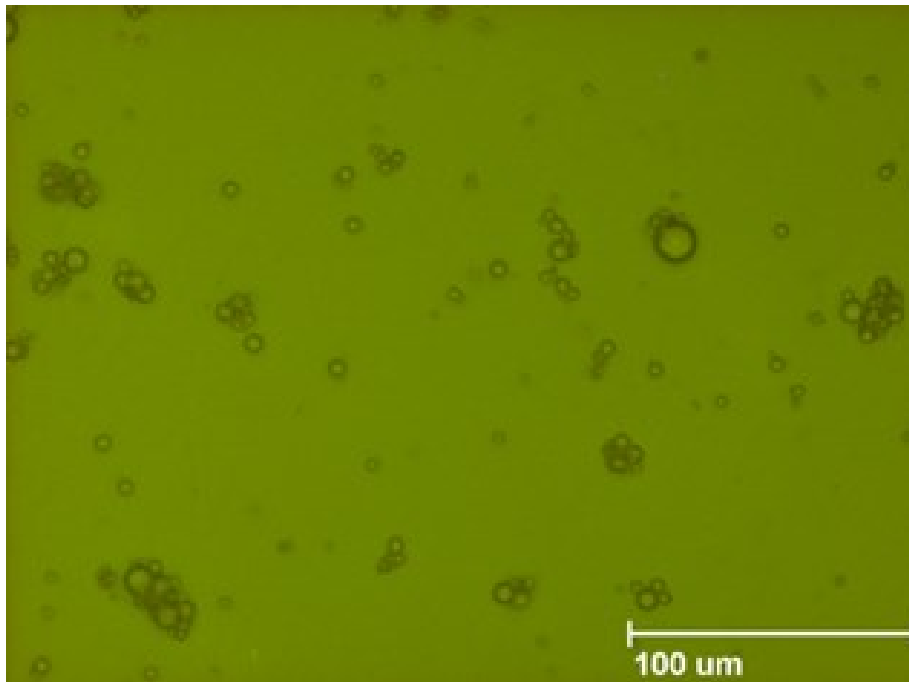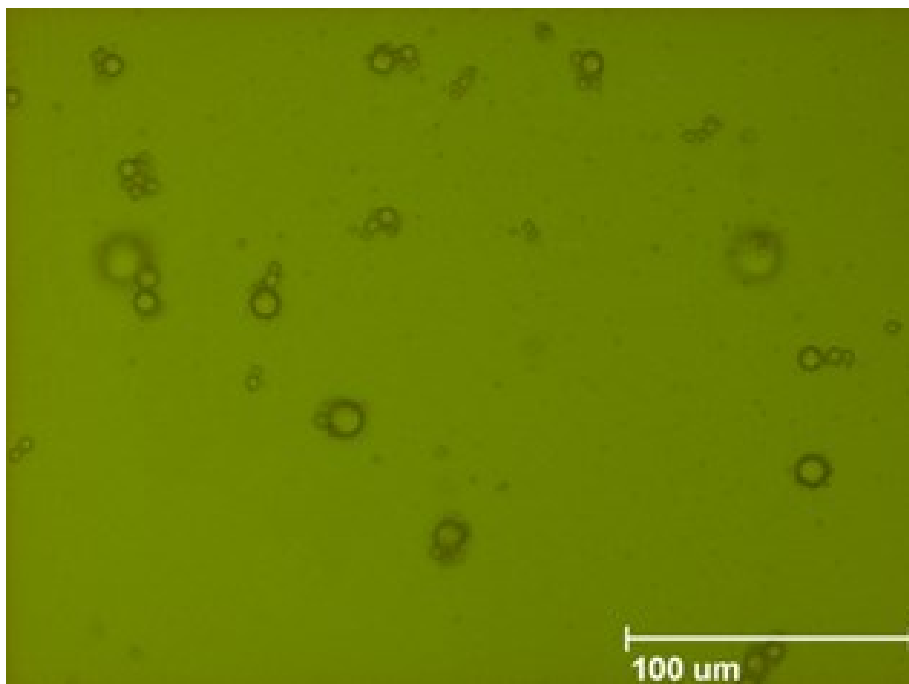
Figure E2.5 Representative microphotograph of the emulsion sample collected at = 0 min of settling for emulsion sheared at 8 RPM.
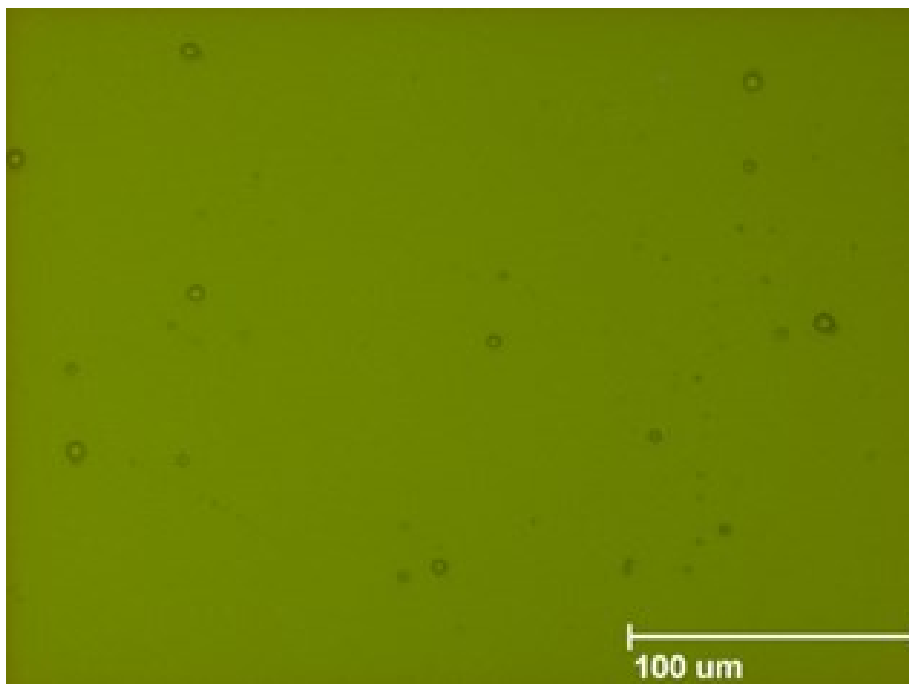
Figure E2.6 Representative microphotograph of the emulsion sample collected at = 60 min of settling for emulsion sheared at 8 RPM.

Figure E2.7 Representative microphotograph of the emulsion sample collected at t = 0 min of settling for emulsion sheared at 12 RPM.

Figure E2.8 Representative microphotograph of the emulsion sample collected at t = 60 min of settling for emulsion sheared at 12 RPM.

Appendix F: Sample calculation for floc size distribution

The steps for the calculation are mentioned as below:

Step -1: MATLAB script -2 mentioned in the appendix C, calculates the area-based diameter of the flocs described as:

$$d_e = \sqrt{\frac{4 * A_f}{\pi}}$$

where, d_e is the equivalent diameter of the floc, and A_f is the area of the floc.
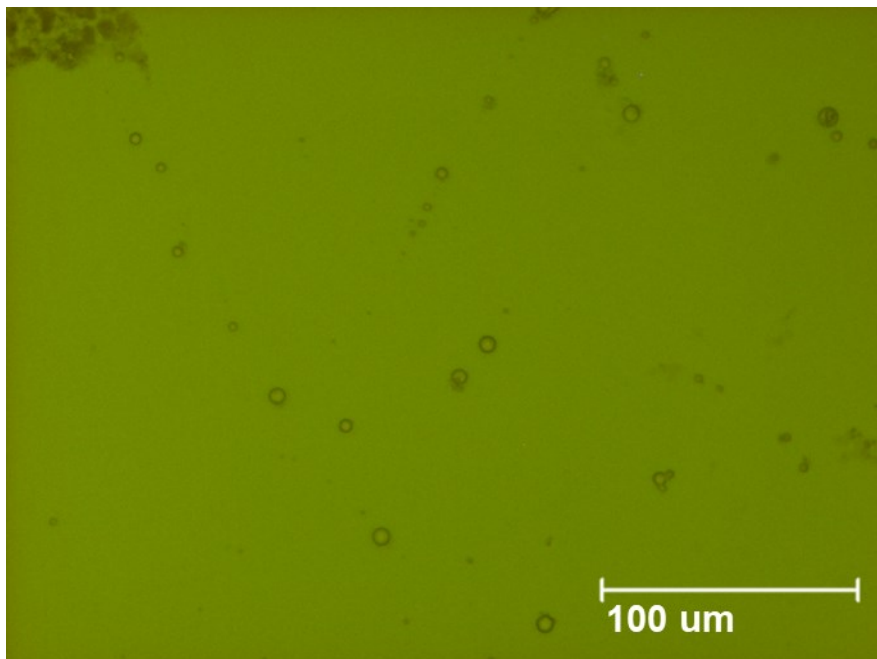
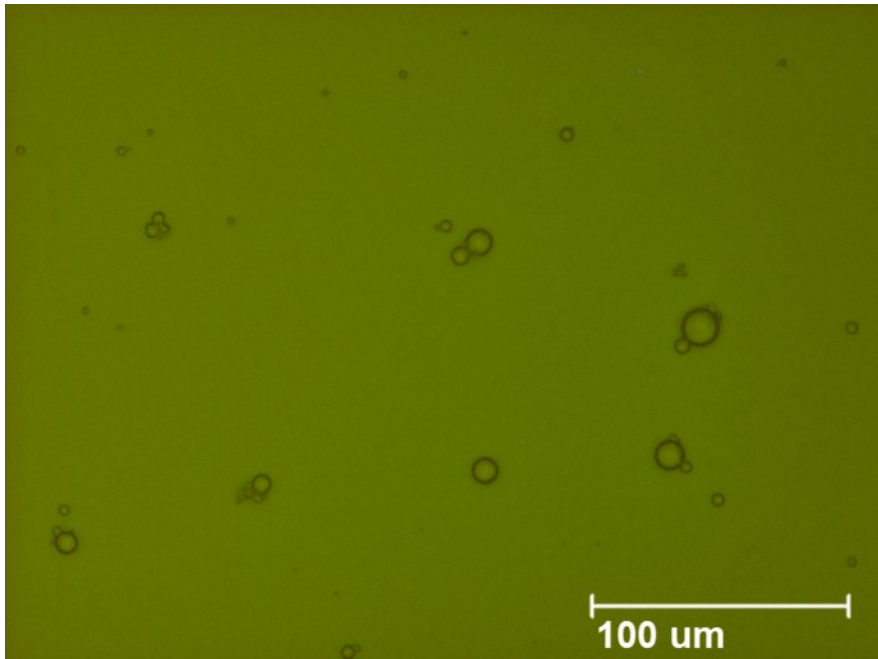Step 2: The volume of floc is then calculated as mentioned below:

$$V = \frac{\pi * d_e{}^3}{6}$$

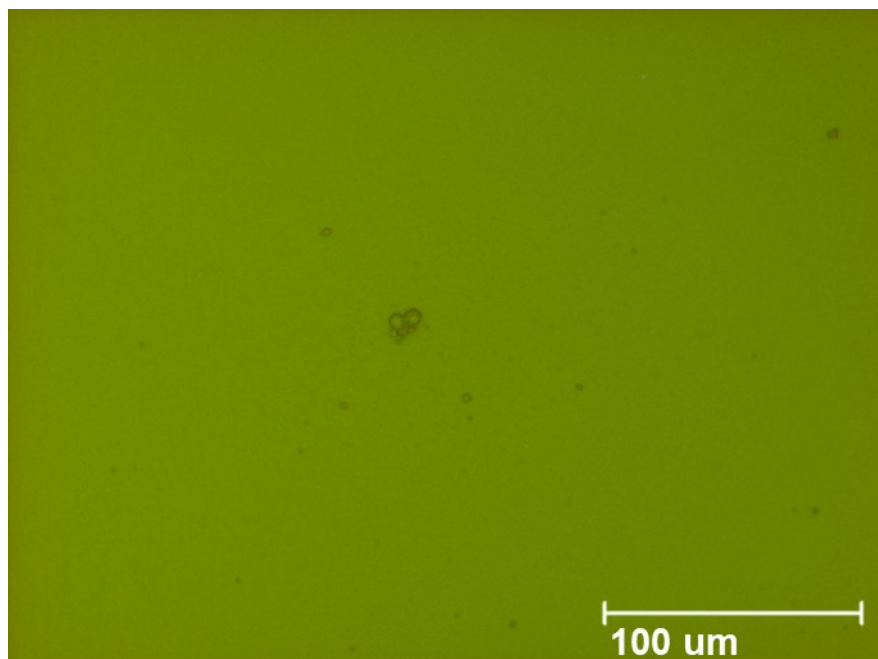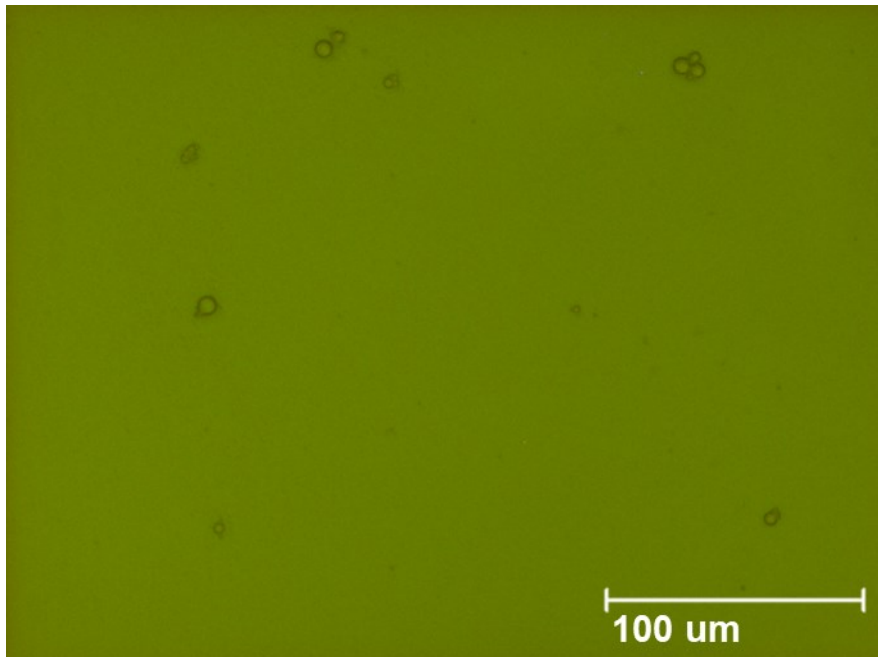The volume of floc as calculated is then used to plot the volume-based floc distributions.

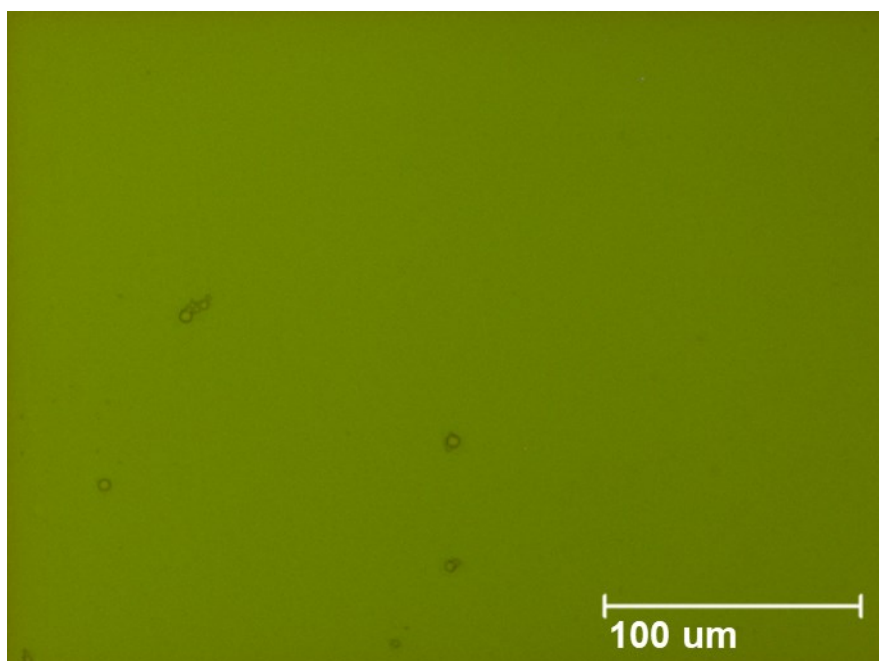# Appendix G: Additional microphotographs of emulsion sheared in Couette cell

G1: Microphotographs of emulsion sample collected at t = 60 min of settling for emulsion sheared at 5 RPM

100 um
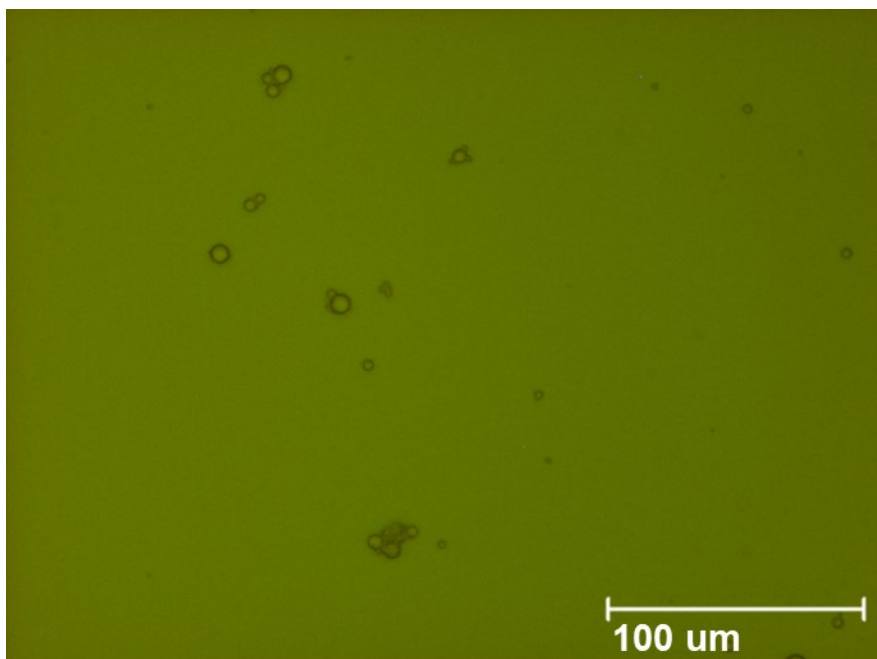
G2: Microphotograph of emulsion sample collected at t = 60 min of
settling for emulsion sheared at 8 RPM

G3: Microphotograph of emulsion sample collected at = 60 min for emulsion sheared at 12 RPM

G3: Microphotograph of emulsion sample collected at = 60 min for emulsion sheared at 12 RPM

100 um